TRANSYLVANIAN REVIEW OF SYSTEMATICAL AND ECOLOGICAL RESEARCH

26.1

The Wetlands Diversity

Editors

Doru Bănăduc, Kevin Cianfaglione & Sophia Barinova

Sibiu – Romania
2024

TRANSYLVANIAN REVIEW OF SYSTEMATICAL AND ECOLOGICAL RESEARCH

26.1

The Wetlands Diversity

Editors

Doru Bănăduc, Kevin Cianfaglione & Sophia Barinova

International Association for Danube Research	"*Lucian Blaga*" University of Sibiu	Ecotur Sibiu Association	Université Catholique de Lille	Broward College, Fort Lauderdale	Institute of Evolution, University of Haifa

Sibiu – Romania
2024

Scientifical Reviewers

Sergey AFANASYEV
Institute of Hydrobiology of the National Academy of Sciences of Ukraine,
Kyiv – Ukraine.

John Robert AKEROYD
Sherkin Island Marine Station,
Sherkin Island – Ireland.

Sophia BARINOVA
Institute of Evolution, University of Haifa,
Haifa – Israel.

Doru BĂNĂDUC
"Lucian Blaga" University of Sibiu,
Sibiu – Romania.

Kevin CIANFAGLIONE
Université Catholique de Lille,
Lille – France.

Constantin DRĂGULESCU
"Lucian Blaga" University of Sibiu,
Sibiu – Romania.

Isa ELEGBEDE
Brandenburg University of Technology Cottbus – Senftenberg,
Cottbus – Senftenberg – Germany.

Nicolae GĂLDEAN
Ecological University of Bucharest,
Bucharest – Romania.

Grant S. MCCALL
Center for Human-Environmental Research,
New Orleans, Louisiana – USA.

Ahmet ÖKTENER
Ministry of Agriculture and Forestry,
Denizli – Turkey.

Erika SCHNEIDER-BINDER
Karlsruhe University, Institute for Waters and River Basin Management,
Rastatt – Germay.

George SECĂREANU
Ovidius University of Constanța,
Constanța – Romania.

David SERRANO
Broward College,
Fort Lauderdale, Florida – USA.

Mark SIXSMITH
University of Plymouth,
Plymouth – Great Britain.

Mikhail O. SON
Institute of Marine Biology of the National Academy of Sciences of Ukraine,
Odessa – Ukraine.

James K. WETTERER
Florida Atlantic University, Wilkes Honors College,
Jupiter – Florida, United States of America.

Editorial Assistants

IN MEMORIAM

Bjørn Grothaug Andersen
(1924 – 2012)

Bjørn Grothaug Andersen was a Norwegian university teacher of Quaternary geology and glaciology who made opening contributions to glacial geology and the in depth understanding of climate change.

Skiing in the winter and fishing in the summer with his father and brothers in his childhood and teenage periods, adored the mountains in Stavanger region, several times he crossed Trollgaren in Ryfylke, this stunning moraine that is fitting to its name. He questioned how it was shaped, and was said by the farmers of the area that it was truly Trolls that had set up the winding fence of gigantic stones, His interest for this natural phenomenon in addition to many others in turn led to his curiosity and attention for nature in general and Ice Age in special.

In 1951 he married Astrid E. Kruse Andersen which supports his activities all along their common life. Subsequently to a research fellowship at Yale University in 1954-1956, *Andersen* was a teaching quaternary geology at the University of Oslo from 1956 to 1970, then at the University of Bergen for nine years until his retirement. He supervised the geological institutes both in Oslo and Bergen. He was in charge for the geological education of over 30 year groups of students, and he unrelenting participated to the academic world activities until autumn 2011, when he was hit by a cancer and he was in poor health.

All along his activity, his students and colleagues benefited from his expertise and international contacts. He conducted field trips to the Antarctic, South America, New Zeeland, Greenland, etc. *Andersen* kept in contact with some of his students until his death.

Andersen's first scientific journey to the South Pole came after a period of small Norwegian interest in the Antarctic after the great achievements of Roald Amundsen in 1911-1912. *Andersen* was the next Norwegian to visit the Pole after the Amundsen successful mission. An America expedition which reached the Pole a week before *Andersen* revered his realisations by naming a mountain escarpment (Andersen Escarpment) after him.

He accompanied along his activity a party of scientists doing research in Norway, Chille, New Zeeland, Greenland, etc.

Among such trips, in 2005 *Andersen* with a group of scientists went on a research voiage to Greenland to measure the ice coverage in connection to climatic change.

All his research led to a succession of works, among them papers in the respected international scientific journals *Nature* and *Science*. In addition, to two significant books on glacial geology, one about the Ice Age in Norway (Ice age Norway: landscapes formed by ice age glaciers) and an international textbook on the World Ice Age (The Ice Age World: an introduction to Quaternary history and research with emphasis on North America and Northern Europe during the last 2.5 million years) were published. Among numerous valuable scientific papers, Amundsen's first paper is one of the most basic papers in Norwegian glacial geology, even thought it was published before C-14 dating was available.

Bjørn Grothaug Andersen was a dedicated naturalist all his adult life, letting an important scientific legacy in his field of activity.

The Editors

CONTENTS

Preface

In a global environment in which the climate changes are observed from few decades no more only through scientific studies but also through day by day life experiences of average people which feel and understand allready the presence of the medium and long-term significant change in the "average weather" all over the world, the most comon key words which reflect the general concern are: heating, desertification, rationalisation and surviwing.

The causes, effects, trends and possibilities of human society to positively intervene to slow down this process or to adapt to it involve a huge variety of aproacess and efforts.

With the fact in mind that these aproaces and efforts shuld be based on genuine scientific understanding, the editors of the *Transylvanian Review of Systematical and Ecological Research* series launch three annual volumes dedicated to the wetlands, volumes resulted mainly as a results of the *Aquatic Biodiversity International Conference*, Sibiu/Romania, 2007-2017.

The therm wetland is used here in the acceptance of the Convention on Wetlands, signed in Ramsar, in 1971, for the conservation and wise use of wetlands and their resources. **Marine/Coastal Wetlands** – Permanent shallow marine waters in most cases less than six metres deep at low tide, includes sea bays and straits; Marine subtidal aquatic beds, includes kelp beds, sea-grass beds, tropical marine meadows; Coral reefs; Rocky marine shores, includes rocky offshore islands, sea cliffs; Sand, shingle or pebble shores, includes sand bars, spits and sandy islets, includes dune systems and humid dune slacks; Estuarine waters, permanent water of estuaries and estuarine systems of deltas; Intertidal mud, sand or salt flats; Intertidal marshes, includes salt marshes, salt meadows, saltings, raised salt marshes, includes tidal brackish and freshwater marshes; Intertidal forested wetlands, includes mangrove swamps, nipah swamps and tidal freshwater swamp forests; Coastal brackish/saline lagoons, brackish to saline lagoons with at least one relatively narrow connection to the sea; Coastal freshwater lagoons, includes freshwater delta lagoons; Karst and other subterranean hydrological systems, marine/coastal. **Inland Wetlands** – Permanent inland deltas; Permanent rivers/streams/creeks, includes waterfalls; Seasonal/intermittent/irregular rivers/streams/creeks; Permanent freshwater lakes (over eight ha), includes large oxbow lakes; Seasonal/intermittent freshwater lakes (over eight ha), includes floodplain lakes; Permanent saline/brackish/alkaline lakes; Seasonal/intermittent saline/brackish/alkaline lakes and flats; Permanent saline/brackish/alkaline marshes/pools; Seasonal/intermittent saline/brackish/alkaline marshes/pools; Permanent freshwater marshes/pools, ponds (below eight ha), marshes and swamps on inorganic soils, with emergent vegetation water-logged for at least most of the growing season; Seasonal/intermittent freshwater marshes/pools on inorganic soils, includes sloughs, potholes, seasonally flooded meadows, sedge marshes; Non-forested peatlands, includes shrub or open bogs, swamps, fens; Alpine wetlands, includes alpine meadows, temporary waters from snowmelt; Tundra wetlands, includes tundra pools, temporary waters from snowmelt; Shrub-dominated wetlands, shrub swamps, shrub-dominated freshwater marshes, shrub carr, alder thicket on inorganic soils; Freshwater, tree-dominated wetlands; includes freshwater swamp forests, seasonally flooded forests, wooded swamps on inorganic soils; Forested peatlands; peatswamp forests; Freshwater springs, oases; Geothermal wetlands; Karst and other subterranean hydrological systems, inland. **Human-made wetlands –** Aquaculture (e. g., fish/shrimp) ponds; Ponds; includes farm ponds, stock ponds, small tanks; (generally below eight ha); Irrigated land, includes irrigation channels and rice fields; Seasonally flooded agricultural land (including intensively managed or grazed wet meadow or pasture); Salt exploitation sites, salt pans, salines, etc.; Water storage areas, reservoirs/barrages/dams/impoundments (generally over eight ha); Excavations; gravel/brick/clay pits; borrow pits, mining pools; Wastewater treatment areas, sewage farms, settling ponds, oxidation basins, etc.; Canals and drainage channels, ditches; Karst and other subterranean hydrological systems, human-made.

The editors of the ***Transylvanian Review of Systematical and Ecological Research*** started and continue the annual sub-series (*Wetlands Diversity*) as an international scientific debate platform for the wetlands conservation, and not to take in the last moment, some last heavenly "images" of a perishing world …

This volume included variated original researches from diverse wetlands around the world.

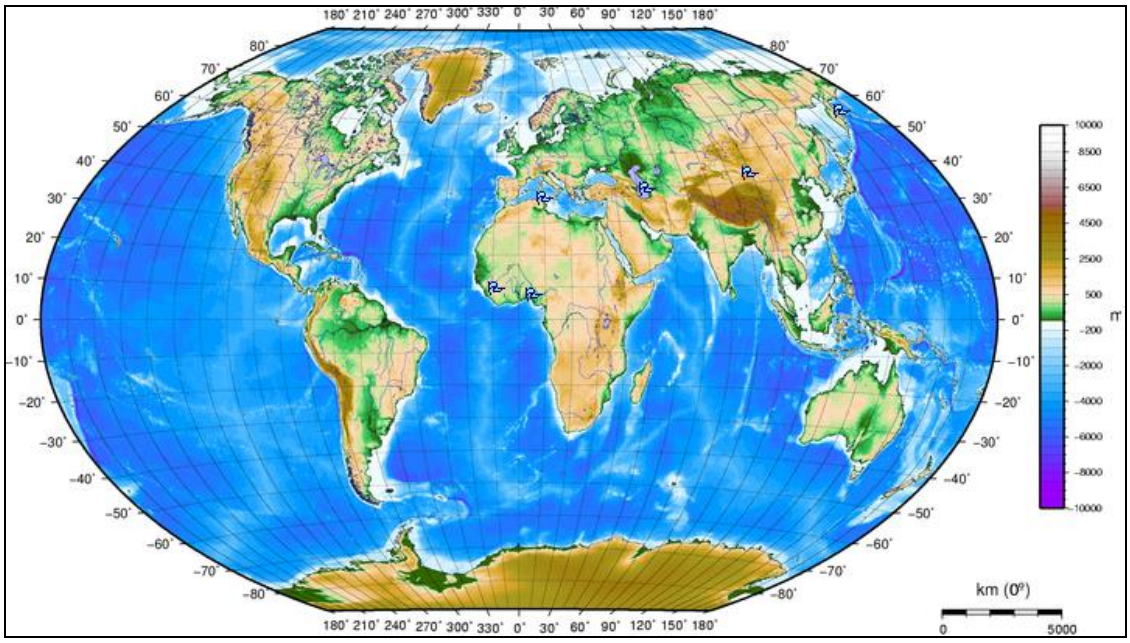

The subject areas (▱) for the published studies in this volume.

No doubt that this new data will develop knowledge and understanding of the ecological status of the wetlands and will continue to evolve.

Acknowledgements

The editors would like to express their sincere gratitude to the authors and the scientific reviewers whose work made the appearance of this volume possible.

The Editor in Chief

Editorial Office:

"*Lucian Blaga" University of Sibiu, Faculty of Science, Dr. Ion Rațiu Street 5-7, Sibiu, Sibiu County, Romania, RO-550012, Doru Bănăduc (ad.banaduc@yahoo.com, doru.banaduc@ulbsibiu.ro)*

(ISSN-L 1841 – 7051; online ISSN 2344 – 3219)

NOVEL SPECIES RECORD OF *ULVA INTESTINALIS* (CHLOROPHYTA, ULVACEAE) FOR KAMCHATKA (NE ASIA) FROM AN ISOLATED INLAND LOCALITY

Roman E. ROMANOV * and *Olga A. CHERNYAGINA* **

* Komarov Botanical Institute of the Russian Academy of Sciences, 2 Professora Popova St., Saint Petersburg, Russian Federation, RU-197376, romanov_r_e@mail.ru, ORCID: 0000-0002-6137-3586.
** Kamchatka Branch of the Pacific Geographical Institute of the Far East Branch of the Russian Academy of Sciences, Petropavlovsk-Kamchatsky, Russian Federation, RU-683000, kamchatika@mail.ru, ORCID: 0000-0003-0801-8961.

DOI: 10.2478/trser-2024-0001

KEYWORDS: Esso, floristic novelty, green algae, Kamchatka, thermal springs.

ABSTRACT

A novel inland record of the green alga *Ulva intestinalis* was found in central Kamchatka, in a brackish stream originating from cooled waters of drilled thermal springs. This species was observed in May 2017, but not encountered again at the same site despite targeted search. Its occurrence in central Kamchatka was surprising given the natural environment, and was probably related to both the presence of thermal springs and human disturbance. The sporadic inland appearance of *U. intestinalis* in this region suggests it may be unable to maintain stable populations in this region, and experience repeated local extinctions and recolonizations.

RÉSUMÉ: Enregistrement d'une nouvelle espèce d'algue, *Ulva intestinalis* (Chlorophyta, Ulvaceae) dans la péninsule du Kamtchatka (Asie du Nord-Est) dans une localité isolée de l'intérieur des terres.

La nouvelle espèce d'algue verte *Ulva intestinalis* (Chlorophyta, Ulvaceae) a été trouvée dans le centre de la péninsule du Kamtchatka, dans un cours d'eau saumâtre provenant des eaux refroidies de sources thermales forées. Cette espèce a été repérée pour la première fois en mai 2017 et n'a plus été revue sur le même site malgré des recherches ciblées. Sa présence dans le centre du Kamtchatka contraste clairement avec le contexte environnemental naturel et était probablement liée à la fois, à la présence de sources thermales et à la transformation humaine de l'environnement. L'apparition sporadique d' *U. intestinalis* à l'intérieur des terres dans cette région suggère qu'elle pourrait être incapable de maintenir des populations stables dans cette région, de connaître des extinctions et des recolonisations locales répétées.

REZUMAT: Înregistrări noi ale speciilor de *Ulva intestinalis* (Chlorophyta, Ulvaceae) pentru Kamchatka (NE Asia) din localitatea izolată interioară.

O nouă înregistrare continentală a algei verzi *Ulva intestinalis*, a fost găsită în centrul Kamchatka, într-un curs de apă salmastru provenit din apele răcite ale izvoarelor termale forate. Această specie a fost observată în mai 2017, dar nu a mai fost întâlnită în același sit, în ciuda căutărilor direcționate. Apariția sa în centrul Kamchatka a fost surprinzătoare, având în vedere mediul natural și a fost probabil legată atât de prezența izvoarelor termale, cât și de perturbarea umană. Apariția sporadică a *U. intestinalis* în această regiune sugerează că ar putea fi incapabilă să mențină populații stabile în această regiune și să experimenteze extincții și recolonizări locale repetate.

INTRODUCTION

Many green algae in the genus *Ulva* L. are economically important; useful in the case of cultivated edible species, or causing grave economic damage in green tide algal blooms (Zhang et al., 2019; Fort et al., 2020; Harsha Mohan et al., 2023). Species with tube thalli, earlier placed in the genus *Enteromorpha* Link (Hayden et al., 2003), can colonize inland waters (Bliding, 1963; Li and Bi, 1998; Messyasz, 2009; Mareš et al., 2011; Rybak, 2015, 2018, 2021; Saber et al., 2018; Škaloud et al., 2018). Inland populations are generally found in hard, brackish waters of arid and semiarid areas that have hot summers, e.g., southeastern Europe (Zhakova, 2006; Zinchenko et al., 2021; iNaturalist, 2024; Romanov, unpubl. data), western and central Asia (Muzafarov, 1965; Nahucrishvili, 1986; Maulood et al., 2013; Zhakova, 2013; Tekebaeva et al., 2014; Sametova et al., 2019; Mohebbi and Zarezadeh, 2023; Romanov, unpubl. data), southern Ural (Yatsenko-Stepanova and Ignatenko, 2018), southern Siberia (Safonova and Ermolaev, 1983; Kuklin, 2017; Efremov, 2018; Tokar, 2018; Bazarova and Kuklin, 2021; Romanov, unpubl. data), Mongolia (Tsegmid and Baigal-Amar, 2018), and China (Li and Bi, 1998). Inland populations are also known from northeastern Siberia (Skvortsov, 1917; Kopyrina et al., 2020) and even in the lowermost locality of the Earth (-455 m below sea level) near Dead Sea (Barinova et al., 2004).

Thermal springs, as well as manmade water bodies, often have temperature regimes and chemical compositions that contrast with surrounding aquatic habitats, analogous biogeographically to isolated islands or oases (Glazier, 2009). Thermal springs are widely recognized as key habitats and biodiversity hotspots (see references in Cantonati, 2022). In addition to species of algae and cyanobacteria (e.g., Elenkin, 1914; Doemel and Brock, 1971; Gromov et al., 1991; Nikitina, 2005; Cantonati et al., 2010; Beauger et al., 2022; see references in Cantonati, 2022), thermal springs can harbor populations of macroscopic algae, e.g., Characeae, far from their main distributional range dictated by climatic and other large-scale ecological factors (e.g., Langangen, 2000; Romanov and Chernyagina, 2018; Langangen et al., 2020; Romanov and Vishnyakov, 2023). The same seems to be true for some water bodies with artificial thermal effluents (Romanov et al., 2018). This paper describes a recent isolated record of *Ulva intestinalis* L. (formerly *Enteromorpha intestinalis* (L.) Link) from central Kamchatka, a humid continental area with subarctic climate, i.e., cold without distinct wet or dry seasons and having cold summers (Köppen-Geiger climate classification = Dfc, Peel et al., 2007), and mostly soft oligotrophic fresh waters (Litvinenko and Zakharikhina, 2020) that are unlike the normal inland habitats of *Ulva* (e.g., Messyasz and Rybak, 2010).

MATERIAL AND METHODS

Study area

The survey of aquatic habitats associated with thermal springs was done around Esso Village, located within Bystrinsky Nature Park, a section of the UNESCO World Heritage "Volcanoes of Kamchatka" area belonging to the Far East monsoon area (Kondratyuk, 1974) and having continental climate with a cold winter (below to –42°C), short warm summer (up to 32°C) and small annual precipitation (390 mm). The natural thermal effluents were altered after human changed the environment. Groundwater with a temperature at drill outlet of 72-100°C is collected from diverse outlets into a pipe and is released into a pool. The *Ulva* was found in the outflow on this pool (Fig. 1). The waters are siliceous (H_2SiO_3 – 169 mg.dm^{-3}), weakly alkaline to alkaline (pH 8.9-9.8), with a salinity of 1.0-1.5 g.dm^{-3}. Components are sulphates (SO_4), calcium, and sodium (Ca–Na), with trace components (As, B, F, Li). The nitrogen is the main dissolved gas (Kiryukhin et al., 2010; Muradov et al., 2013).

Sampling and laboratory study

The plants were collected by hand and stored in 70% ethanol. The images were taken using a Carl Zeiss Axiolab A microscope equipped with an AxioCam MRs-5 digital camera. A voucher specimen was deposited in the collection of algae of the herbarium of the Komarov Botanical Institute of the Russian Academy of Sciences (LE). The species was identified using key references (Bliding, 1963; Vinogradova, 1974, 1979; Moshkova and Hollerbach, 1986; Li and Bi, 1998; Ichihara et al., 2009; Mareš et al., 2011; Škaloud et al., 2018). Taxonomy follows the most recent reference for continental species (Škaloud et al., 2018). Although morphological variability of this genus complicates species identification and sometimes require genetic analyses (Bartolo et al., 2022; Steinhagen et al., 2023), the morphological traits of the studied population were clear enough for identifying our specimens as *U. intestinalis*.

Figure 1: General appearance of *Ulva intestinalis*
in a stream flowing from the swimming basin collecting water
from the drilled thermal springs in the villages of Esso,
Kamchatka during May 2017.

RESULTS AND DISCUSSION

Studied plants, their description and habitat

Studied specimens

Kamchatka Krai, Bystrinsky District, settlement of Esso, a stream outflow from the pool receiving water from thermal effluents, 55.924135° N, 158.701082° E, 490 m a.s.l., attached to the stones, at the depth of few cm, mainly in upper water layer, at water temperature of 22-23°C, 29 May 2017, abundant, O. A. Chernyagina (LE).

Description of specimens

The light fresh green wrinkled tubular thalli were harboring air bubbles inside, attached to the stones in clusters, up to 10 cm in length, less than 0.5 cm in width, had more or less uniform width throughout most of the plant, gradually narrowed to the base, unbranched at general appearance, very rarely shortly branched (Figs. 1 and 2). The branches were not filiform. They were always short in comparison with main tube width. No branches of second order and proliferations were found. Cells were placed without any order throughout thallus, and only short irregular lines of cells could be spotted at short branches and in basal parts of plants. Cells were more or less isodiametric to somewhat elongated, up to 2 times longer of width, 9.0-10.7 x (4.8)5.4-8.4 μm. Almost exclusively one pyrenoid per cell was traceable.

The studied specimens were in good agreement to descriptions of this species (see list of references in "Materials and methods"), but did differ with smaller cell size. They were overlapping in this trait expression, but were not identical in all characters with *Enteromorpha intestinalis* f. *saprobia* Vinogr. reported from the Sea of Japan and the Black Sea (Vinogradova, 1974; Moshkova and Hollerbach, 1986).

Habitat and frequency of occurrence

The ice-free stream (Fig. 1) from the large water-cooling swimming pool collecting cooled waters from drilled natural thermal springs called Esso springs after their use for house heating. The plants were found in May 2017 only, and not found at the same site in August 2017, nor during subsequent visual surveys conducted 2-3 times per year in 2018-2024 by O. A. Chernyagina.

Ecology and distribution of *U. intestinalis* in neighboring regions

The closest known inland localities of *U. intestinalis* are from thermokarst lakes in the basin of the Lena River in NE Siberia (Skvortsov, 1917; Kopyrina et al., 2020) similar climate, i.e., cold, without dry season and with very cold winter (Köppen-Geiger classification = Dfd, Peel et al., 2007), and in urban stream in Primorye Territory (Kukharenko, 1989) from cold, with dry winter and warm summer (Dwb; Peel et al., 2007). In southern Siberia, this species was found in hardwater, circumneutral to alkaline, slightly to properly brackish, mesotrophic and eutrophic lakes, ponds, endorheic rivers in steppe and forest-steppe (Tripolitowa, 1928; Pirozhnikov, 1929; Yakubova, 1953; Andreev et al., 1963; Khalfina, 1964; Ermolaeva, 1967; Safonova and Ermolaev, 1983; Safonova and Shishkina, 1986; Sviridenko, 2000; Kipriyanova and Romanov, 2010; Efremov and Sviridenko, 2016; Sviridenko et al., 2016; Tokar, 2018; Romanov, unpubl. data), as well as in rivers with elevated sulphates, brackish endorheic lakes, and in drainage waterbodies of the ash yard of big thermal power in steppe landscapes (Kuklin and Zamana, 2011; Kuklin, 2017; Bazarova and Kuklin, 2021). These sites are sited in areas with two types of climate: mostly cold, without dry season, with warm summer and mostly cold, with dry winter, with cold summer (Dfb and Dwc; Peel et al., 2007). The continental sites of this species are broadly spread across Eurasia, but seem to be concentrated in arid and subarid regions with brackish water bodies (see all references cited above).

Figure 2: Key morphological traits of *Ulva intestinalis* from a stream flowing from the basin collecting water from the drilled thermal springs in Esso village, Kamchatka in May 2017 (LE): a, b – wrinkled tubular thalli with short robust primary branches (arrowhead), c – short robust primary branch, d – cells at primary branch illustrated at c, e – view of tangential irregular cross section at basal part of plant, f – lateral view of basal part of plant with narrow strip of cells having different general appearance, i.e., more narrow, elongated and with degraded chloroplasts, a filament of *Tribonema viride* Pascher (Ochrophyta, Xanthophyceae, Tribonemataceae) is visible at low right corner, g, h – irregular placement of cells with solitary pyrenoids in wide parts of plant, view from above. Scale bars: a, b – 400 μm, c – 200 μm, d-g – 40 μm, h – 20 μm.

It is unclear if *U. intestinalis* can sustain reproduction in study locality. This species could be occasionally colonize the site, in agreement with the *r*-strategy of opportunistic *Ulva* species (Burkholder and Glibert, 2013; Fort et al., 2020). Such species are widely known benefit from excessive anthropogenic nitrogen (Fort et al., 2020), making them useful ecological indicators of eutrophic waters (e.g., Areco et al., 2021; Rybak, 2021). Considering rare and unstable occurrence of *U. intestinalis* in inland Kamchatka, it could be there as a rare aquatic weed unable to maintain a stable population. Aquatic birds, known to transport and disperse a wide spectrum of plants, may be their main dispersal vectors (Lovas-Kiss et al., 2018).

Whereas seacoasts and estuaries are typical habitats for *Ulva* species worldwide (see references in Rybak, 2018; Bartolo et al., 2022), species with tubular thalli (former genus *Enteromorpha*) are also known from inland localities (Bliding, 1963; Moshkova and Hollerbach, 1986; Li and Bi, 1998; Ichihara et al., 2009; Messyasz, 2009; Mareš et al., 2011; iNaturalist, 2024). *Ulva intestinalis* has not been reported from new sites in marine habitats of Kamchatka and neighboring areas after its first records by Ruprecht and Woronichin from southern coasts of this peninsula (Ruprecht, 1850; Woronichin, 1914; Vinogradova, 1974, 1979; Klochkova and Berezovskaya, 1997, 2001; Klochkova et al., 2009a, b; Selivanova and Zhigadlova, 1997a, b, 2009a, b). According to Vinogradova (1979), *U. intestinalis* is not typical for Far East seas. The same can be suggested for continental water bodies of Primorye Territory (Kukharenko, 1989; Medvedeva and Nikulina, 2014). Close marine localities are known from the Okhotsk Sea and the Sea of Japan in Sakhalin Region, Khabarovsk Territory and Primorye Territory (Ruprecht, 1850; Sinova, 1928; Nagai, 1940; as *E. intestinalis* f. *saprobia*; Vinogradova, 1974; Kudrjaschov et al., 1976; Levenets, 2011; Kozhenkova, 2020).

CONCLUSIONS

A population of *Ulva intestinalis* living more than 200 km from the ocean in central Kamchatka, a region with a largely unsuitable climate and water chemistry, seems to be possible in only waters originating from thermal springs and experiencing eutrophication. Sporadic records of this species from Kamchatka suggest it may be unable to maintain stable populations in this region, and experience repeated local extinctions and recolonizations.

ACKNOWLEDGEMENTS

The authors are grateful to James K. Wetterer for English improvement of our manuscript. The research of R. E. Romanov was supported by of the state assignments of the Komarov Botanical Institute of the Russian Academy of Sciences, the project “Flora and taxonomy of algae, lichens and bryophytes in Russia and phytogeographically important regions of the world” (no. 121021600184-6), the research by O. A. Chernyagina was supported by the state assignment of the Kamchatka Pacific Institute of Geography of the Far East Branch of the Russian Academy of Sciences, the project “Terrestrial and marine ecosystems of Kamchatka and north-eastern part of Pacific region: study of biodiversity, development of methodological framework for sustainable use of natural resources” (no. of the state registration 122011400140-4). The research was done using equipment of the core facilities center “Cell and molecular technologies in plant science” at the Komarov Botanical Institute RAS (St. Petersburg, Russia).

REFERENCES

1. Andreev G. P., Goryacheva G. I., Skabitchevsky A. P., Chernyavskaya M. A. and Chistyakov L. D., 1963 – The algae of Irtysh River and its drainage basin, in *The nature of Ob River floodplain and its development*, Tomsk, Tomsk State University Press, 69-103. (in Russian)
2. Areco M. M., Salomone V. N. and Afonso M. S., 2021 – Ulva lactuca: A bioindicator for anthropogenic contamination and its environmental remediation capacity, *Marine Environmental Research*, 171, 105468, DOI: https://doi.org/10.1016/j.marenvres.2021.105468.
3. Barinova, S.S., Tsarenko, P.M., Nevo, E., 2004. Algae of experimental pools on the Dead Sea coast, Israel. *Israel Journal of Plant Science*, 52, 3, 265-275. DOI 10.1560/V889-764E-MCDY-NPDP

   Bartolo A. G., Zammit G. and Küpper F. C., 2022 – Ulva L. biodiversity in the central Mediterranean Sea: cryptic species and new records, *Cryptogamie, Algologie*, 43, 14, 215-225, DOI: https://doi.org/10.5252/cryptogamie-algologie2022v43a14.
4. Bazarova B. B. and Kuklin A. P., 2021 – Dynamics of the vegetation cover of soda lakes in the southeast of Transbaikalia, in *Diversity of soils and biota of Northern and central Asia*. IV All-Russian conference with international participation, 15-18 June 2021, Ulan-Ude, Buryatia Scientific Center of the Siberian Branch of RAS Press, 46-48. (in Russian)
5. Beauger A., Wetzel C., Voldoire O., Allain E., Breton V., Miallier D. and Ector L., 2022 – *Fontina* gen. nov. (Bacillariophyta): a new diatom genus from a thermo-mineral spring of the French Massif Central, *Diatom Research*, 37, 1, 51-61, DOI: https://doi.org/ff10.1080/0269249X.2022.2033327.
6. Bliding C., 1963 – A critical survey of European taxa in Ulvales. Part I. Capsosiphon, Percursaria, Blidingia, Enteromorpha, Opera Botanica, 8, 3, 1-160.
7. Tsegmid B. and Baigal-Amar T., 2018 – The conspectus of algae in Mongolia, Ulaanbaatar, Bembi, 314.
8. Burkholder J. M. and Glibert P. M., 2013 – Eutrophication and oligotrophication, in Levin S. A. (ed.), *Encyclopedia of Biodiversity, 2nd Edition*, Amsterdam, Academic Press, 347-371, DOI: https://doi.org/10.1016/b978-0-12-384719-5.00047-2.
9. Cantonati M., 2022 – Springs – groundwater-borne ecotones – a typology, with an overview on the diversity of photoautotrophs in springs, in Mehner T., Tockner K. (eds.), *Encyclopedia of Inland Waters, 2nd edition, vol. 3*, Amsterdam, Elsevier, 488-509, DOI: https://doi.org/10.1016/B978-0-12-819166-8.00178-X.
10. Cantonati M., Lange-Bertalot H., Scalfi A. and Angeli N., 2010 – Cymbella tridentina sp. nov. (Bacillariophyta), a crenophilous diatom from carbonate springs of the Alps, *Journal of the North American Benthological Society*, 29, 775-788, DOI: https://doi.org/10.1899/09-077.1.
11. Doemel W. and Brock T. D., 1971 – The physiological ecology of Cyanidium caldarium, *Journal of General Microbiology*, 67, 1, 17-32, DOI: https://doi.org/10.1099/00221287-67-1-17.
12. Efremov A. N., 2018 – Records of little-known cattails (Typha L., Typhaceae) in Siberia, *Bulletin of Moscow Society of Naturalists. Biological Series*, 123, 6, 69-70. (in Russian)
13. Efremov A. N. and Sviridenko B. F., 2016 – On distribution of rare hydrophytes in Omsk Region, *Botanicheskii Zhurnal*, 101, 8, 923-927, DOI: https://doi.org/10.1134/S0006813616080044. (in Russian)
14. Elenkin A. A., 1914 – Die Süswasseralgen Kamtschatka's, in *Expedition à Kamtchatka, organisée par Th. P. Riabouchinsky avec le concours de la Société Impériale Russe de Géographie. Section de Botanique. II. Plantes cryptogames de Kamchatka: 1) Algues, 2) Champignons*, Moscou, Maison d'édition Ryabushinsky, 2-402, 579-591. (in Russian)
15. Ermolaeva L. M., 1967 – The phytobenthos of ponds of Bolsherechensky District, *Proceedings of the Kuybyshev Omsk State Medical Institute*, 77, 42-46. (in Russian)

16. Fort A., Mannion C., Fariñas-Franco J. M. and Sulpice R., 2020 – Green tides select for fast expanding Ulva strains, *Science of the Total Environment*, 698, 1, 134337, DOI: https://doi.org/10.1016/j.scitotenv.2019.134337.
17. Glazier D. S., 2009 – Springs, in Likens G. E. (ed.), *Encyclopedia of Inland Waters, vol. 1*, Oxford, Elsevier, 734-755, DOI: https://doi.org/10.1016/B978-012370626-3.00259-3.
18. Gromov B. V., Nikitina V. N. and Mamkayeva K. A., 1991 – Ochromonas vulcania sp. nov. (Chrysophyceae) from the acidic spring on the Kunashir Island (Kurile Islands), *Algologia*, 1, 2, 76-79. (in Russian)
19. Harsha Mohan E., Madhusudan S. and Baskaran R., 2023 – The sea lettuce Ulva sensu lato: Future food with health-promoting bioactives, *Algal Research*, 71, 103069, DOI: https://doi.org/10.1016/j.algal.2023.103069.
20. Hayden H. S., Blomster J., Maggs C. A., Silva P. C., Stanhope M. J. and Waaland J. R., 2003 – Linnaeus was right all along: Ulva and Enteromorpha are not distinct genera, *European Journal of Phycology*, 38, 3, 277-294, DOI: https://doi.org/10.1080/1364253031000136321.
21. Ichihara K., Arai S., Uchimura M., Fay E. J., Ebata H., Hiraoka M. and Shimada S., 2009 – New species of freshwater Ulva, Ulva limnetica (Ulvales, Ulvophyceae) from the Ryukyu Islands, Japan, *Phycological Research*, 57, 2, 94-103, DOI: https://doi.org/10.1111/j.1440-1835.2009.00525.x.
22. iNaturalist, 2024. – *iNaturalist.org*, available online: http://www.inaturalist.org, accessed on 20 January 2024.
23. Khalfina N. A., 1964 – Towards hydrobiology of forest-steppe water bodies of West Siberia, *Izvesitya SO AN SSSR, Seriya Biologo-meditsinskikh Nauk*, 4, 1, 41-48. (in Russian)
24. Kipriyanova L. M. and Romanov R. E., 2010 – Communities of macroalgae, in Ravkin Yu. S. (ed.-in-chief), *The biodiversity of Karasuk-Burla area (West Siberia)*, Novosibirsk, SB RAS Press, 81-84. (in Russian)
25. Kiryukhin A. V., Kiryukhin V. A. and Manukhin Yu. F., 2010 – The hydrogeology of volcanogens, Saint Petersburg, Nauka, 395. (in Russian)
26. Klochkova N. G. and Berezovskaya V. A., 1997 – The algae of Kamchatka shelf. Distribution, biology, chamical composition. Vladivostok, Petropavlovsk-Kamchatskiy, Dalnauka, 155. (in Russian)
27. Klochkova N. G. and Berezovskaya V. A., 2001 – The macrophytobenthos of the Avacha Bay and its anthropogenic destruction, Vladivostok, Dalnauka, 208. (in Russian)
28. Klochkova N. G., Korolyova T. N. and Kusidi A. E., 2009a – Marine algae of Kamchatka and surrounding areas, vol. 1, Petropavlovsk-Kamchatskiy, KamchatNIRO, 217. (in Russian)
29. Klochkova N. G., Koroleva T. A. and Kusidi A. E., 2009b – Species composition and peculiarities of vegetation on the algae-macrophytes at the coasts of Starichkov Island, in *Biota of Starichkov Island and adjacent waters of Avacha Gulf* / *Proceedings of the Kamchatka Branch of the Pacific Institute of Geography, Far Eastern Division, Russian Academy of Sciences*, 8, 67-198. (in Russian)
30. Kondratyuk V. I., 1974 – The climate of Kamchatka, Moscow, Gidrometeoizdat, 204. (in Russian)
31. Kopyrina L., Pshennikova E. and Barinova S., 2020 – Diversity and ecological characteristic of algae and cyanobacteria of thermokarst lakes in Yakutia (northeastern Russia), *Oceanological and Hydrobiological Studies*, 49, 2, 99-122, DOI: https://doi.org/10.1515/ohs-2020-0010.
32. Kozhenkova S. I., 2020 – Checklist of marine benthic algae from the Russian continental coast of the Sea of Japan, *Phytotaxa*, 437, 4, 177-205, DOI: https://doi.org/10.11646/phytotaxa.437.4.1.
33. Kudrjaschov V. A., Tarakanova T. F. and Ivanova M. B., 1976 – On the fauna and the flora of the intertidal zone of the Shantar Islands. Coastal communities of the Far Eastern seas, *Transactions of the Institute of Marine Biology of the Far East Science Center of the Academy of Sciences of the USSR*, 6, 22-63. (in Russian)

34. Kukharenko L. A., 1989 – The algae of freshwater water bodies of Primorye Territory, Vladivostok, FEB AS USSR, 152. (in Russian)
35. Kuklin A. P., 2017 – Geochemical conditions of the landscape as a factor of formation of the species of macroscopic algae in small rivers of the Baikal and Amur basins, *Issues of modern algology*, 1, 13, 1-9. (in Russian)
36. Kuklin A. P. and Zamana L. V., 2011 – Macroalgae – indicators of river drainage of urban territories (by the example of a district of Chita), in *Evolution of biogeochemical systems (factors, processes, patterns) and problems of ecosystems exploitation. Geo-ecological, economic and social problems of ecosystem exploitation*, Chita, ZabSHPU, 106-108. (in Russian)
37. Langangen A., 2000 – Charophytes from the warm springs of Svalbard, *Polar Research*, 19, 2, 143-153, DOI: https://doi.org/10.3402/polar.v19i2.6541.
38. Langangen A., Ballot A., Nowak P. and Schneider S. C., 2020 – Charophytes in warm springs on Svalbard (Spitsbergen): DNA barcoding identifies Chara aspera and Chara canescens with unusual morphological traits, *Botany Letters*, 167, 2, 179-186, DOI:. https://doi.org/10.1080/23818107.2019.1672104.
39. Levenets I. R., 2011 – Macroalgae of fouling communities in shallow waters of southern Primorye, Vladivostok, Dalnauka, 188. (in Russian)
40. Li S. and Bi L. (eds.), 1998 – Flora algarum sinicarum aquae dulcis. Vol. 5. Ulothricales, Ulvales, Chaetophorales, Trentepohliales, Sphaeropleales, Beijing, Science Press, 136. (in Chinese)
41. Litvinenko Y. S. and Zakharikhina L. V., 2020 – Hydrochemical zoning of the river network of Kamchatka, *Water Resources*, 47, 2, 269-281, DOI: https://doi.org/10.1134/S0097807820020098.
42. Lovas-Kiss A., Sánchez M. I., Wilkinson D. M., Coughlan N. E., Alves J. A. and Green A. J., 2018 – Shorebirds as important vectors for plant dispersal in Europe, *Ecography*, 42, 5, 956-967, DOI: https://doi.org/10.1111/ecog.04065.
43. Mareš J., Leskinen E., Sitkowska M., Skácelová O. and Blomster J., 2011 – True identity of the European freshwater Ulva (Chlorophyta, Ulvophyceae) revealed by a combined molecular and morphological approach, *Journal of Phycology*, 47, 1177-1192, DOI: https://doi.org/10.1111/j.1529-8817.2011.01048.x.
44. Maulood B. K., Hassan F. M., Al-Lami A. A., Toma J. J. and Ismail A. M., 2013 – Checklist of algal flora in Iraq, Baghdad, Ministry of Environment, 94.
45. Medvedeva L. A. and Nikulina T. V., 2014 – Catalogue of freshwater algae of the southern part of the Russian Far East, Vladivostok, Dalnauka, 271. (in Russian).
46. Messyasz B., 2009 – Enteromorpha (Chlorophyta) populations in the Nielba River and Lake Laskownickie, *Oceanological and Hydrobiological Studies*, 38, suppl., 1-9.
47. Messyasz B. and Rybak A., 2010 – Abiotic factors affecting the development of Ulva sp. (Ulvophyceae; Chlorophyta) in freshwater ecosystems, *Aquatic Ecology*, 45, 75-87, DOI: https://doi.org/10.1007/s10452-010-9333-9.
48. Mohebbi F. and Zarezadeh S., 2023 – A review of Ulva intestinalis, the only macroscopic alga of Urmia Lake, *Iranian Journal of Botany*, 29, 1, 83-88, DOI: https://doi.org/10.22092/IJB.2023.361068.
49. Moshkova N. A. and Hollerbach M. M., 1986 – The identification manual of freshwater algae of the USSR. Iss. 10. Chlorophyta: Ulotrichophyceae, Ulotrichales, Leningrad, Nauka, 360. (in Russian)
50. Muradov S. V., Kirichenko S. V. and Rogatykh S. V., 2013 – The thermomineral springs and therapeutic muds of Kamchatka Territory, Petropavlovsk-Kamchatskiy, RIOiP KKT, 238. (in Russian)
51. Muzafarov A. M., 1965 – The flora of algae of water bodies of Middle Asia, Tashkent, Nauka, 568. (in Russian)

52. Nagai M., 1940 – Marine algae of the Kurile Islands, I, *Journal of the Faculty of Agriculture, Hokkaido Imperial University*, 46, 1-137.
53. Nahucrishvili I. G. (ed.), 1986 – Flora of Cryptogamous Plants of Georgia: Conspectus, Tbilisi, Meznierba, 885. (in Russian)
54. Nikitina V. N., 2005 – The blue-green algae (cyanobacteria) of natural thermal biotopes, Saint Petersburg, Saint Petersburg University Press, 110. (in Russian)
55. Peel M. C., Finlayson B. L. and McMahon T. A., 2007 – Updated world map of the Köppen-Geiger climate classification, *Hydrology and Earth System Sciences*, 11, 5, 1633-1644, DOI: https://doi.org/10.5194/hess-11-1633-2007.
56. Pirozhnikov P. L., 1929 – Towards knowledge of Lake Sartlan in limnological, hydrobiological and fishery sides, *Proceedings of the Siberian Scientific Fishery Station*, 4, 2, 3-116. (In Russ.).
57. Romanov R. E. and Chernyagina O. A., 2018 – Chara braunii, in *Red Data Book of Kamchatka Territory. Vol. 2. Plants*, Petropavlovsk-Kamchatsky, Kamchatpress, 274. (in Russian)
58. Romanov R. E., Patova E. N, Teteryuk B. Yu. and Chemeris E. V., 2018 – Charophytes (Charales, Charophyceae) on the north-eastern edge of Europe: is it something different across Northern Europe in their diversity and biogeography, *Nova Hedwigia, Beihefte*, 147, 161-181, DOI: https://doi.org/10.1127/nova-suppl/2018/016
59. Romanov R. E. and Vishnyakov V. S., 2023 – Chara globata Mig., in *Red Data Book of Republic of Buryatia: Plants and fungi. 4th edition, updated*, Belgorod, Konstanta, 91. (in Russian)
60. Ruprecht F. J., 1850. – Algae ochotenses. Die ersten sicheren Nachrichten über die Tange des Ochotskischen Meeres, St. Petersburg, Buchdruckerei der Kaiserlichen Akademie der Wissenschaften, 243. (in German)
61. Rybak A. S., 2015 – Revision of herbarium specimens of freshwater Enteromorpha-like Ulva (Ulvaceae, Chlorophyta) collected from Central Europe during the years 1849–1959, *Phytotaxa*, 218, 1, 1-29, DOI: https://doi.org/10.11646/phytotaxa.218.1.1.
62. Rybak A. S., 2018 – Species of Ulva (Ulvophyceae, Chlorophyta) as indicators of salinity, *Ecological Indicators*, 85, 253-261, DOI: https://doi.org/10.1016/j.ecolind.2017.10.061.
63. Rybak A. S., 2021 – Freshwater macroalga, Ulva pilifera (Ulvaceae, Chlorophyta) as an indicator of the trophic state of waters for small water bodies, *Ecological Indicators*, 121, 106951, DOI: https://doi.org/10.1016/j.ecolind.2020.106951.
64. Saber A. A., Mareš J., Guella G., Anesi A., Štenclová L. and Cantonati M., 2018 – Polyphasic approach to a characteristic Ulva population from a limno–rheocrenic, mineral (chloride, sodium, sulphate) spring in the Siwa Oasis (Western Desert of Egypt), *Fottea*, 18, 227-242, DOI: https://doi.org/10.5507/FOT.2018.008.
65. Safonova T. A. and Ermolaev V. I., 1983 – The algae of water bodies of Lake Chany complex, Novosibirsk, 153. (In Russ.).
66. Safonova T. A. and Shishkina L. N., 1986 – The algae of rivers Kargat and Chulym, in *New about flora of Siberia*, Novosibirsk, 31-41. (in Russian)
67. Sametova E. S., Nurashov S. B. and Jiyenbekov A. K., 2019 – Algoflora of the rivers of desert low mountains of the southeast of Kazakhstan, *Problems of botany of South Siberia and Mongolia*, 18, 1, 390-392, DOI: https://doi.org/10.14258/pbssm.2019079. (in Russian)
68. Selivanova O. N. and Zhigadlova G. G., 1997a – Macrophytes of the Commander Islands, in *Benthic flora and fauna of the shelf zone of the Commander Islands*, Vladivostok, Dalnauka, 11-58. (in Russian)
69. Selivanova O. N. and Zhigadlova G. G., 1997b – Marine algae of the Commander Islands, preliminary remarks on the revision of the flora. I. Chlorophyta, *Botanica Marina*, 40, 1-8, DOI: https://doi.org/10.1515/botm.1997.40.1-6.1.
70. Selivanova O. N. and Zhigadlova G. G., 2009a – Marine algae-macrophytes of the coastal waters of Starichkov Island, in *Biota of Starichkov Island and adjacent waters of Avacha Gulf: proceedings of Kamchatka Branch of Pacific Institute of Geography, Far Eastern Division, Russian Academy of Sciences*, 8, 25-57. (in Russian)

71. Selivanova O. N. and Zhigadlova G. G., 2009b – Marine benthic algae of the South Kamchatka state wildlife sanctuary (Kamchatka, Russia), *Botanica Marina*, 52, 4, 317-329, DOI: https://doi.org/10.1515/BOT.2009.003.
72. Sinova E. S., 1928 – Algae maris japonensis. Chlorophyceae, *Bulletins of Pacific Ocean Scientific Fishery Research Station*, 2, 2, 1-62. (in Russian)
73. Skvortsov B., 1917 – Contributions à la flore des algues de la Russie d'Asie, *Journal de la Société Botanique de Russie*, 2, 10-20. (in Russian)
74. Škaloud P., Rindi F., Boedeker C. and Leliaert F., 2018 – Freshwater flora of Central Europe, Vol 13: Chlorophyta: Ulvophyceae (Süßwasserflora von Mitteleuropa, Bd. 13: Chlorophyta: Ulvophyceae), Berlin, Springer Spektrum, 288, DOI: https://doi.org/10.1007/978-3-662-55495-1.
75. Steinhagen S., Hoffmann S., Pavia H. and Toth G. B., 2023 – Molecular identification of the ubiquitous green algae Ulva reveals high biodiversity, crypticity, and invasive species in the Atlantic-Baltic Sea region, *Algal Research*, 73, 103132, DOI: https://doi.org/10.1016/j.algal.2023.103132.
76. Sviridenko B. F., 2000 – Flora and vegetation of water bodies of Northern Kazakhstan, Omsk, Omsk State Pedagogical University, 196. (in Russian)
77. Sviridenko B. F., Murashko Yu. A., Sviridenko T. V. and Efremov A. N., 2016 – Tolerance of hydromacrophytes to active reaction, mineralization and water hardness in natural and man-maid water bodies of the West Siberian Plain, *Bulletin of Nizhnevartovsk State University*, 2, 8-17. (in Russian)
78. Tekebaeva Zh. B., Kanaev D. B. and Zhamangara A., 2014 – Towards study of species composition and ecology of phytoplankton of Shchuchinsk-Borovoe zone, in *Proceedings of the IX International Scientific Conference for students and young scholars «Science and education – 2014»*, Astana, 350-358. (in Russian)
79. Tokar O. E., 2018 – Hydromacrophytes composition in water reservoirs of the north-eastern part of the Kurgan Region, *Samara Journal of Science*, 7, 2, 120-125. (in Russian)
80. Tripolitowa T. K., 1928 – Beiträge zûr Flora der Sporen-Pflanzen des Altais und des Guvernements Tomsk. II. Algen, *Transactions of Tomsk State University*, 79, 4, 271-325. (in German)
81. Vinogradova K. L., 1974 – Ulvacean algae (Chlorophyta) of seas of the USSR, Leningrad, Nauka, 166. (in Russian)
82. Vinogradova K. L., 1979 – The identification manual for algae of Far East seas of the USSR. Green algae, Leningrad, Nauka, 147. (in Russian)
83. Woronichin N. N., 1914 – Die Meeresalgen Kamtschatka's, in *Expedition à Kamtchatka, organisée par Th. P. Riabouchinsky avec le concours de la Société Impériale Russe de Géographie. Section de Botanique. II. Plantes cryptogames de Kamchatka: 1) Algues, 2) Champignons*, Moscou, Maison d'édition Ryabushinsky, 475-524, 592-593. (in Russian)
84. Yakubova A. I., 1953 – The vegetation of the Lake Sartlan and its changes in connection with water level oscillations, *Trudy Tomskogo Gosudarstvennogo Universiteta, 125, Seriya biologicheskaya*, 223-248. (in Russian)
85. Yatsenko-Stepanova T. N. and Ignatenko M. E., 2018 – About some results of the research of the algal flora of the specially protected area "Tuzlukkolsky Muds" (Orenburg Region, Belyaevsky District), *Bulletin of the Orenburg Scientific Center, Ural branch, Russian Academy of Sciences*, 4, 1-17, DOI: https://doi.org/10.24411/2304-9081-2019-14003. (in Russian)
86. Zhakova L. V., 2006 – Check-list for Caspian Sea macroalgae, in *Caspian Biodiversity Project under umbrella of Caspian Sea Environment Program*, https://www.zin.ru/projects/caspdiv/caspian_macroalgae.html

87. Zhakova L. V., 2013 – Effect of long-term changes of the salinity on the water flora composition and distribution of macrophytes in the Aral, *Proceedings of the Zoological Institute of the Russian Academy of Sciences*, 317, suppl. 3, 113-119. (in Russian)
88. Zhang Y., He P., Li H., Li G., Liu J., Jiao F., Zhang J., Huo Y., Shi X., Su R., Ye N., Liu D., Yu R., Wang Z., Zhou M. and Jiao N., 2019 – Ulva prolifera green-tide outbreaks and their environmental impact in the Yellow Sea, China, *National Science Review*, 6, 4, 825-838, DOI: https://doi.org/10.1093/nsr/nwz026.
89. Zinchenko T. D., Golovatyuk L. V., Gorokhova O. G., Abrosimova E. V., Umanskaya M. V., Popchenko T. V., Shitikov V. K., Gusakov V. I., Bolotov S. E., Lazareva V. I., Selivanova E. A., Balkin A. S. and Plotnikov A. O. 2021 – Functional features of the structural organization of plankton and bottom communities in highly mineralized rivers of the hyperhaline Lake Elton Basin (Russia), *Ecosystems: Ecology and Dynamics*, 5, 1, 5-72, DOI: https://doi.org/10.24411/2542-2006-2021-10077. (in Russian)

LANDSCAPE FRAGMENTATION AND DEFORESTATION IN SIERRA LEONE, WEST AFRICA, ANALYSED USING SATELLITE IMAGES

Polina LEMENKOVA *, **

* Paris Lodron University of Salzburg (PLUS), Faculty of Digital and Analytical Sciences, Department of Geoinformatics, Schillerstraße 30, Salzburg, Austria, A-5020, polina.lemenkova@plus.ac.at
** Alma Mater Studiorum – University of Bologna, Department of Biological, Geological and Environmental Sciences, Via Irnerio 42, Bologna, Emilia-Romagna, Italia, IT-40126, polina.lemenkova2@unibo.it, ORCID- 0000-0002-5759-1089.

DOI: 10.2478/trser-2024-0002

KEYWORDS: West Africa, Sierra Leone, coastal landscapes, remote sensing, satellite image analysis, forests, mapping, GRASS GIS.

ABSTRACT

Monitoring rainforests in West Africa is necessary for natural resource management. Remote sensing is valuable for mapping tropical ecosystems and evaluation of landscape heterogeneity. This study presents landscape analysis in Sierra Leone which affects wildlife habitats and biodiversity. Methods include modules "r.mapcalc", "r.li.mps", "r.li.edgedensity", and "r.forestfrag" of GRASS GIS for satellite image processing by computation of mean patch size, edge density index and landscape fragmentation with six levels: exterior, patch, transitional, edge, perforated, and interior. The results demonstrate increased deforestation and landscape fragmentation in Sierra Leone over a 10-year period (2013 to 2023).

RÉSUMÉ: Fragmentation du paysage et déforestation en Sierra Leone, Afrique de l'Ouest, analysées à l'aide d'images satellite.

Le suivi des forêts tropicales en Afrique de l'Ouest est nécessaire à la gestion des ressources naturelles. La télédétection est précieuse pour cartographier les écosystèmes tropicaux et évaluer l'hétérogénéité des paysages. Cette étude présente une analyse du paysage en Sierra Leone qui affecte les habitats fauniques et la biodiversité. Les méthodes incluent les modules "r.mapcalc", "r.li.mps", "r.li.edgedensity" et "r.forestfrag" de GRASS GIS pour le traitement d'images satellite par calcul de la taille moyenne des parcelles, de l'indice de densité des bordures et de la fragmentation du paysage avec six niveaux: extérieur, point, transitionnel, bordure, perforé et intérieur. Les résultats démontrent une déforestation accrue et une fragmentation du paysage en Sierra Leone sur une période de 10 ans (2013 à 2023).

REZUMAT: Fragmentarea peisajului și defrișările din Sierra Leone, Africa de Vest, analizate folosind imagini din satelit.

Monitorizarea pădurilor tropicale din Africa de Vest este necesară pentru gestionarea resurselor naturale. Teledetecția este valoroasă pentru cartografierea ecosistemelor tropicale și evaluarea eterogenității peisajului. Acest studiu prezintă analiza peisajului din Sierra Leone, care afectează habitatele faunei sălbatice și biodiversitatea. Metodele includ modulele „r.mapcalc", „r.li.mps", „r.li.edgedensity" și „r.forestfrag" ale GRASS GIS pentru procesarea imaginilor satelitare prin calcularea dimensiunii medii a patch-ului, indicele de densitate a marginilor și fragmentarea peisajului cu șase niveluri: exterior, petic, tranzițional, margine, perforat și interior. Rezultatele demonstrează creșterea defrișărilor și fragmentării peisajului în Sierra Leone într-o perioadă de 10 ani (2013-2023).

INTRODUCTION

The crucial role of remote sensing data for landscape analysis and environmental assessment, both in a technical and scientific sense, has major implications for the way in which they can be analysed and used. In fact, information that can be retrieved from the satellite images is useful for ecological mapping in two different ways: detecting spatial heterogeneity of landscapes of land cover types (Lemenkova and Debeir 2023a; Fimbel, 1994;) and monitoring temporal changes that take place over a certain period of time (García-Álvarez et al., 2022; Tarawally et al., 2021). Combining both approaches enables to detect a spatial-temporal dynamics (Mustafa et al., 2021). While evaluating temporal changes in landscapes can be performed using comparative analysis of satellite images as a time series analysis for analysis of deforestation or landscape fragmentation (Lemenkova and Debeir, 2023b; Wilson et al., 2022; Haas et al., 2009), detecting spatial mosaic of landscape patterns is implemented by analysis of vegetation (Lemenkova and Debeir, 2023c; Nyerges and Green, 2000; Reid, 2016).

The use of remote sensing data is especially valuable for tracking environmental changes in Sierra Leone (Fig. 1). A small-sized coastal country of West Africa, it has a unique reserve of tropical rainforests and at the same time, notable level of deforestation (Nyerges, 1994). High pressure from human activities and development of infrastructure (Akiwumi and Butler, 2008) aggravated by civil unrest (Kaplan et al., 2022) resulted in recent land cover changes and deforestation in Sierra Leone with a general trend of declining areas of natural vegetation and expanding urban areas (Brandt et al., 2018). Environmental problems of Sierra Leone are diverse and in general, triggered by recent trends of climate change in West Africa which include increase in temperatures, decrease of precipitation and droughts (Bangura et al., 2013). The consequences of climate effects on the landscapes of Sierra Leona include flooding of wetlands and alluvial lowlands, deforestation, decrease of mangroves, and retreat of natural types of vegetation replaced by croplands.

Wetlands of the Sierra Leone area are a precious hotspot of biodiversity and habitats for species adapted to temporarily flooded ecosystems such as rare birds and endemic species (Field, 1968). Nevertheless, wetland areas in Sierra Leone are recently reported to be a subject of substantial (51%) decrease (Lahai et al., 2022). Moreover, Duncan et al. (2018) recently reported the processes of sea level rise that affect the distribution of mangrove forests in Sierra Leone. This raises questions of conservation of these precious ecosystems in coastal and riparian areas of Sierra Leone. Besides natural value, mangrove ecosystems of Sierra Leone are invaluable agro-ecological entries since rice yields are higher in temporarily flooded areas, swamps, coastal and riparian wetlands due to suitability of soil properties (Baggie et al. 2018).

Cultivating rice in wetlands of Sierra Leone has a rich history. Wetlands create favourable climate conditions, distribution of lowlands and repetitively flooded areas that create perfect conditions for rice plantations. As a result, rice is the major staple food in households of Sierra Leone. At the same time, climate and environmental issues resulted in reported problems with rice cultivations such as rice disease and crop losses (Fomba and Singh, 1990; Fomba, 1984). This may have consequences for food availability and sustainable development, thereby illustrating the link between the environmental and social issues.

Climate factors are aggravated by the increased anthropogenic pressure that includes urbanization, restructuring of landscapes, agricultural activities, increase of artificial areas and cropland fields and development of industrial facilities in Sierra Leone (Tarawally et al., 2019). Thus, West African landscapes are particularly vulnerable for social pressure and experience consequences of overuse of natural resources.

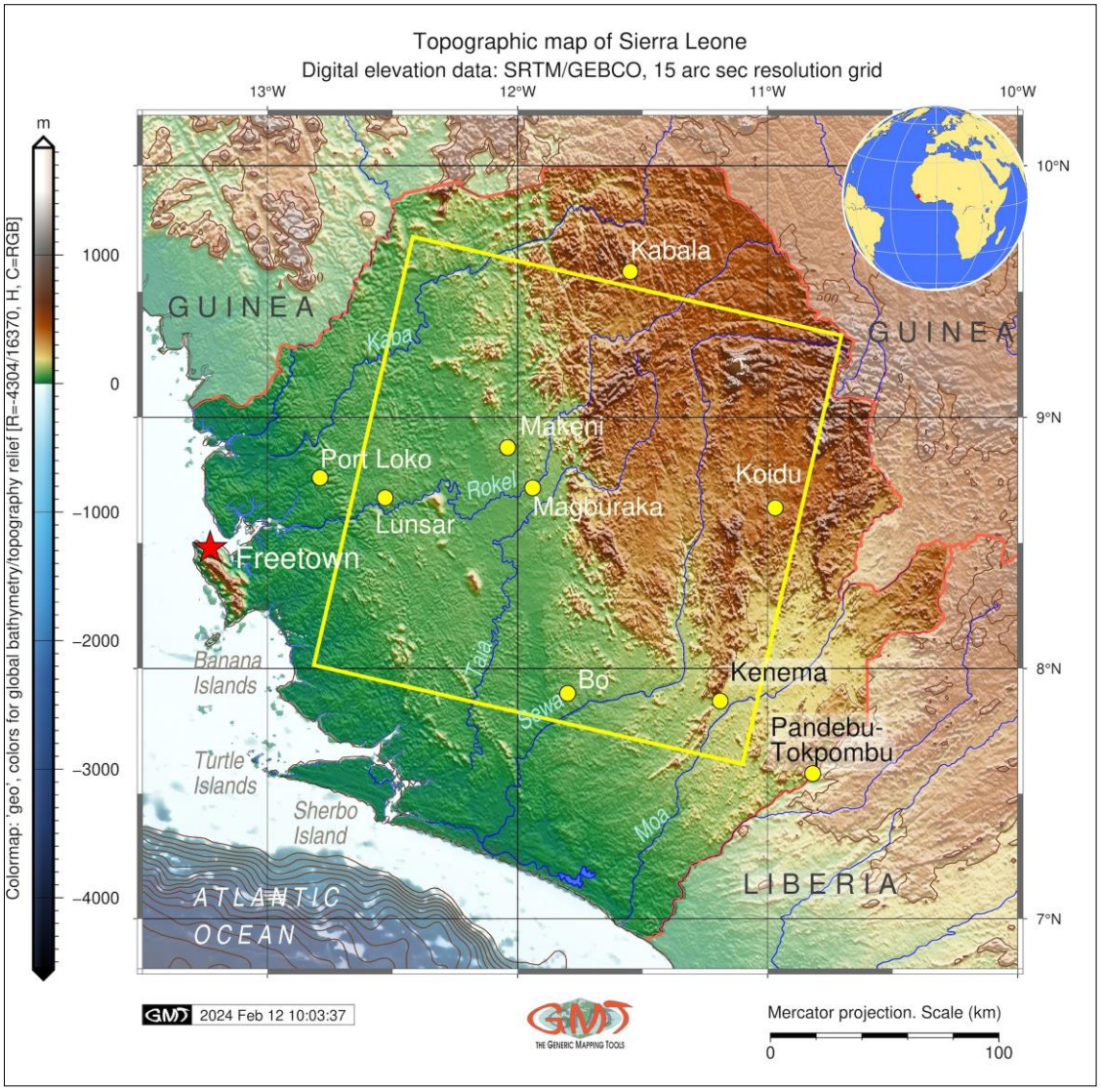

Figure 1: Topographic map of Sierra Leone showing the extent of study area (rotated yellow square). Data source: GEBCO. Software: GMT scripting toolset.

Recently, rainforests of the Sierra Leone area have been reported to be decreasing. For instance, the highest rates of rapid forest degradation associated with urbanization are detected since 2005 (Jin et al., 2020). Besides natural process of the increase in population that necessarily requires more land areas to be used for food production and agricultural activities (Herrmann et al., 2020), there are restructuring process that involves developing of infrastructure, business as well as increase of land areas intended for use in industrial purposes. In this regard, Gornitz (1985) raises questions of cumulative effects from anthropogenic and climate factors on vegetation changes in West Africa. At the same time, reorganisation of land and environmental changes may cause social consequences. Thus, Yengoh and Armah (2016) reported continuing process of restructuring of land use system in Sierra Leone which in turn has led to the restructured access to the suitable for agriculture areas.

Besides wetlands, other land cover types in Sierra Leone include complex mosaic of tropical rainforests, rainfed and aquatic croplands, flooded and irrigated vegetation along the coasts, broadleaved deciduous forests and woodlands, cultivated areas, grasslands and shrubland, evergreen and deciduous trees with different level of fragmentation (open/closed forests). The complex distribution of the landscape types and landscape patterns in Sierra Leone are shown in figure 2.

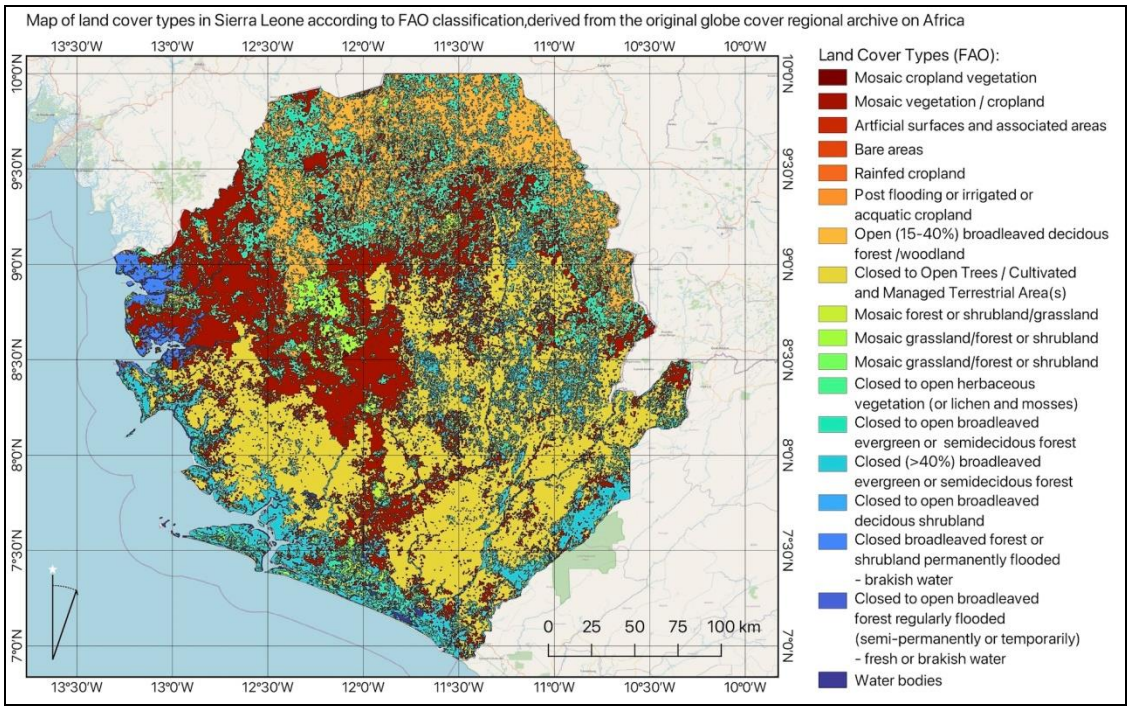

Figure 2: Land cover types and habitats in Sierra Leone. Data source: vector layers obtained from Food and Agriculture Organization (FAO) data repository.

A viewpoint commonly shared among the GIS community is that the advanced methods and operational tools for spatial data management significantly expand the dissemination of the proper techniques to the practice of cartographic data processing and empirical analysis in environmental studies. As argued at length in previous studies (Lemenkova, 2022b), the process of mapping becomes more efficient when using scripts because programming codes automate repetitive workflow, iterative steps and functions (Lemenkova and Debeir, 2022b). Consequently, specialized techniques of GRASS GIS that use modules enable to facilitate and advance landscape analysis. With a few exceptions, current mapping approaches in Sierra Leone lack such applications and mostly include the use of traditional GIS software that operates with user interface (Bah and Tsiko, 2011). In this study, we proposed using scripting approach of GRASS GIS to processing remote sensing data with aim to detect changes in forest areas of coastal Sierra Leone and analyse landscape fragmentation. Technical basis for the cartographic implementation of this research is the use of several modules of GRASS GIS involved in spatial analysis of satellite images.

MATERIAL AND METHODS

The data include two satellite images, Landsat 8-9 OLI/TIRS taken on 24.12.2013 and 27.02.2023 and covering Sierra Leone. The data originally produced by the USGS were obtained from the EarthExplorer website (Fig. 3). The Landsat images were selected as a data source since remote sensing provides a valuable source of information which can be retrieved using image processing methods as reported in numerous environmental studies (Lemenkova P. and Debeir O. 2022a; Lemenkova, 2020a; Heiskanen et al., 2019; Hillson et al., 2019).

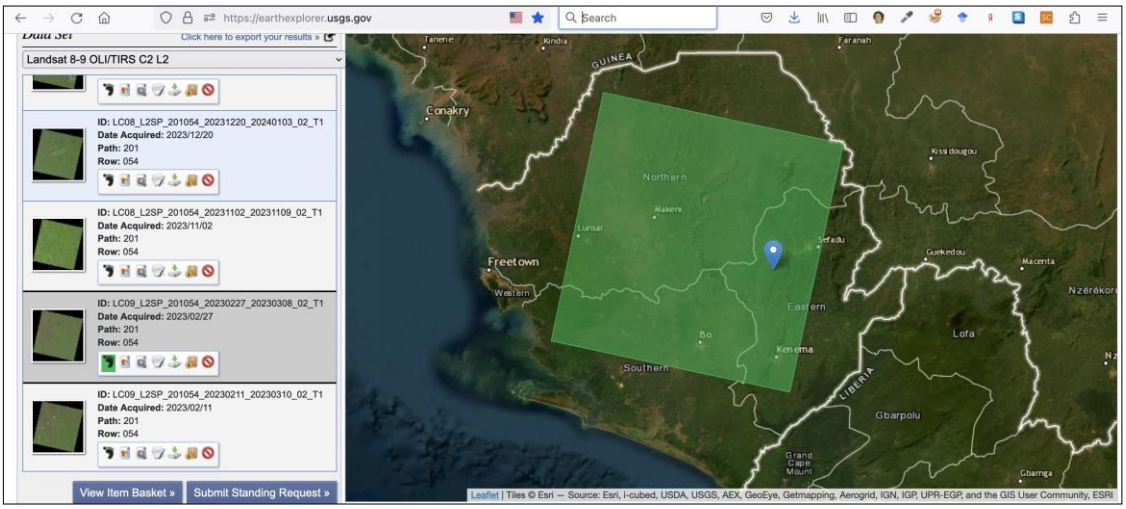

Figure 3: Data collection: satellite images Landsat 8-9 OLI/TIRS covering Sierra Leone obtained from the USGS EarthExplorer repository.

The original unprocessed satellite images are demonstrated in figure 4 where the scenes are represented in RGB in natural colours. The landscape analysis was performed using Geographic Resources Analysis Support System (GRASS) Geographic Information System (GIS) software (Neteler and Mitasova, 2008; Neteler et al., 2008). The effectiveness and powerful functionality of the open source GRASS GIS has been explained with demonstrated maps created using scripts (Lemenkova, 2022a, 2020b). Therefore, it has been selected as a main cartographic software for processing raster images. The topographic map in figure 1 was created using Generic Mapping Tools (GMT) software (Wessel et al., 2019) with applied existing methodology of scripts (Lemenkova, 2021a,b).

The forest fragmentation process was performed from the GRASS GIS console using codes organized in scripts as consecutive process that employs several GRASS GIS modules.

The first stage involves the classification of the two images and then reclassifying clusters into land cover types (Figs. 5 and 6). First, the computational region was set to match the scene using the following command: “g.region raster=L_2013_01 -p”. Then, the group of bands was created for each of the images to include all the multispectral scenes as follows: “i.group group=L_2013 subgroup=res_30m input=L_2013_01,<...>,L_2013_07”. Afterwards, clustering was done using “i.cluster” module which generates signature file and reports results using k-means: “i.cluster group = L_2013 subgroup=res_30m signaturefile=cluster_L_2013 classes=10 reportfile=rep_clust_L_2013.txt”. Finally, the classification is performed using “i.maxlik” module for both images as follows: “i.maxlik group=L_2013 subgroup=res_30m signaturefile=cluster_L_2013 output=L_2013_Cl reject=L_2013_Cl_reject”.

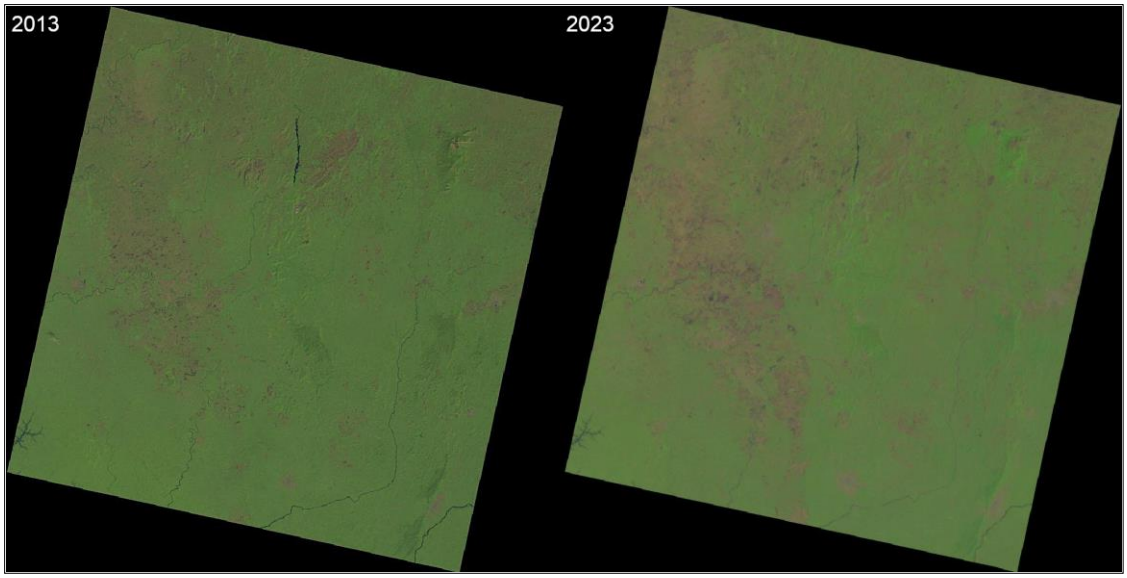

Figure 4: Satellite images Landsat 8-9 OLI/TIRS covering Sierra Leone in natural colors as raw data with a 10-year time gap. (a): 24 December 2013; (b): 27 February 2023.

Then, the categories of the raster file were checked to explore the range of values contained in the original map layer. This was done using the commands "r.category L_2013_cluster_classes" for a quick reference and "r.describe L_2013_cluster_classes" for a more detailed description of the file content and its categories. The rasters contained classes from Class 1 to Class 10, undetermined. Therefore, the classified images were examined and the classes assigned using the following code: "echo" 1 = 1 water 2 = 2 agriculture 3 = 3 shrubland 4 = 4 savannah 5 = 5 herbaceous 6 = 6 forest 7 = 7 grassland 8 = 8 bare soil 9 = 9 cropland 10 = 10 urban "> landuserecl.txt". Hence, the file with descriptors "landuserecl.txt" was then used for reclassification and renaming the categories. The category "forest" was then used in the next step for computing fragmentation of forest areas and assessment of deforestation from 2013 to 2023. The reclassified maps are shown in figures 5 and 6.

The reclassification was performed by "r.reclass" module of GRASS GIS using the following code: r.reclass input=L_2013_cluster_classes output=SL_LCC_2013 rules=landuserecl.txt title="LCC 2013". The areas of forests were selected on both of the maps using map algebra and logical queries which selected target class from all the categories as follows: "r.mapcalc" "orests2013 = if(L_2013_cluster_classes == 6, 1, null())" "--overwrite". The resulting maps showing only the areas of forests are shown in figure 7.

Afterwards, the landscape analysis was performed using r.li series of GRASS GIS modules. First, the definition were created using g.gui.rlisetup. Then, mean patch size (MPS) was computed using the following code which applied "r.li.mps" module: "r.li.mps input=forests conf=movwindow7 out=forests_mps_mov7". Uplon execution, the data were checked using the "r.univar" module as follows: "r.univar forests_richness_mov7". The maps of MPS are visualised in this research in figure 8 for comparative analysis of 2013 and 2023.

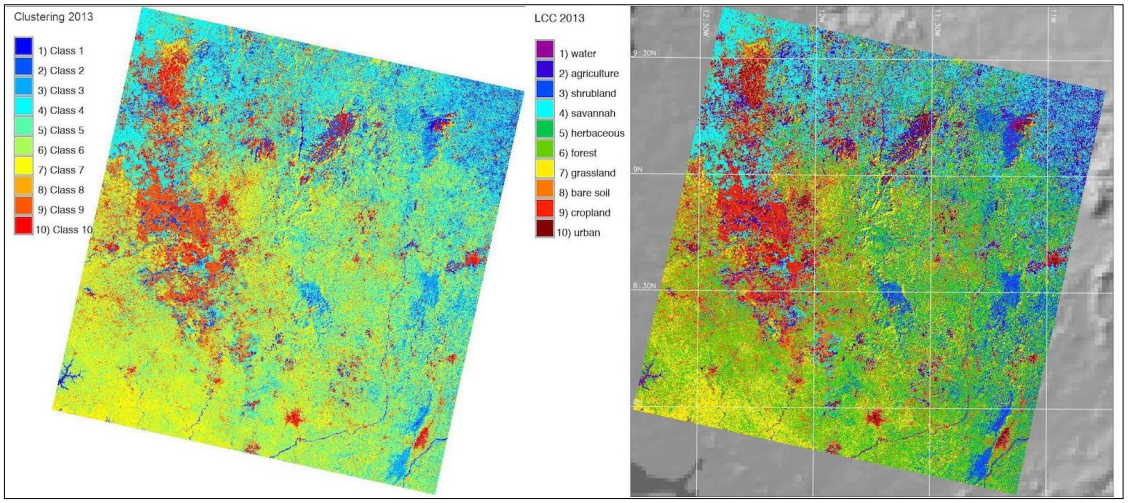

Figure 5: (a) Classification the Landsat 8-9 OLI/TIRS on 24.12.2013 of the coastal regions of Sierra Leone using clustering method. (b) Reclassified image Landsat 8-9 OLI/TIRS on 24.12.2013 with indicated 10 land cover types.

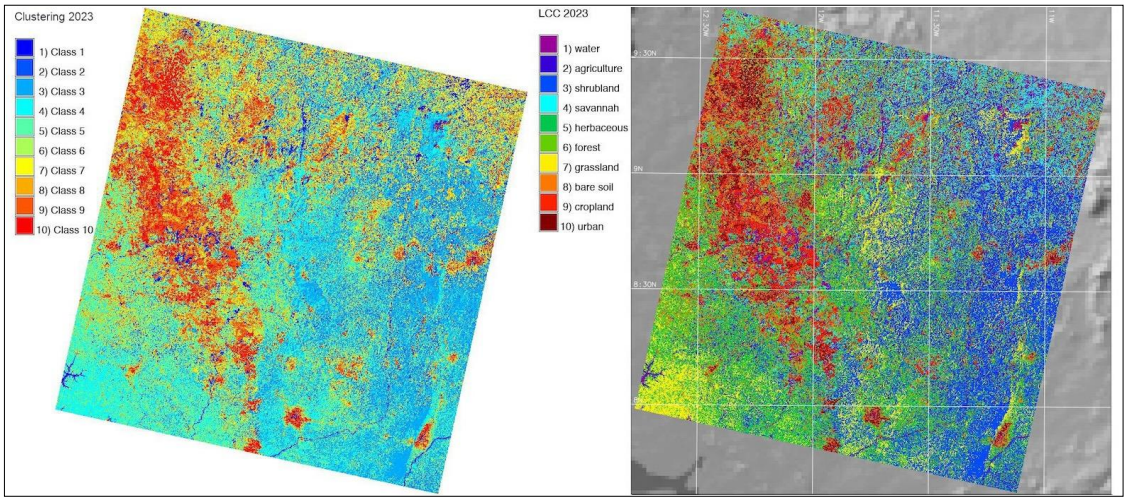

Figure 6: (a) Classification the Landsat 8-9 OLI/TIRS on 27.02.2023 of the coastal regions of Sierra Leone using clustering method. (b) Reclassified image Landsat 8-9 OLI/TIRS on 27.02.2023 with indicated 10 land cover types.

The edge density was computed using "r.li.edgedensity" module using the code: "r.li.edgedensity input=forests2013_SL conf=movwindow7 out=forests_ED_mov7_SL_2013". Afterwards, the data were inspected using modules r.univar, r.category and r.describe and plotted in figure 9 where the results are shown for 2013 and 2023. Forest fragmentaion has been calculated using "r.forestfrag" module of the GRASS GIS by using the following code: "r.forestfrag input=forests2013_new output=fragment_2013 window=7". The results of mapping are shown in figure 10.

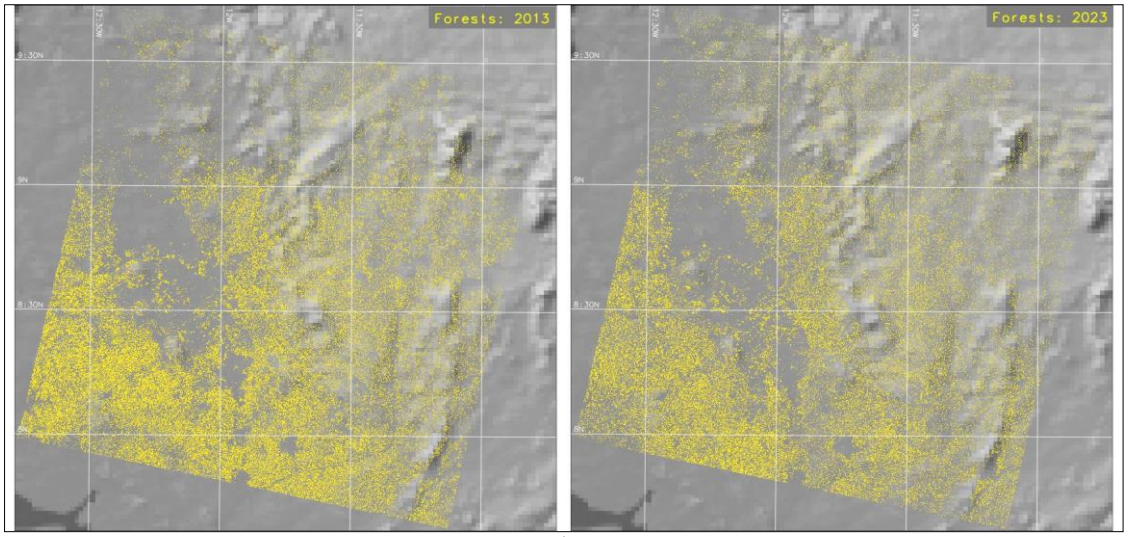

Figure 7: Distribution of rainforests in Sierra Leone. (a) in 2013, detected using classes "forests" in classified Landsat 8-9 OLI/TIRS image. (b) in 2023, detected using classes "forests" in classified Landsat 8-9 OLI/TIRS image by methods of map algebra, GRASS GIS.

The maps were then plotted using a series of cartographic commands used for visualization, as explained in previous works (Lemenkova, 2023a,b) using the following codes: d.mon wx0; d.rast shaded_relief; d.rast fragment_2013; d.grid -g size=00:30:00 color=white width=0.1 fontsize=10 text_color=white; d.legend raster=fragment_2013 title="Fragmentation 2013" title_fontsize=14 font="Helvetica" fontsize=13 bgcolor=white border_color=white; d.out.file output=Fragment_2013 format=jpg.

RESULTS AND DISCUSSION

Figure 8 shows the computed Mean Patch Size (MPS) in Sierra Leone which differs in the range from 0 to 4.4.

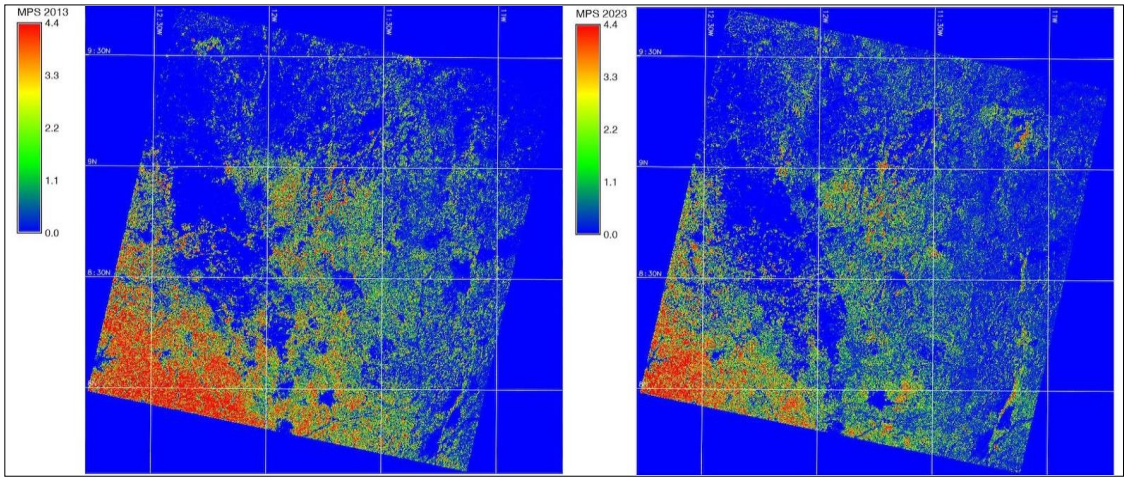

Figure 8: Computed Mean Patch Size (MPS) in the rainforests of Sierra Leone. (a) in 2013, detected using processed Landsat 8-9 OLI/TIRS image. (b) in 2023, detected using processed Landsat 8-9 OLI/TIRS image by methods of landscape analysis, GRASS GIS.

The maps demonstrate the average number of pixels of the patches in the coastal landscapes of Sierra Leone in 2013 and 2023 which visualise the difference. The comparison of the information on this landscape metrics in both maps reveals that patch size in the south-western region became smaller. Since this is the region corresponding to the lowland and wetland areas, it indicates that the decrease of landscape patches in wetlands is affected by fragmentation that is related to the decline of mangroves. This spatial attribute enables to examine the landscape structure and shows that higher MPS is related to the croplands.

Figure 9 shows the computed edge density which equals all edges in the landscape in relation to the landscape area in the study area of Sierra Leone for 2013 and 2023. The range of values differing from 190 to 1333 shows the difference in values calculated for all patches within forest land cover type indicating the length of edge per area of patch over rainforests. Tropical rainforests of Sierra Leone should be protected for conservation of flora and fauna, and as a precious source of commercial exploitation for timber. Nevertheless, the overexploitation of woodland and natural resources can lead to the deforestation and landscape fragmentation, as demonstrated in the maps. Increased forest fragments result from the activities of traditional landowners and local communities in Sierra Leone which can affect environmental sustainability of the country through unbalanced use of resources. Therefore, forest monitoring should be implemented with the aim of sustainable and reasonable use of natural resources that enable local population use resources in balanced way.

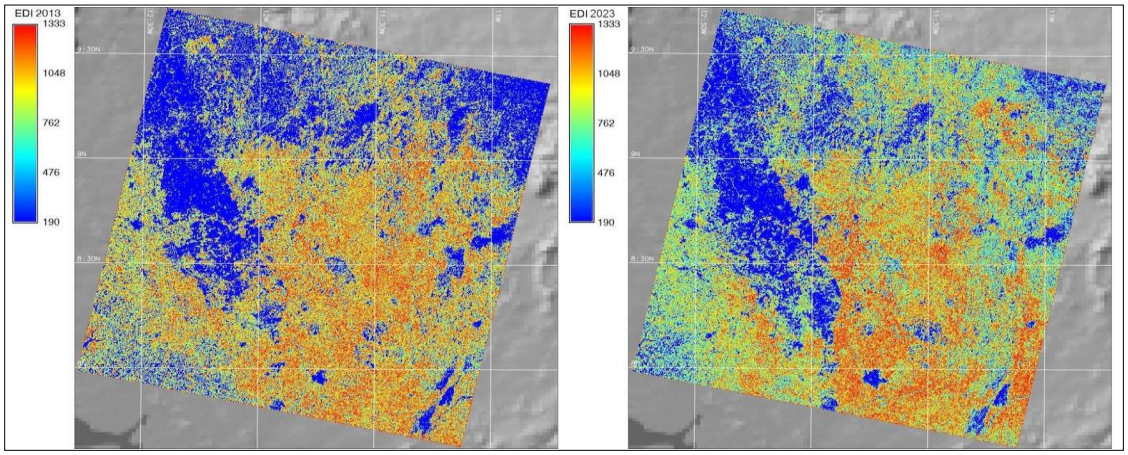

Figure 9: Edge density index computed on two raster maps using methods of landscape analysis in module r.li.edgedensity of GRASS GIS. The analysis includes the rainforests of Sierra Leone. (a) in 2013, using Landsat 8-9 OLI/TIRS image. (b) in 2023, using Landsat 8-9 OLI/TIRS image.

The specific features of edge density index of landscape patches are that it presents a class-level metric which is useful for quantification habitat network. Hence, for biodiversity analysis, it can be applied for monitoring migration ways of species within an area that use ecological corridors for habitat changes of rainforest in Sierra Leone from 2013 to 2023. In view of this, the results of the performed landscape analysis and computed edge density index contribute to the environmental monitoring of Sierra Leone through presented landscapes analysis based on remote sensing data. The comparison of the regions occupied by forests in 2013 and 2023 indicated their decline which pointed at continued deforestation in the eastern regions of Sierra Leone. Such results confirm previously reported studies on deforestation in Sierra Leone (Karg et al., 2020; Mansaray et al. 2016; Kim et al., 2015) and contribute to the environmental monitoring of tropical rainforests.

Figure 10 shows dynamics of landscape fragmentation in Sierra Leone from 2013 to 2023 which indicates disintegration of continuous habitat areas into smaller clusters of patches. Here, six levels of fragmentation are detected as follows: 1 exterior, 2 patch, 3 transitional, ; 4 edge, 5, perforated, and 6 interior. These level indicate changes landscape structure such as physical discontinuity and increased discrepancy in the landscape mosaic which is caused by construction of urban or transport network, expansion of agricultural fields that replace natural communities and increased heterogeneity and division of landscapes in Sierra Leone.

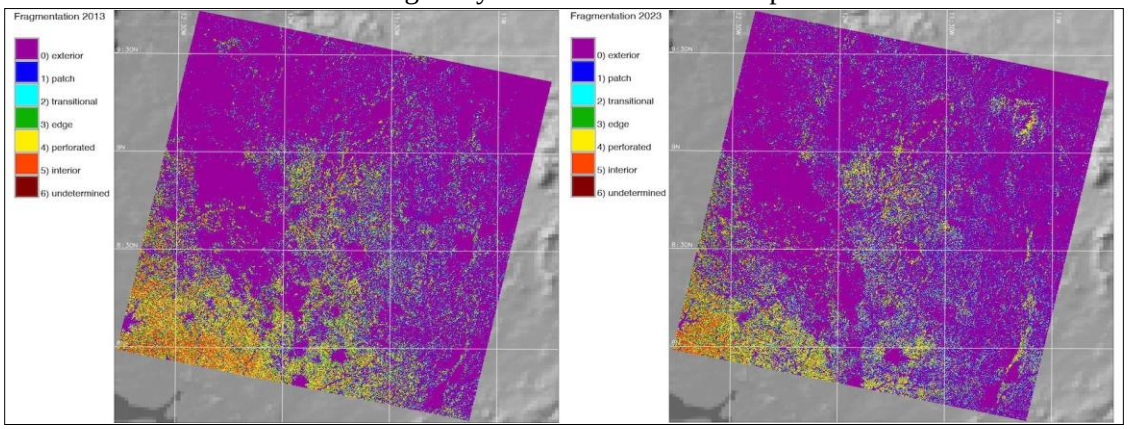

Figure 10: Landscape fragmentation with six levels of fragmentation: 1 exterior, 2, patch, 3 transitional, 4 edge, 5 perforated, and 6 interior. The analysis includes the rainforests of Sierra Leone. (a) in 2013, using Landsat 8-9 OLI/TIRS image. (b) in 2023, using Landsat 8-9 OLI/TIRS image by methods of landscape analysis, GRASS GIS.

Hence, increased landscape fragmentation within forests shows that parts of a habitat are destroyed, leaving behind smaller isolated areas of rainforest patches. This occurred both naturally and also due to human activities. Tropical rainforests form an essential element in the natural ecosystems in Sierra Leone. The complex matrix of their landscapes is characterized by a mosaic of fragments of patches. Local communities of Sierra Leone use diverse types of landscapes to maintain their livelihood (cotton, baobabs) and as a source of diverse products: wood, biomass fuel, nutrition (rice plantations, fruits, nuts, cocoa, coffee beans, and leaves), as well as for traditional medicine. Some products are used for export and therefore have an international commercial value, for instance, such as cocoa which is the biggest export product of Sierra Leone. At the same time, maintaining the balance of environmental sustainability and economic prosperity is important for ecosystems. In view of this, keeping a sustainable mosaic of agriculture-forest landscapes in Sierra Leone is essential due to the diverse and multi-facetted benefits of biodiversity and ecosystem services. In this regard, environmental monitoring using data visualization and analysis is important for nature resource management in agroforestry systems of Sierra Leone.

Landscapes of Sierra Leone include rainforests that present an essential part of Upper Guinea forest ecosystems in West Africa. Therefore, protecting valuable tropical forests in Sierra Leone has a high priority for nature conservation which can be performed through measures on habitat restoration. Mapping landscape dynamics and implementing landscape analysis in Sierra Leone can be assured by detecting changes in rainforest patches and analysis of landscape fragmentation using remote sensing data and advanced cartographic techniques. Such methods are presented in this paper, which applies GRASS GIS advanced scripting cartographic software for processing satellite images covering Sierra Leone.

CONCLUSIONS

This article has demonstrated how rainforest areas and fragmented patch sites in the landscapes of Sierra Leone can be mapped and analysed using GRASS GIS approach of scripts. Moreover, the satellite images used for mapping demonstrated their potential for identification of rainforest areas through map algebra used for analyses of diverse vegetation patterns by spectral signatures in the multispectral bands of Landsat 8-9 OLI/TIRS images. Complex vegetation mosaic which is formed by different landscape patches within rainforests and diverse land cover types of Sierra Leone were identified using scripting methods of image analysis implemented in GRASS GIS. These features are essential elements of the landscape structure which was analysed using distinct patterns of patches detected on raster images.

Deforestation of rainforests in West Africa indicate decreased connectivity of patches which is essential for globally important wildlife species. Recorded from the analysed satellite images and visualised using GRASS GIS scripts, maps of landscape patch distribution can be used to analyse the areas with high level of landscape fragmentation and deforestation. In turn, detected endangered regions can be selected as protected areas for conservation of landscapes to mitigate the consequences of landscape transformation through agriculture field expansion. Hence, this study contributes to the practical development of cartographic methods on mapping and data visualization to achieve these goals. Technically, the data were processed using scripting approach of GRASS GIS applied for landscape analysis in Sierra Leone using Earth observation data. Processing Landsat 8-9 OLI/TIRS by GRASS GIS methodology proved to be a powerful tool for detecting deforestation and land cover classification to evaluate landscape fragmentation in Sierra Leone using modules of landscape analysis ("r.li.edgedensity", "r.li.mps", "r.forestfrag") and raster calculation by "r.mapcalc".

Streamlining existing GIS techniques is invaluable to process and model geospatial data such as satellite images in order to retrieve information regarding land cover types using raster analysis and computational map techniques. Scripts written using GRASS GIS syntax targeted for automation of data processing facilitates cartographic workflow. Such approach is essential for implementing landscape analysis in areas of highly heterogeneous landscapes. At the same time, evaluating distribution of forest, tree canopies, and wetlands helps to detect areas for land cover protection. Detecting land cover changes and fragmented landscapes using advanced GIS approaches is useful for selecting areas of priority landscapes to secure endangered habitats. Complementary cartographic approach included image analysis through classification and landscape analysis supported by visual interpretation. Demonstrated GRASS GIS techniques of image processing support environmental monitoring in tropical landscapes of Sierra Leone, West Africa.

ACKNOWLEDGEMENTS

Funding from the University of Salzburg, Department of Geoinformatics, Faculty of Digital and Analytical Sciences, award GZ: P29085/L-2O23 is gratefully acknowledged.

REFERENCES

1. Akiwumi F. A. and Butler D. R. 2008 – Mining and environmental change in Sierra Leone, West Africa: a remote sensing and hydrogeomorphological study, *Environmental Monitoring and Assessment*, 142, 309-318.
2. Baggie I., Sumah F., Zwart S. J., Sawyerr P., Bandabla T. and Kamara C. S. 2018 – Characterization of the mangrove swamp rice soils along the great scarcies river in Sierra Leone using principal component analysis, *CATENA*, 163, 54-62.
3. Bah Y. and Tsiko R. G. 2011 – Landfill site selection by integrating geographical information systems and multi-criteria decision analysis: a case study of freetown, Sierra Leone, *African Geographical Review*, 30, 1, 67-99.
4. Bangura K. S., Lynch K. and Binns J. A. 2013 – Coping with the impacts of weather changes in rural Sierra Leone, *International Journal of Sustainable Development & World Ecology*, 20, 1, 20-31.
5. Brandt M., Rasmussen K., Hiernaux P., Herrmann S., Tucker C. J., Tong X., Tian F., Mertz O., Kergoat L., Mbow C., David J. L., Melocik K. A., Dendoncker M., Vincke C. and Fensholt R., 2018 – Reduction of tree cover in West African woodlands and promotion in semi-arid farmlands, *Nature Geoscience*, 11, 328-333.
6. Duncan C., Owen H. J. F., Thompson J. R., Koldewey H. J., Primavera J. H. and Pettorelli N. 2018 – Satellite remote sensing to monitor mangrove forest resilience and resistance to sea level rise, *Methods in Ecology and Evolution*, 9, 1837-1852.
7. Field , G. D. 1968 – Utilization of mangroves by birds on the Freetown Peninsula, Sierra Leone, *Ibis*, 110, 354-357.
8. Fomba S. N. 1984 – Rice disease situation in mangrove and associated swamps in Sierra Leone, *Tropical Pest Management*, 30, 1, 73-81.
9. Fomba S. N. and Singh N. 1990 – Crop losses caused by rice brown spot disease in mangrove swamps of northwestern Sierra Leone, *Tropical Pest Management*, 36, 4, 387-393.
10. García-Álvarez D., Camacho Olmedo M. T., Mas J. F. and Paegelow M. 2022 – Land use cover mapping, modelling and validation, A background, in García-Álvarez D., Camacho Olmedo M. T., Paegelow M., Mas J. F. (eds), *Land Use Cover Datasets and Validation Tools*, Springer, Cham.
11. Gornitz V. 1985 – A survey of anthropogenic vegetation changes in West Africa during the last century – climatic implications, *Climatic Change*, 7, 285-325.
12. Haas E. M., Bartholomé E. and Combal B. 2009 – Time series analysis of optical remote sensing data for the mapping of temporary surface water bodies in sub-Saharan western Africa, *Journal of Hydrology*, 370, 52-63.
13. Heiskanen J., Adhikari H., Piiroinen R., Packalen P. and Pellikka P. K. E., 2019 – Do airborne laser scanning biomass prediction models benefit from Landsat time series, hyperspectral data or forest classification in tropical mosaic landscapes? *International Journal of Applied Earth Observation and Geoinformation*, 81, 176-185.
14. Herrmann S. M., Brandt M., Rasmussen K. and Fensholt R. 2020 – Accelerating land cover change in West Africa over four decades as population pressure increased, *Communications Earth & Environment*, 1, 53.
15. Hillson R., Coates A., Alejandre J. D., Jacobsen K. H., Ansumana R., Bockarie A. S., Bangura U., Lamin J. M. and Stenger D. A. 2019 – Estimating the size of urban populations using Landsat images: a case study of Bo, Sierra Leone, West Africa, *International Journal of Health Geographics*, 18, 16.
16. Fimbel C. 1994 – The relative use of abandoned farm clearings and old forest habitats by primates and a forest antelope at Tiwai, Sierra leone, West Africa, *Biological Conservation*, 70, 3, 277-286.

17. Jin W., Cui Y., Wu S. and Cheng D. 2020 – Ecological risk resonance of urbanization and its effect on geohazard disaster: the case of Freetown, Sierra Leone, *Urban Ecosystems*, 23, 1141-1152.
18. Kaplan G., Rashid T., Gasparovic M., Pietrelli A. and Ferrara V., 2022 – Monitoring war-generated environmental security using remote sensing: A review, *Land Degradation & Development*, 33, 10, 1513-1526.
19. Karg H., Drechsel P., Dittrich N. and Cauchois A. 2020 – Spatial and temporal dynamics of croplands in expanding West African cities, *Urban Agriculture & Regional Food Systems*, 5, e20005.
20. Kim D.-H., Sexton J. O. and Townshend J. R., 2015 – Accelerated deforestation in the humid tropics from the 1990s to the 2000s, *Geophysical Research Letters*, 42, 3495-3501.
21. Lahai M. K., Kabba V. T. S. and Mansaray L. R. 2022 – Impacts of land-use and land-cover change on rural livelihoods: Evidence from eastern Sierra Leone, *Applied Geography*, 147, 102784.
22. Lemenkova P., 2020a – Sentinel-2 for high resolution mapping of slope-based vegetation indices using machine learning by SAGA GIS, *Transylvanian Review of Systematical and Ecological Research*, 22, 3, 17-34.
23. Lemenkova P., 2020b – GRASS GIS for topographic and geophysical mapping of the Peru-Chile Trench, *Forum Geografic*, 19, 2, 143-157.
24. Lemenkova P., 2021a – Geophysical mapping of Ghana using advanced cartographic tool GMT, *Kartografija i Geoinformacije*, 20, 36, 16-37.
25. Lemenkova, P. 2021b – Using GMT for 2D and 3D Modeling of the Ryukyu Trench Topography, Pacific Ocean, *Miscellanea Geographica*, 25, 4, 213-225.
26. Lemenkova P. 2022a – GRASS GIS scripts for satellite image analysis by raster calculations using modules r.mapcalc, d.rgb, r.slope.aspect, *Tehnicki Vjesnik*, 29, 6, 1956-1963.
27. Lemenkova P., 2022b – Mapping climate parameters over the territory of Botswana using GMT and Gridded Surface Data from TerraClimate, *ISPRS International Journal of Geo-Information*, 11, 9, 473.
28. Lemenkova P. and Debeir O. 2022a – Satellite image processing by Python and R using Landsat 9 OLI/TIRS and SRTM DEM data on Côte d'Ivoire, West Africa, *Journal of Imaging*, 8, 12, 317.
29. Lemenkova P. and Debeir O. 2022b – R libraries for remote sensing data classification by K-Means Clustering and NDVI computation in Congo River basin, DRC, *Applied Sciences*, 12, 24, 12554.
30. Lemenkova, P., 2023a – Monitoring seasonal fluctuations in saline lakes of Tunisia using Earth observation data processed by GRASS GIS, *Land*, 12, 1995.
31. Lemenkova P., 2023b – A GRASS GIS scripting framework for monitoring changes in the ephemeral salt lakes of Chotts Melrhir and Merouane, Algeria, *Applied System Innovation*, 6, 4, 61.
32. Lemenkova P. and Debeir O., 2023a – Multispectral satellite image analysis for computing vegetation indices by R in the Khartoum Region of Sudan, Northeast Africa, *Journal of Imaging*, 9, 5, 98.
33. Lemenkova P. and Debeir O. 2023b – Time series analysis of Landsat images for monitoring flooded areas in the inner Niger Delta, Mali, *Artificial Satellites*, 58, 4, 278-313.
34. Lemenkova P. and Debeir O. 2023c – Computing vegetation indices from the satellite images using GRASS GIS scripts for monitoring mangrove forests in the coastal landscapes of Niger Delta, Nigeria, *Journal of Marine Science and Engineering*, 11, 4, 871.
35. Mansaray L. R., Huang J. and Kamara,A. A. 2016 – Mapping deforestation and urban expansion in Freetown, Sierra Leone, from pre- to post-war economic recovery, *Environmental Monitoring and Assessment*, 188, 470.

36. Mustafa E. K., Abd El-Hamid H. T. and Tarawally M. 2021 – Spatial and temporal monitoring of drought based on land surface temperature, Freetown City, Sierra Leone, West Africa, *Arabian Journal of Geosciences*, 14, 1013.
37. Neteler M. and Mitasova H., 2008 – Open Source GIS – A GRASS GIS Approach, 3 ed., Springer: New York, NY, USA.
38. Neteler M., Beaudette D. E., Cavallini P., Lami L. and Cepicky J., 2008 – GRASS GIS, in Open source approaches in spatial data handling, 865, Springer, Berlin, Heidelberg, 171-199.
39. Nyerges A. E. 1994 – Deforestation history and the ecology of swidden fallows in Sierra Leone, *Culture & Agriculture*, 14, 6-12.
40. Nyerges A. E. and Green G. M. 2000 – The ethnography of landscape: GIS and remote sensing in the study of forest change in West African Guinea savanna, *American Anthropologist*, 102, 271-289.
41. Reid S. H. 2016 – Satellite remote sensing of archaeological vegetation signatures in coastal West Africa, *African Archaeological Review*, 33, 163-182.
42. Tarawally M., Wenbo X., Weiming H., Darlington Mushore T. and Kursah M. B., 2019 – Land use/land cover change evaluation using land change modeller: A comparative analysis between two main cities in Sierra Leone, *Remote Sensing Applications: Society and Environment*, 16, 100262.
43. Tarawally M., Xu W., Kursah M. B. and Kamara A. B. 2021 – Intra-seasonal variations in urban land surface temperature in two cities in Sierra Leone: the challenge of using a single-date image to represent a whole season, *Spatial Information Research*, 29, 937-947.
44. Wessel P., Luis J. F., Uieda L., Scharroo R., Wobbe F., Smith W. H. F. and Tian D. 2019 – The generic mapping tools version 6, *Geochemistry, Geophysics, Geosystems*, 20, 5556-5564.
45. Wilson S. A., Wilson C. O. and Moise I. K. 2022 – Livelihood impacts of iron ore mining-induced land change in Sierra Leone: A time series analysis, *Applied Geography*, 144, 102713.
46. Yengoh G. T. and Armah F. A., 2016 – Land access constraints for communities affected by large-scale land acquisition in Southern Sierra Leone, *GeoJournal*, 81, 103-122.

MODELING PROCESS OF THE SPATIAL-TEMPORAL CHANGES OF VEGETATION COVER AND ITS RELATIONSHIP WITH DRIVERS IN DRYLANDS AND WETLANDS IN XIANJIANG (CHINA)

Seyed Omid Reza SHOBAIRI *, **, *Lingxiao SUN* *, **(C.A.), *Haiyan ZHANG* *, **, *Chunlan LI* *, **, *Jing HE* *,***, *Behnam Asghari BEIRAMI* ***, *Samira Hemmati ROUDBARI* **** and *Qirghizbek AYOMBEKOV* *

* Xinjiang Institute of Ecology and Geography, Chinese Academy of Sciences, 818 South Beijing Road, Urumuqi, China, CN-830011, omidshobeyri214@gmail.com, ORCID: 0000-0002-6528-8653 (S. O. R. S.); sunlx@ms.xjb.ac.cn, ORCID: 0000-0002-1702-5445 (L. S.); hyzhang@ms.xjb.ac.cn, ORCID: 0000-0002-5250-1865 (H. Z.); lichunlan@ms.xjb.ac.cn, ORCID: 0009-0001-9837-7556 (C. L.); hejing@ms.xjb.ac.cn, ORCID: 0001-0001-7013-1266 (J. H.); ayombekqarghizbek@gmail.com, ORCID: 0009-0002-2400-1481 (Q. A.).

** University of Chinese Academy of Sciences, 19 Yuquan Road, Beijing, CN-100049, China, CN-100049, omidshobeyri214@gmail.com, ORCID: 0000-0002-6528-8653 (S. O. R. S.); sunlx@ms.xjb.ac.cn, ORCID: 0000-0002-1702-5445 (L. S.); hyzhang@ms.xjb.ac.cn, ORCID: 0000-0002-5250-1865 (H. Z.); lichunlan@ms.xjb.ac.cn, ORCID: 0009-0001-9837-7556 (C. L.); hejing@ms.xjb.ac.cn, ORCID: 0001-0001-7013-1266 (J. H.).

*** K. N. Toosi University of Technology, 470 Mirdamad Ave. West, Tehran, Iran, IR-19697, behnam.asghari1370@gmail.com, ORCID: 0000-0002-0314-1912 (B. A. B.).

**** University of Zanjan, Faculty of Agriculture, University Blvd., 45371-38791, Iran, IR-45371-38791, ss.hemmati82.sh@gmail.com, ORCID: 0009-0000-0002-1702-0907, (S. H. R.).

DOI: 10.2478/trser-2024-0003

KEYWORDS: vegetation, NDVI, drivers, ecoregions, spatial distribution, OLS.

ABSTRACT

Findings reveal that the majority of studied areas are classified as bare lands, while the lowest amount is covered by lichens and mosses. Grassland and cropland occupy major areas of the region, with highest normalized difference vegetation index (NDVI) value saw in 2020, showing dense vegetation in the western, northwestern and northern regions. Afforestation efforts shown positive results, with a 4% increase in forested area between 2000 and 2022.

RÉSUMÉ: Processus de modélisation des changements spatio-temporels de la couverture végétale et de sa relation avec les facteurs de changement dans les zones arides et humides du Xianjiang (Chine).

Les résultats révèlent que la majorité des zones étudiées sont classées comme des terres nues, tandis que la plus petite partie est couverte de lichens et de mousses. Les prairies et les terres cultivées occupent une grande partie de la région, la valeur la plus élevée de l'indice de végétation par différence normalisée (NDVI) étant observée en 2020, ce qui indique une végétation dense dans les régions de l'ouest, du nord-ouest et du nord. Les efforts de reboisement ont donné des résultats positifs, avec une augmentation de 4% de la superficie forestière entre 2000 et 2022.

REZUMAT: Procesul de modelare a schimbărilor spațio-temporale ale acoperirii vegetale și relația acesteia cu factori ai zonelor uscate și zonelor umede din Xianjiang (China).

Rezultatele arată că majoritatea ariilor studiate sunt clasificate ca terenuri goale, cea mai mică proporție este acoperită de licheni și mușchi. Pajiștile și terenurile cultivate ocupă arii mari ale regiunii, cu o valoare mare a indicelui de vegetație (NDVI) în 2020, indicând vegetație densă în regiunile de vest, nord-vest și nord. Eforturile de împădurire au arătat rezultate positive, cu o creștere cu 4% a suprafeței împădurite între 2000 și 2022.

INTRODUCTION

Vegetation plays a key role in Earth's biosphere, influencing biogeochemical cycles, carbon balance regulation, and climate stability (He et al., 2023; Zhuang et al., 2019; Jiang et al., 2017). It also provides environmental protection, defence of soil from erosion, wind and sand damage, and preventing desertification (Wang et al., 2023; Zhuang et al., 2019). Additionally, vegetation contributes to the energy cycle by reducing greenhouse gas, supporting global carbon balance, and ensuring climate stability (Zhuang et al., 2019). Thus, it is vital to monitor changes in vegetation over time and understand the underlying mechanisms to effectively manage ecological processes and protect the environment (Li et al., 2021).

Many studies conducted worldwide saw significant changes in vegetation across various scales (Gadiga, 2015). These studies have highlighted the influence of both natural and human factors, such as climate change, land use modifications, and ecological interventions on the dynamics of vegetation patterns (Wang et al., 2023; Wang et al., 2022; Gadiga, 2015). Natural factors exert long-term control, for instance, weather conditions determine the type of vegetation, and alterations in rainfall deeply impact vegetation growth and health. On the other hand, social factors play a significant role in short-term scales. Growth of urban economies and rise in urban population contribute to the expansion of urban areas (Hu and Hu, 2019).

When a large-scale change in vegetation occurs in an area, it affects the energy balance of the surface, which may cause heating or cooling effects (Han et al., 2022), land use change is one of the main challenges that affects natural landscapes and has raised concerns about sustainable development and food security (Hu and Nacun, 2018; Li et al., 2015). That is why, countries and organizations around the world have accepted the risks of reducing vegetation cover and considered measures for protection (Wang et al, 2023). IGBP (International Geosphere-Biosphere Program) and IHDP (Global Change Human Factors Program) proposed the research program "land use/change of cover" (LULC) in 1995 (Liu et al., 2022). As one of the most active economies in the world, China has undergone many changes in land use over the past decades, increasingly contributing to environmental crises (Zhu et al, 2022; Yin et al, 2018). In the last fifty years, China has implemented some measures to protect the Loess plateau, aiming to mitigate soil erosion and enhance ecological conditions. Among these initiatives, the "project of restoring cultivated land to forests and grasses" has emerged as a prominent ecological revitalization scheme. This project, initiated in 1999, has yielded ample improvements in vegetation quantity and quality on the Loess plateau (Zhang et al., 2020). However previous studies have shown that between 1700 and 1950 there was an increasing trend in arable land in China, although they show diverse magnitudes and rates (Miao et al., 2016). Consequently, vegetation is a comprehensive indicator of environmental change, and therefore, spatial and temporal changes in vegetation and its response to climate change have become key issues in global change research (Xianfeng et al., 2014). Xiao and Weng (2007) examined land use changes in southern China from 1991 to 2001, showing that agricultural land decreased and forest land increased slightly. In the study of spatial-temporal dynamic changes in vegetation, the plant Normalized Difference index (NDVI), is an important factor for assessing plant growth status and vegetation distribution pattern (Duan et al., 2021). Gadiga (2015) studied the state and dynamics of vegetation in the Mubi Region in Nigeria using the NDVI index, and the vegetation in the region has suffered record degradation due to the growth of urbanization. Zhuang et al. (2020) conducted a study investigating vegetation dynamics in China's Xinjiang province from 1981 to 2018 using the normalized vegetation difference index (NDVI). Their findings revealed that multiple factors, including precipitation, influenced vegetation changes in the region. Areas with notable vegetation dynamics were primarily concentrated on the northern and southern slopes of the

Tianshan Mountains, the Ely River Valley, and the Altai region. Meng et al. (2020) assessed the temporal and spatial variations in the NDVI index in Mongolia and examined natural and human factors influencing these changes. The results indicated major degradation in desert steppe and the Gobi Desert within arid regions, while grassland steppe and Alpine steppe exhibited significant upward trends. The researchers also observed that climatic parameters, such as precipitation, had a positive impact on vegetation distribution. Overall, these studies highlight the influence of factors such as precipitation on vegetation dynamics and underscore the specific regions affected by these changes in China's Xinjiang province and Mongolia.

Xinjiang Province, in northwestern China, has been susceptible to the effects of climate change, experiencing warming over the last four decades. The region has witnessed notable transformations in vegetation patterns during last years (Han et al., 2022; Zhuang et al., 2019). Understanding the changes in vegetation cover is crucial in realising the temporal and spatial dynamics of this region and the feedback between vegetation and the atmosphere.

This study aimed to analyze and model the detection of vegetation cover changes in various areas of Xinjiang Province over a 23-year period. By harnessing the connectivity of sensor datasets from remote sensing platforms, time series data was utilized to track these changes. Examining the relationship between vegetation dynamics and climate and environmental stimuli is vital in the context of global warming and climate change research, as it provides insights into the dynamic responses of terrestrial ecosystems to these phenomena. The study employed the ArcGIS platform to predict the impact of climate and environmental factors on plant indicators, leveraging open-source data and coding techniques.

MATERIAL AND METHODS

Study area

Xinjiang Province is situated in northwestern China, spanning from 73°20'E to 96°25'E and 34°15'N to 49°10'N (Jiapaer et al., 2015). With a total land area of 1.66 million km^2, it accounts for approximately one-sixth of China's land area (Yu et al., 2020). The province encompasses a delicate ecological zone characterized by a complex arid environment, with mountainous areas comprising 51.4% and plain areas comprising 48.6% of the total land area (Luo et al., 2019; Jiapaer et al., 2015). Xinjiang exhibits diverse landforms, including the Altai Mountains in the north, the Kunlun Mountains and A-erh-chin Mountains in the south, and the Tian Shan Mountains spanning the central part of the province. These major mountain ranges encircle the Junggar Basin and the Tarim Basin (Zhao et al., 2022), which serve as the sources of numerous rivers (Luo et al., 2019). The Tian Shan Mountains, Altai Mountains, and Kunlun Mountains harbor extensive forest and grassland vegetation, while oases and cities are located in the valley plains. As of 2018, forest land and grassland accounted for 31.29% of the land area, with grassland being the predominant vegetation type (Zhuang et al., 2020). The Junggar and Tarim Basins are characterized by typical temperate desert vegetation. Despite belonging to a temperate continental climate, Xinjiang exhibits distinct differences between its northern and southern regions due to its extensive north-south span. The annual precipitation in northern Xinjiang ranges from 100 to 500 mm, with average temperatures ranging from 4 to 8°C. In southern Xinjiang, annual precipitation ranges from 20 to 100 mm, while average temperatures range from 10 to 13°C (Cao and Gao, 2022). Figure 1 provides a visual representation of Xinjiang Province's geographical location and its ecoregions.

Preparation of vegetation data from 2000 to 2023

Modeling the study is based on calculating satellite data. Calculations were completed with the help of the Google Earth Engine (GEE) platform and catalogs of raster files on the platform.Other open sources of data were used such as MODIS/061/myd13a1-NDVI (16 daily-2000 to 2023 – with a spatial resolution of 250 meters – global scale, and data sets of drivers such as daily LST (Kelvin), precipitation (mm/d), global land cover extracted from Sentinel-1 and 2 data and Global 30 Arc-Second Elevation to extract DEM and slope. Data through ArcGIS platform was extracted to track vegetation cover changes, areas, and calculation of the drivers affecting the vegetation. The main sources and characteristics of the data collected are displayed in table 1.

Table 1: Main sources of data with the satellite products specifications.

Sattelite/ Model	Product name	Date name	Unit	Spatial resolution	Temporal resolution	Time extent
Modis/ Terra	MOD11A1.061 Terra Land Surface Temperature and Emissivity Daily Global 1 km	LST_Day 1 km LST_Night 1 km	Kelvin	1,000 m	Daily	2000-02-24
Modis/ Terra	Vegetation Indices	NDVI	–	500 m	Daily	2000-02-18
Modis/ Terra	Vegetation Indices	NDVI	–	500 m	Daily	2000-02-18
CHIRPS	CSB-CHG/CHIRPS/ DAILY	Precipitation	mm/d	–	Daily	1981-01-01T00:00:00 Z–2023-06-30T00:00:00
Sentinel-1 and 2 data	ESA World Cover 2020	Global Land cover product	–	10 m	Annually	2020-2021
GTOPO30	Global 30 Arc-Second Elevation	DEM	m	1 km	NaN	1996

Ecoregion data

Ecoregions, defined as regions with similar ecosystems, have become increasingly significant in the evaluation and administration of environmental matters. They offer a comprehensive framework that allows for flexible and comparative analysis of intricate environmental issues (Lovland and Merchant, 2004). We downloaded Ecoregion data from https://ecoregions.appspot.com and cropped it for Xinjiang Province. There are 14 terrestrial biomes and 846 ecoregions worldwide. Plant communities within a given biome may exhibit comparable structural characteristics while harboring distinct species compositions. Table 2, list the 17 ecoregions and five biomes in Xinjiang Province. Figure 1 shows the positions of each of the ecoregions of Xianjian Province.

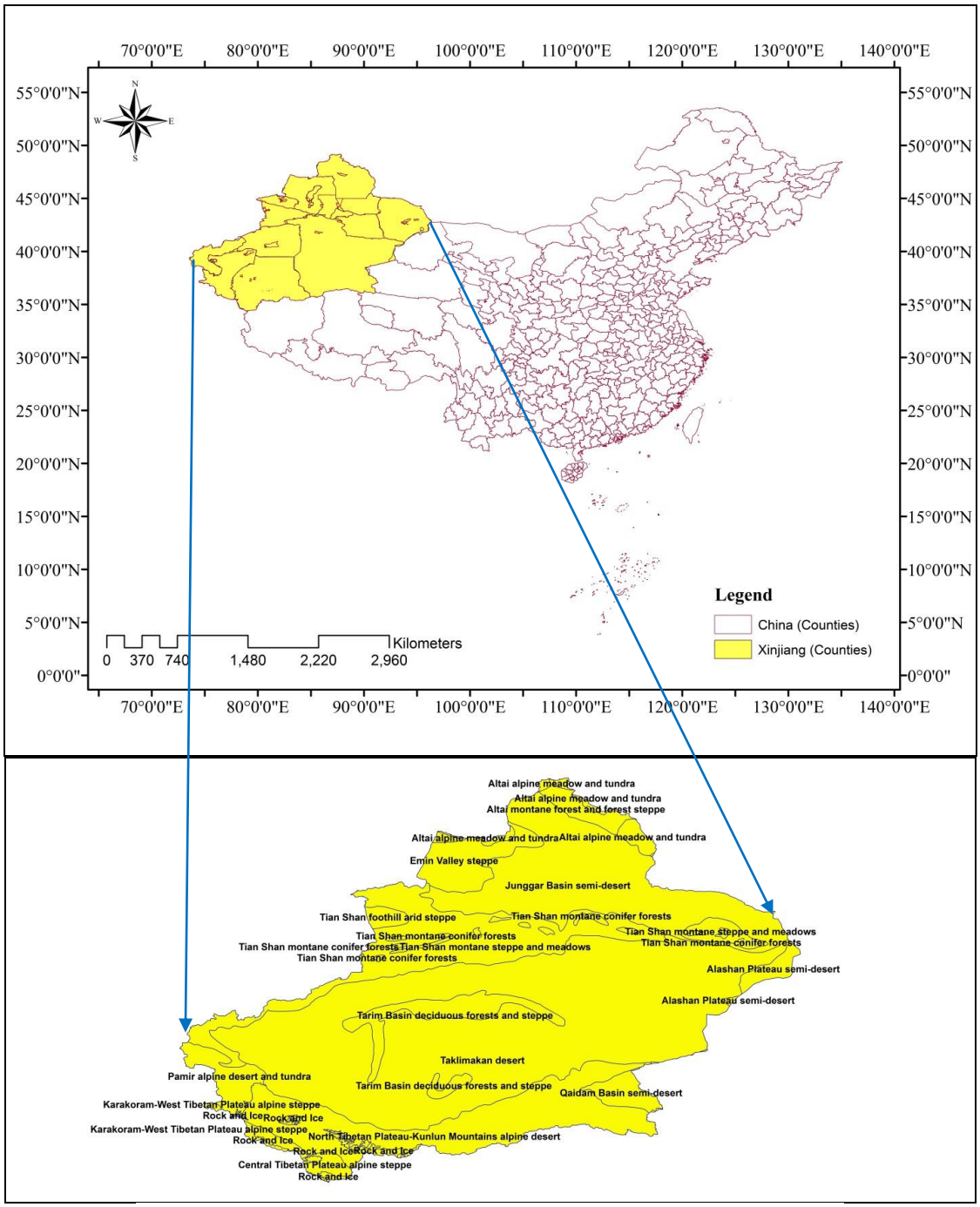

Figure 1: Positions of each of the ecoregions in the Xianjiang, China.

Taklimakan Desert ecoregion with 742,657 km^2 accounts for 18.1% of the province and Tian Shan montane conifer forests ecoregion with 27,568 km^2 covers 0.67% of the province, representing the largest and smallest areas among the Xinjiang-Tian Shan ecoregions (Tab. 2).

Table 2: Xinjiang ecoregions, classified by name, area, percentage.

Ecoregions	Area km^2	%
Alashan Plateau semi-desert	674,352	16.498
Altai alpine meadow and tundra	90,434	2.212
Altai montane forest and forest steppe	142,875	3.495
Altai steppe and semi-desert	83,192	2.035
Central Tibetan Plateau alpine steppe	629,190	15.393
Emin Valley steppe	65,135	1.594
Junggar Basin semi-desert	304,938	7.460
Karakoram-West Tibetan Plateau alpine steppe	143,265	3.50
North Tibetan Plateau-Kunlun Mountains alpine desert	374,494	9.162
Pamir alpine desert and tundra	118,072	2.889
Qaidam Basin semi-desert	192,147	4.701
Rock and Ice	34,830	0.852
Taklimakan Desert	742,657	18.169
Tarim Basin deciduous forests and steppe	54,533	1.334
Tian Shan foothill arid steppe	129,231	3.162
Tian Shan montane conifer forests	275,68	0.674
Tian Shan montane steppe and meadows	280,611	6.865

Implementation phases

Tracking and analysis of the models took place in several phases: Identifying the current state of the study border; Calculation and zoning of vegetation at the study boundary (time series 2000 to 2023) and determination of maximum and minimum density; Analysis of spatial-temporal distribution of vegetation since 2000 by classification method; Areas where the value of NDVI is greater than 0.5 and vice versa areas where the value of NDVI is less than 0.5.; Estimation of vegetation density using kernel density and point density: 1) Monitoring and evaluation of vegetation cover from the past 23 years using land surface measurements (Divisions by municipalities), 2) Monitoring and evaluation of vegetation cover from 2000-2023 using land surface measurements (Divisions by ecoregions); Estimation of the area and percentage of afforestation and deforestation at the beginning and end of the desired time period (2000-2022); Identifying the pattern of spatial distribution of vegetation in the study border with spatial autocorrelation with a confidence level above 90%, Average Nearest Neighbor; Estimation of hot spots and cold spots of vegetation in the border of the study with a confidence level above 90% using hot spot analysis, clusters and outliers; Identification of factors affecting the distribution of vegetation in the study border (land use, land surface temperature, rainfall, slope, elevation); Spatial modeling of factors affecting vegetation (OLS).

RESULTS

Identifying the current state of the study border

Figure 2 shows patterns for the digital elevation model (A), slope (B), precipitation parameter (C) and LULC variations calculated. According to the digital elevation model, the area studied has expanded between 152 m and 7,553 m, which will create a wide range of plant species, each plant specific to an elevation surface.

As much as altitude increase, precipitation increase, temperature decrease, dry stress decrease, and the vegetation develops, this trend continues till higher altitudes where low temperatures reduces the vegetation. The gradient variation pattern (Fig. 2B) also represents gradient fluctuations of 0 to 356 degrees in the study area, which is very diverse. There is a question of which slopes in the Xinjiang ecoregions have more vegetation?

For the northern hemisphere of the Earth, including Xinjiang, which is wide and rich in diversity, the slopes facing south receive more sunlight and become drier and warmer, support drought-resistant vegetation and are less favorable for trees, while the slopes facing north retain moisture and are cold and humid and are suitable for humid plants.

The rain pattern is displayed in figure 2C. The highest rainfall was 704 mm and the lowest was 13 mm. Precipitation is one of the most important factors affecting the growth and development of vegetation. According to studies conducted in many Xinjiang ecosystems, especially grasslands and arable land, the growth of seasonal plants occurs entirely within the rainy season. In times of drought, vegetation grows poorly in these ecosystems. If it rains, the sudden growth of vegetable plants actually turns. Unsure what is being communicated.

By manipulating the Sentinel-1 and 2 satellite data sets, tracking land use and land cover changes, for 2020, LULC was considered as one of the drivers that reflected vegetation in the ecoregions of Xinjiang. Figure 2D shows this classification visually, and table 3 examines the classification of LULC and their area and percentage.

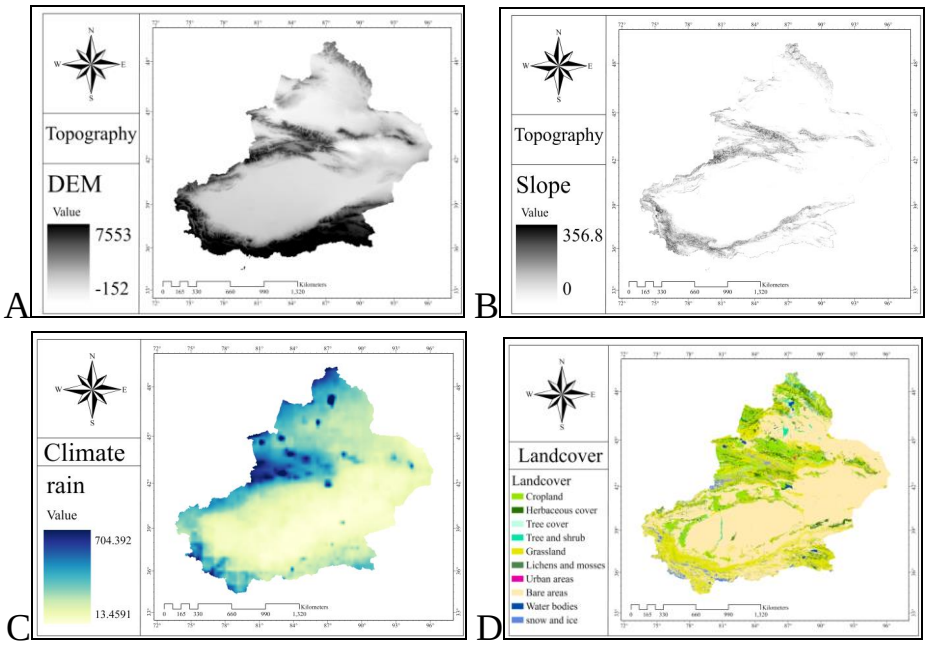

Figure 2: Digital elevation model (A), slope (B), precipitation (C) and LULC (D).

Table 3 shows, the largest area is the Bare area class, (139,433.7 km^2, or ying 61.49%), and the smallest area is the Lichens and Mosses class (41.8 km^2, or 0.018%). Bare land refers to areas where dominant vegetation covers under 90%. This category contains areas without artificial cover and includes regions with less than 4% vegetative cover. Examples include bare rock regions, sandy areas, and deserts. Table 3 shows that mosses and lichens has the smallest area, however it is argued that it plays a very important role in study area. Both mosses and lichens have a significant role in maintaining a healthy environment as they contribute to the absorption of carbon dioxide and other air pollutants. Lichens, in particular, possess valuable detoxifying properties that make them highly beneficial to various organisms.

Table 3: Classification of LULC alignments, area and percentage.

LULC	Area km^2	%
Crop land	16,263.74	7.17
Herbaceous cover	13,615.37	6
Tree cover	2,038.06	0.89
Tree and shrub	1,989.67	0.87
Grassland	48,112	21.2
Lichens and mosses	41.8	0.018
Urban areas	261.83	0.11
Bare areas	139,433.7	61.49
Water bodies	1,306.74	0.57
Snow and ice	3,692.84	1.62

Table 3 is divided into valuable LULC classes and their respective area and percent coverage of the study area. These classes together create an incredibly diverse and complex BioCycle and any changes in urban area, cropland and bare area classes will greatly affect the quality and quantity of valuable classes.

Calculation and zoning of vegetation at the study boundary in time series 2000 to 2023 and determination of maximum and minimum density

Satellites carry numerous sensors that measure the reflection of red and near-infrared light waves from land surfaces. By utilizing mathematical algorithms, scientists convert the raw satellite data related to these light waves into vegetation indices. These indices serve as indicators of vegetation greenness, representing the relative density and health of vegetation for each pixel in a satellite image. Among various vegetation indices, the Normalized Difference Vegetation Index (NDVI) is widely employed. NDVI values range from +1.0 to –1.0. Barren areas such as rocks, sand, or snow typically exhibit very low NDVI values, often 0.1 or less. Regions with sparse vegetation like shrubs, grasslands, or aging crops show moderate NDVI values ranging from approximately 0.2 to 0.5. High NDVI values, around 0.6 to 0.9, correspond to dense vegetation found in temperate and tropical forests or crops during their peak growth stage (Tahir et al., 2019; Elsu et al., 2017). Researchers can utilize raw satellite data to convert it into NDVI values, which enables the creation of images and other products that provide a general assessment of vegetation characteristics, quantity, and condition on a global scale. NDVI is particularly valuable for monitoring vegetation at continental to global levels, as it can account for variations in lighting conditions, surface slope, and viewing angles. However, it should be noted that NDVI may become saturated in areas with dense vegetation and is influenced by the color of the underlying soil. By averaging NDVI values over time, researchers can establish a baseline for normal growing conditions in a specific region during a particular time of year. Subsequent analysis can then evaluate the relative health of vegetation compared to this baseline. Over time, NDVI analysis can identify areas where vegetation is flourishing or experiencing stress, as well as detect changes in vegetation patterns resulting from human activities like deforestation, natural disturbances such as wildfires, or shifts in plants' phenological stages (*).

Figure 3 shows the visual patterns of vegetation classification calculated with the average NDVI value for the time series 2000 to 2023. The highest value of NDVI is for 2020 (Fig. 3E), with a value of 0.933 predicted, and according to the classification of NDVI value balances; it represents areas with dense vegetation. The lowest value of -0.199 corresponds to 2010 (Fig. 3C), representing areas with the presence of abundant sand, rocks, and snow.

Based on the NDVI value patterns depicted in figure 3, the western, northwestern, and northern areas of Xinjiang Province exhibit the highest NDVI values. These regions encompass various ecoregions, including the arid steppe of the Tian Shan foothills, conifer forests of the Tian Shan Mountains, steppe and meadows of the Tian Shan montane region, steppe in the Emin Valley, steppe and semi-desert in Altai, forest and forest steppe in Altai Mountains, and alpine meadow and tundra in Altai.

The average value of NDVI is estimated to be approximately between 0.2 and 0.5 which are spread in the central, western and northwestern and southwestern regions, are also broadcasted in the form of spots in the eastern regions of Xinjiang Province, which this type of classification represents scattered vegetation, savanna, shrubs, meadows, and agricultural lands. The classification of certain areas within the Tian Shan montane steppe and meadow ecoregion serves as a notable illustration of this categorization.

Ecoregions like Taklimakan Desert, north Tibetan Plateau-Kunlun mountains alpine desert and junggar basin semi desert positioned in the central, central south, southern and northern regions of Xinjiang Province respectively experienced the lowest value of NDVI, and are covered with very scattered vegetation, sand, barren rock and rarely snow (Fig. 3).

Analysis of spatial-temporal distribution of vegetation 2000-2023 by classification method (Areas with NDVI > 0.5 and NDVI < 0.5).

The temporal and spatial distribution of the average annual NDVI value was examined. This classification specifically identifies regions where the NDVI value exceeds 0.5, and regions where the NDVI value is below 0.5, based on data from 2000 to 2023 (Fig. 5). 2015 had the highest area of the regions, with a NDVI value greater than 0.5 in Xinjiang Province, which has an area of 149,450.6 km^2 (Tab. 4, Fig. 5D). 2000 also experienced the largest area with a NDVI less than 0.5, this value includes 1,614,503.6 km^2 (Tab. 4, Fig. 5A). In summary, the range of NDVI values spans from –1.0 to 1.0. Negative values represent clouds and water, values close to zero indicate bare soil, and higher positive values of NDVI correspond to varying levels of vegetation density, ranging from sparse vegetation (0.1-0.5) to dense green vegetation (0.6 and above). 2015 has experienced the highest level of dense vegetation, and 2000 is also covered with a sporadic and vast vegetation community.

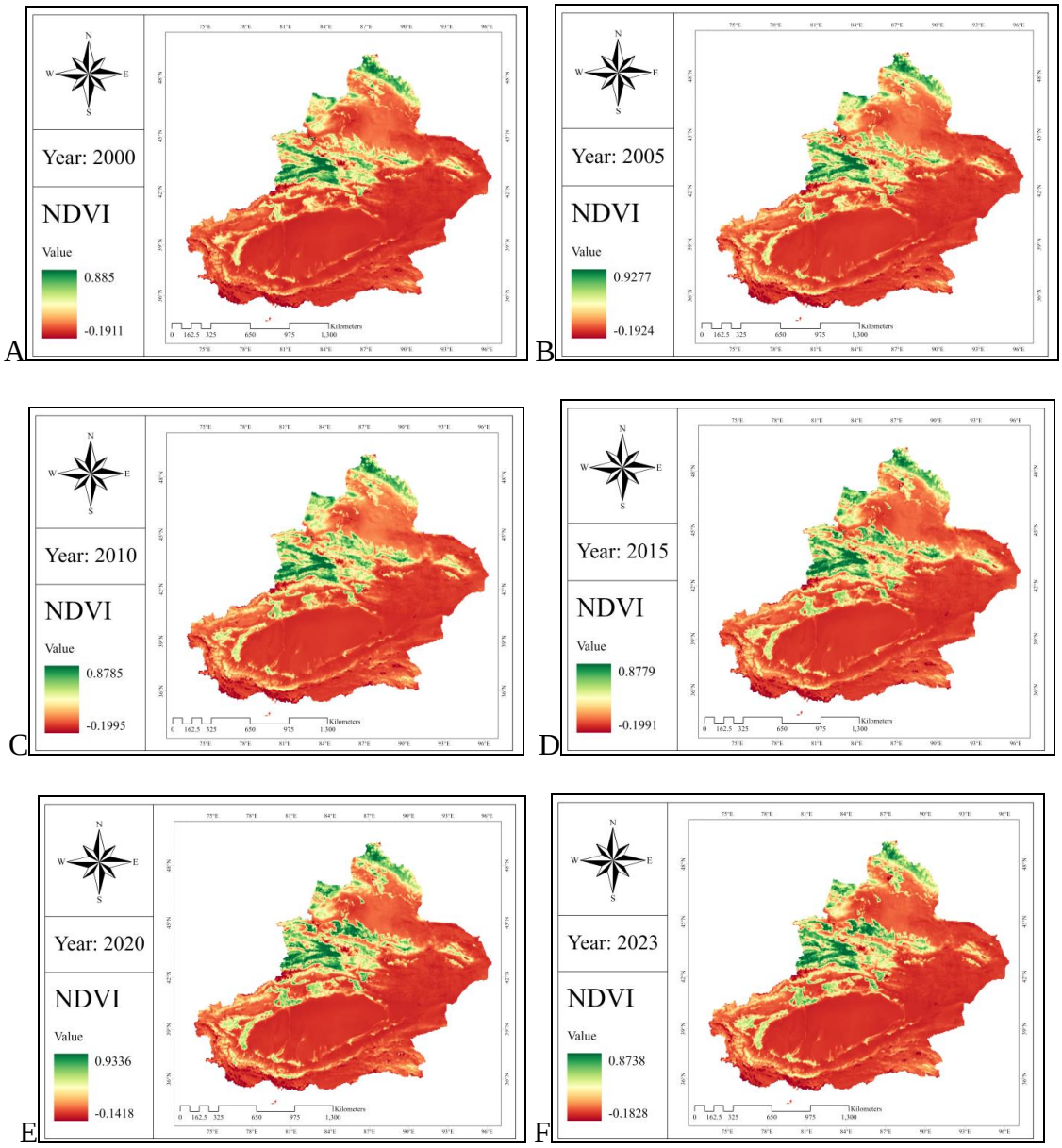

Figure 3: Visual patterns of temporal and spatial changes of vegetation calculated by the mean value of NDVI for the time series 2000 to 2023.

Table 4: Statistics on area in km^2 from 2000 to 2023.

Year	2000	2005	2010	2015	2020	2023
Area (km^2) of arenas where the value of the NDVI < 0.5	1614503.61	1600279.06	1587131.76	1574324.40	1583306.92	1578566.28
Area (km^2) of arenas where the value of the NDVI > 0.5	109396.39	123345.94	136518.24	149450.60	142168.08	146908.72

Figure 4 describes changes in boundary areas from 2000-2023. Figure 4A clearly shows a decrease in area for arenas with a NDVI of less than 0.5. On the other hand figure 4B shows a unique phenomenon, where area of areas with NDVI more than 0.5 is increasing, indicating the existence of suitable conditions for vegetation development as well as correct management of the arenas. The increasing quantity of positive NDVI values signifies a rise in the presence of green vegetation. What are the factors that affect NDVI? NDVI is an important indicator that reflects the state of the regional climate and the environment, which is affected by precipitation, temperature, the water content of the soil, humans, etc. For instance, Yao et al. (2023) conducted a study utilizing GeoDetector to investigate the impact of various factors on NDVI, such as climate, soil, topography, and human activities. Their findings revealed that the primary contributing factors were night light brightness (51.9%), annual average air temperature (47%), and annual average atmospheric pressure (45.8%). Additional research has demonstrated that NDVI exhibits a stronger correlation with changes in rainfall (R = 0.75) compared to temperature and elevation. Generally, NDVI values tend to decrease under extremely high and low temperature conditions. Furthermore, the growth pattern of NDVI varies with altitude, with a more pronounced response observed between 70 m and 1,500 m above sea level. These aspects will be further examined in the subsequent sections of this article, exploring the relationship between NDVI and rainfall, land use and land cover changes, elevation, slope, and LST, as well as modeling the interconnectedness of these factors.

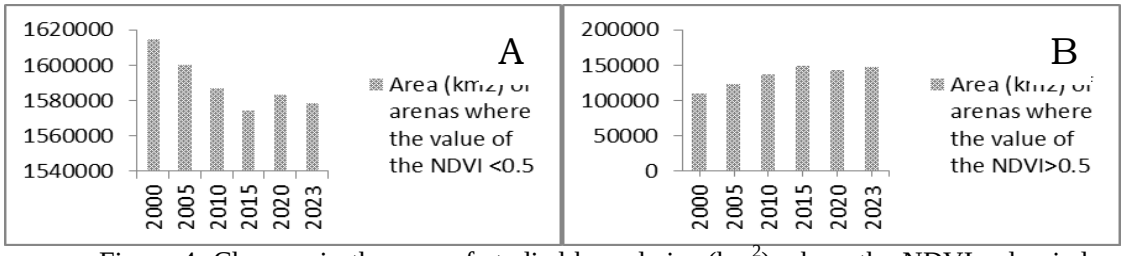

Figure 4: Changes in the area of studied boundaries (km^2) where the NDVI value is less than 0.5.(A) and NDVI value is more than 0.5 (B).

Figure 5 reports visual patterns of NDVI value, for the northern regions of Xinjiang such as Altai Mountains forest and forest steppe, Altai alpine meadow and tundra, parts of the Emin Valley steppe and large parts of the Tian Shan ecoregions. Likewise it reports the montane steppe meadows, the montane conifer forest and the foothill arid steppe and the central parts of this province are seen as spots that have experienced NDVI values >5 from 2000 to 2023. This value reached its highest value in 2015 (Tab. 4, Fig. 4B), After a hiatus in 2020, it increased again until 2023. Areas that had NDVI values <5 and have scattered vegetation, bare land, sand and agricultural land (displayed in red), with the exception of 2020, have experienced a downward trend (Fig. 4A). Overall the very positive ecological event is taking shape and every year we see an increase in conservation, restoration, and development of vegetation coverage in all parts of the Xinjiang Province. This constructive process is more prominent in central and western parts such as the Tian Shan Mountains and northern areas such as the Altai Mountains and the Emin Valley (Fig. 5).

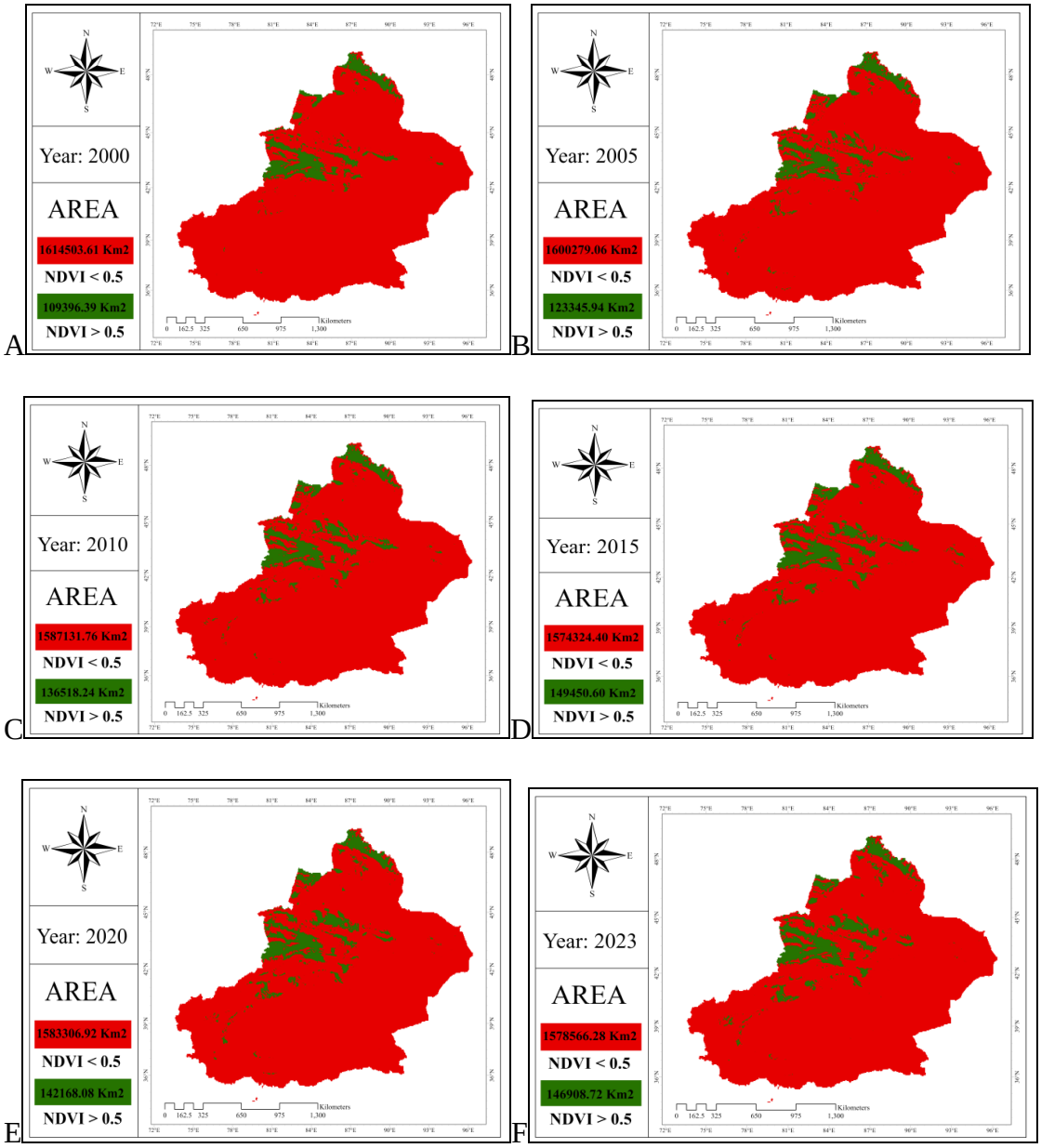

Figure 5: Visual patterns of NDVI temporal and spatial distribution along with area of arenas with a value greater than 0.5 and less than 0.5 for 2000 to 2023.

Estimation of vegetation density using kernel density and point density monitoring and evaluation of vegetation cover from 2000-2023 using land surface measurements (Divisions by municipalities)

Figure 6 shows temporal and spatial patterns of monitoring and evaluating vegetation changes using land surface measurements, which are borders of counties, and have modeled changes since 2000. The NDVI value is an average of the total months of the year. The modeling process relies on assessing vegetation density and leverages the kernel density method. This approach involves calculating the density of point features surrounding each output raster cell. Essentially, a smooth curved surface is fitted over each point in the model. Kernel density estimation, a statistical technique, is utilized for estimating the probability density function of a random variable using kernel smoothing. In this case, the variable of interest is the annual average NDVI value.

Kernel estimator results argue that the maximum values close to NDVI >0.55 with green, and the minimal values are close to NDVI <0.07, highlighted in red. The range between maximum and minimum is aligned with yellow and orange colors (Fig. 6). In general, the northern and western counties of Xinjiang Province have experienced the development of vegetation, in other words the southern and eastern counties have lost the harmony of warm red and orange colors and turned into pale yellow and green colors (Fig. 6).

According to table 5, the highest average NDVI value is related to Ili Kazakh County, which experienced a value of 0.54 in 2000. The lowest average NDVI value of 0.07 also belongs to Khotan County.

According to NASA Earth Observatory website (***), extremely low NDVI values (0.1 and below) indicate barren areas such as rock, sand, or snow. Moderate values (0.2 to 0.3) correspond to shrub and grassland, while high values (0.6 to 0.8) signify temperate and tropical rainforests. Applying this principle, it can be observed that Khotan County predominantly consists of very sparse vegetation, desert, sand, and rock, whereas Ili Kazakh County and Shihezi County exhibited a relatively moderate vegetation situation in 2000, characterized by grasslands, shrubs, as well as broadleaf and coniferous species (Fig. 7).

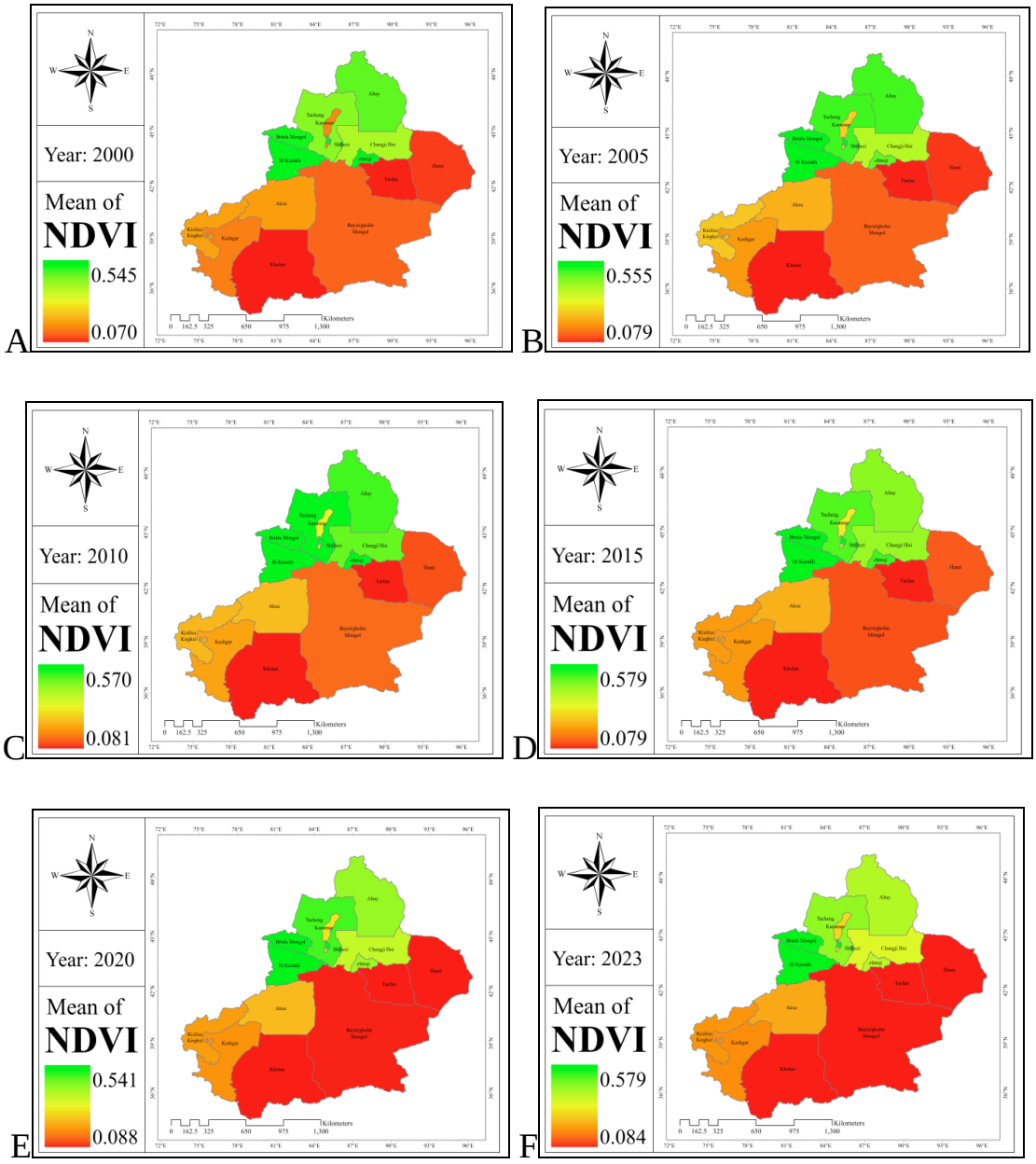

Figure 6: Examination of spatial and temporal patterns of vegetation density using Kernel density estimation.

Table 5: Classification of vegetation cover (NDVI) based on county divisions in two.

No.	Name	Minimum	Maximum	Mean
1	Aksu	–0.052921	0.691787	0.136181
2	Altay	–0.123229	0.859978	0.270487
3	Bayin'gholin	–0.191100	0.878285	0.104023
4	Bortala	–0.171962	0.874815	0.290748
5	Changji Hui	–0.033705	0.803515	0.233974
6	Hami	–0.027253	0.678575	0.088444
7	Ili Kazakh	–0.043728	0.885946	0.54512
8	Karamay	0.03571	0.541906	0.124138
9	Kashgar	–0.075600	0.536531	0.118364
10	Khotan	–0.117503	0.677344	0.070696
11	Kizilsu	–0.054392	0.547	0.137629
12	Shihezi	0.201837	0.640216	0.484435
13	Tacheng	–0.156277	0.819484	0.253239
14	Turfan	–0.038627	0.58874	0.082853
15	Urümqi	–0.038954	0.724495	0.307904

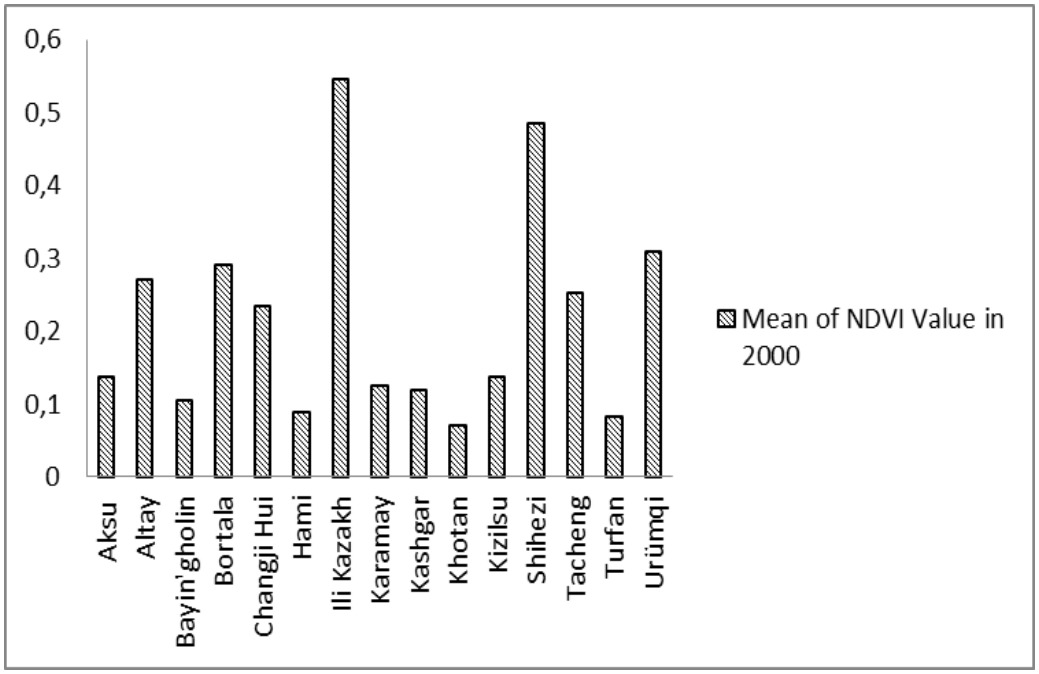

Figure 7: Statistics of average annual NDVI value
based on the division of county boundaries in 2000.

Tables 5-10 as well as figures 7-12 show the NDVI values of the cities of Xinjiang Province 2000-2003. The results showed that Ili Kazakh city and then Shihezi city had the highest NDVI value during the period studied. The lowest NDVI value was for Khotan city. Examining the NDVI index values in Ili Kazakh city 2000 to 2023 showed that the amount of vegetation has grown significantly and improved. In this city, the NDVI value in 2000 was 0.54, which gradually increased in 2005, 2010, and 2015 (0.55, 0.57, and 0.57, respectively).

Table 6: Classification of vegetation cover (NDVI) based on couty divisions in 2005.

No.	Name	Minimum	Maximum	Mean
1	Aksu	–0.122748	0.742965	0.148695
2	Altay	–0.192430	0.927757	0.279236
3	Bayin'gholin	–0.184302	0.869611	0.10498
4	Bortala	–0.155703	0.875777	0.307521
5	Changji Hui	–0.027991	0.773594	0.229612
6	Hami	–0.073582	0.669499	0.088761
7	Ili Kazakh	–0.046839	0.88735	0.555844
8	Karamay	–0.042529	0.670178	0.169616
9	Kashgar	–0.175655	0.563468	0.135556
10	Khotan	–0.074800	0.60319	0.079338
11	Kizilsu Kirghiz	–0.055451	0.5445	0.1639
12	Shihezi	0.170395	0.704664	0.521317
13	Tacheng	–0.048387	0.808383	0.279653
14	Turfan	0.011559	0.578973	0.084733
15	Urümqi	–0.030313	0.695617	0.269192

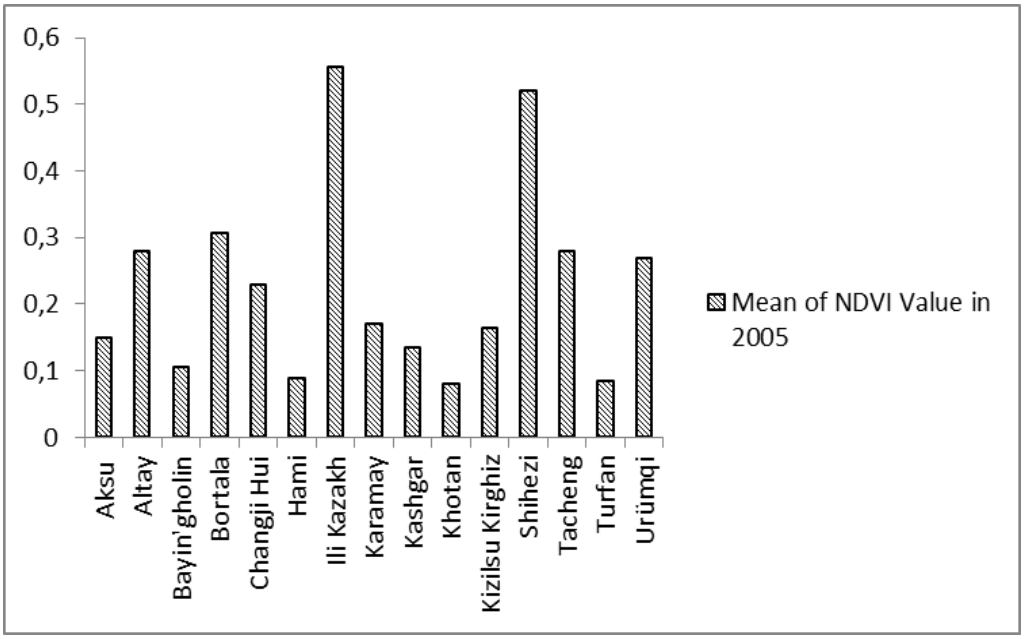

Figure 8: Statistics of average annual NDVI value
based on the division of county boundaries in 2005.

Table 7: Classification of vegetation cover (NDVI) based on couty divisions in 2010.

No.	Name	Minimum	Maximum	Mean
1	Aksu	–0.065500	0.687213	0.160299
2	Altay	–0.116237	0.864199	0.286228
3	Bayin'gholin Mongol	–0.187300	0.869814	0.111299
4	Bortala Mongol	–0.190533	0.820894	0.315226
5	Changji Hui	–0.023896	0.81202	0.274984
6	Hami	–0.072722	0.68649	0.099629
7	Ili Kazakh	–0.033036	0.878573	0.570325
8	Karamay	–0.025764	0.712739	0.204186
9	Kashgar	–0.080600	0.684593	0.143876
10	Khotan	–0.074623	0.694637	0.081276
11	Kizilsu Kirghiz	–0.064005	0.662137	0.156734
12	Shihezi	0.261811	0.7112	0.56347
13	Tacheng	–0.128363	0.807561	0.305837
14	Turfan	0.011221	0.593036	0.086799
15	Urümqi	–0.033983	0.75133	0.304136

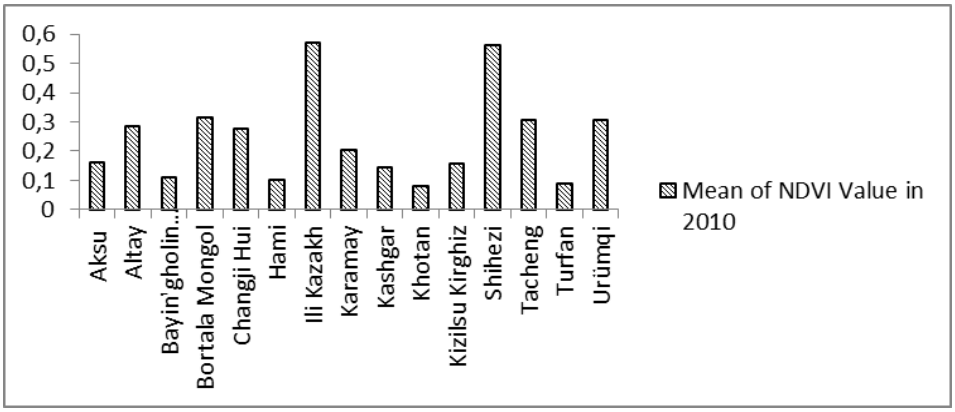

Figure 9: Statistics of average annual NDVI value based on the division of county boundaries in 2010.

Table 8: Classification of vegetation cover (NDVI) based on couty divisions in 2015.

No.	Name	Minimum	Maximum	Mean
1	Aksu	–0.060800	0.666599	0.167056
2	Altay	–0.199042	0.866951	0.279071
3	Bayin'gholin Mongol	–0.199100	0.857465	0.111562
4	Bortala Mongol	–0.150868	0.83892	0.337688
5	Changji Hui	–0.038100	0.841333	0.271983
6	Hami	–0.085294	0.737637	0.11500
7	Ili Kazakh	–0.041731	0.877921	0.579145
8	Karamay	0.007897	0.780512	0.210299
9	Kashgar	–0.086180	0.682347	0.151257
10	Khotan	–0.080100	0.592517	0.079768
11	Kizilsu Kirghiz	–0.056029	0.521963	0.152814
12	Shihezi	0.19053	0.760908	0.510827
13	Tacheng	–0.189183	0.830494	0.30230
14	Turfan	0.005873	0.629756	0.096969
15	Urümqi	–0.049939	0.726139	0.30828

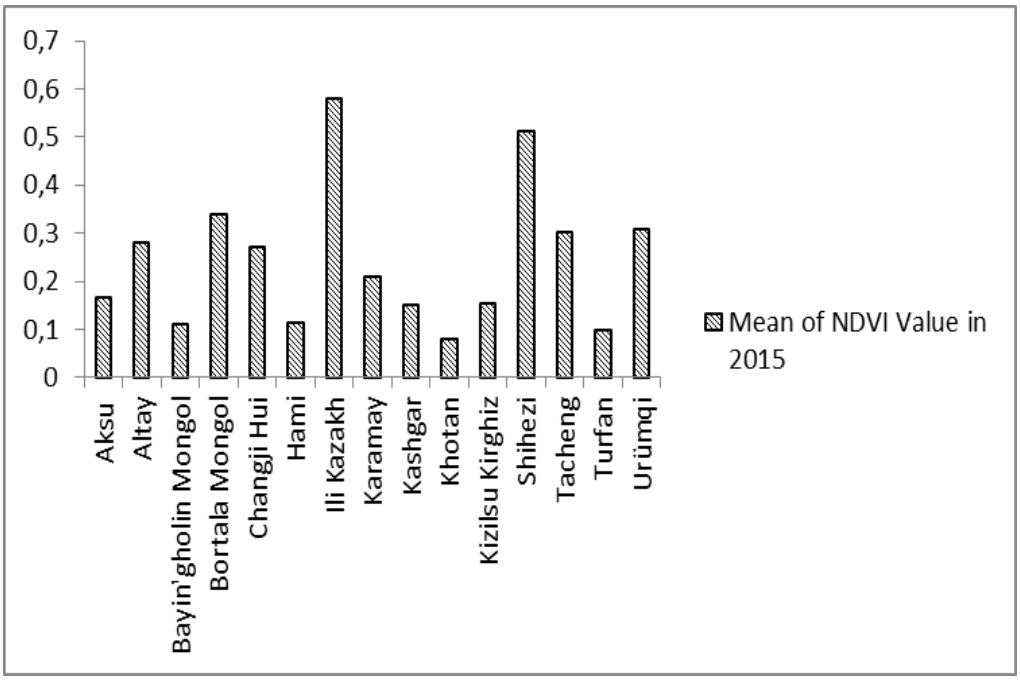

Figure 10: Statistics of average annual NDVI value based on the division of county boundaries in 2015.

Table 9: Classification of vegetation cover (NDVI) based on couty divisions in 2020.

No.	Name	Minimum	Maximum	Mean
1	Aksu	–0.069200	0.779886	0.18251
2	Altay	–0.141897	0.848825	0.27150
3	Bayin'gholin Mongol	–0.127306	0.822712	0.115179
4	Bortala Mongol	–0.135692	0.933632	0.330082
5	Changji Hui	–0.019654	0.797883	0.246454
6	Hami	–0.030933	0.652469	0.091052
7	Ili Kazakh	–0.039898	0.865697	0.541766
8	Karamay	0.036021	0.781246	0.211123
9	Kashgar	–0.057445	0.646838	0.160216
10	Khotan	–0.076941	0.614853	0.08908
11	Kizilsu Kirghiz	–0.051024	0.52605	0.166212
12	Shihezi	0.134233	0.817762	0.5278
13	Tacheng	–0.043740	0.825483	0.30307
14	Turfan	0.013841	0.592871	0.0888
15	Urümqi	–0.033376	0.67819	0.267829

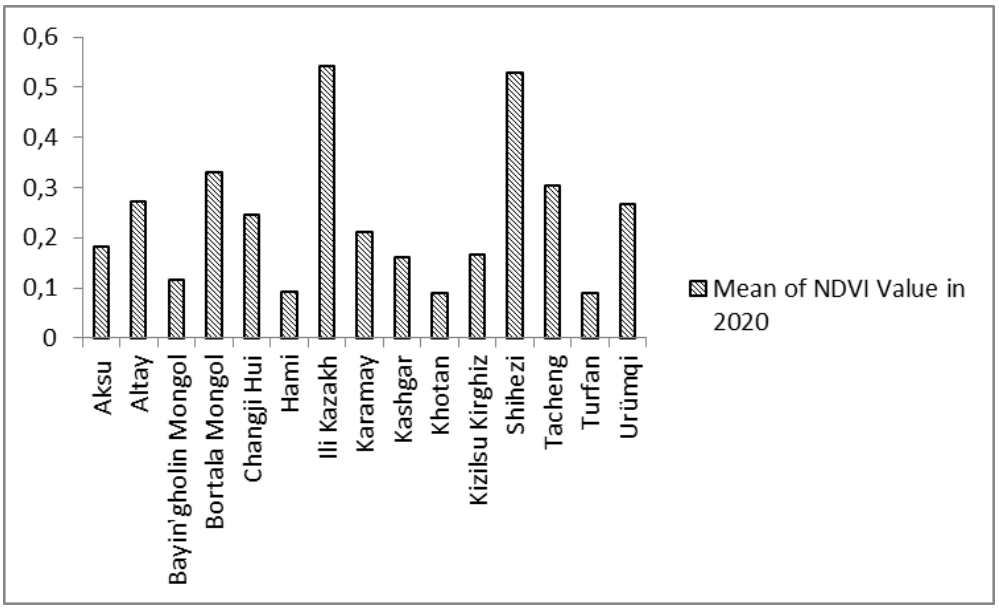

Figure 11: Statistics of average annual NDVI value based on the division of county boundaries in 2020.

Table 10: Classification of vegetation cover (NDVI) based on couty divisions in 2023.

No.	Name	Minimum	Maximum	Mean
1	Aksu	–0.060800	0.736774	0.178739
2	Altay	–0.182885	0.83864	0.271577
3	Bayin'gholin Mongol	–0.162868	0.833813	0.113792
4	Bortala Mongol	–0.177081	0.847629	0.3529
5	Changji Hui	–0.009055	0.800372	0.24254
6	Hami	–0.058832	0.640684	0.08512
7	Ili Kazakh	–0.037388	0.87388	0.579248
8	Karamay	0.038863	0.790834	0.210868
9	Kashgar	–0.076800	0.651084	0.16133
10	Khotan	–0.076644	0.558047	0.08468
11	Kizilsu Kirghiz	–0.052250	0.661522	0.166611
12	Shihezi	0.136324	0.814858	0.5312
13	Tacheng	–0.039781	0.841734	0.29065
14	Turfan	0.019744	0.576473	0.088044
15	Urümqi	–0.011569	0.687454	0.264764

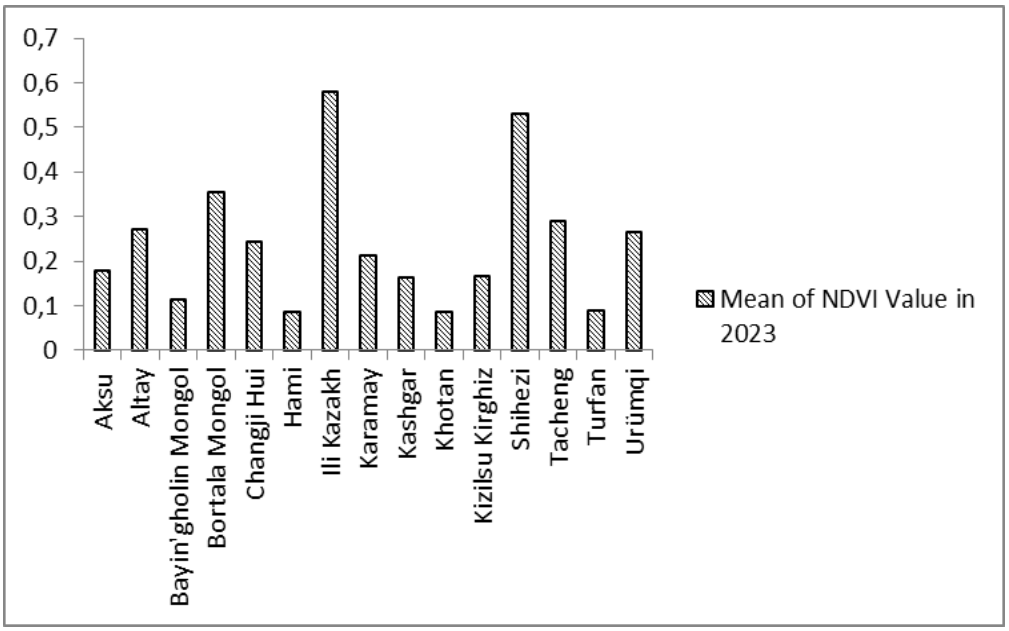

Figure 12: Statistics of average annual NDVI value based on the division of county boundaries in 2023.

However, in 2020, the NDVI value in Ili Kazakh city area decreased slightly (0.54), then increased again in 2023 (0.58). In Shihezi city, this significant trend of vegetation growth was observed, with average NDVI value reaching from 0.48 in 2000 to 0.53 in 2023.

This growth trend was seen NDVI index values for Khotan County, which had the lowest NDVI rate among the different counties of Xinjiang Province. According to tables 5-10, as well as figures 7-12, the NDVI value in Khotan County in 2000 and 2005 averaged 0.07, which gradually reached 0.08 in 2010, 2015, 2020 and 2023.

According to the information provided on the NASA Earth Observatory website (***), it is stated that low NDVI values (0.1 and below) indicate barren areas consisting of rock, sand, or snow. Moderate values (0.2 to 0.3) suggest the presence of shrubs and meadows, while high values (0.6 to 0.8) are associated with temperate and tropical rainforests. Applying this principle, it can be argued that the region of Khotan has minimal vegetation, predominantly comprising desert, sand, and rock. On the other hand, the cities of Ili Kazakh and Shihezi exhibit a relatively moderate level of vegetation, including meadows, shrubs, as well as broadleaf and coniferous species.

Monitoring and evaluation of vegetation cover from 2000-2023 using land surface measurements (Divisions by ecoregions)

Figure 13 shows the pattern of spatial and temporal changes in vegetation cover in the ecoregions of Xinjiang Province during 2000-2023 using the kernel density function.

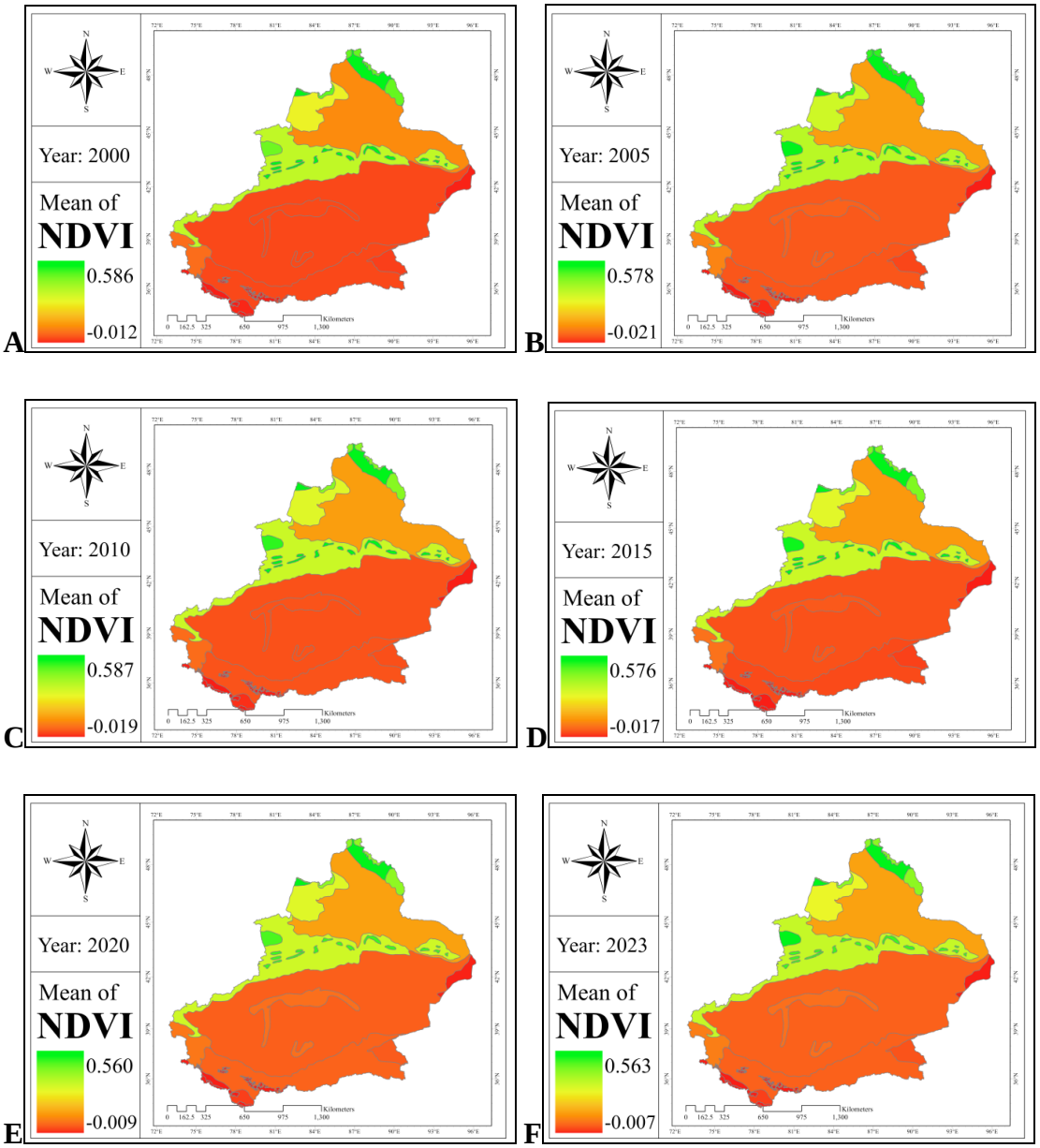

Figure 13: Patterns of temporal and spatial changes in vegetation cover using kernel density estimators in the borders of the ecorigens Xinjiang Province.

Most of the Taklimakan Desert is completely devoid of vegetation, but hardy plants such as Halogeton, Halostachys, and camelthorn grow in its foothills. Although the value of NDVI in this ecoregion is low, it has had a growing trend during the studied years, the value of NDVI increased from 0.08 in 2000 to 0.09 in 2005 and 2010 and gradually increased to 0.1 in 2015, 2020 and 2023 (Tabs. 11-16, Fig. 13).

This growing trend in the amount of vegetation was also observed in other ecoregions that have thin and scattered vegetation. Among them are the ecoregions of North Tibetan Plateau-Kunlun Mountains alpine, Junggar Basin semi-desert, Tarim Basin deciduous forests and steppe, and Pamir alpine desert and tundra, respectively in the southern, northern, central and southwest of Xinjiang Province. Therefore, in these ecoregions, the vegetation is sparse and the NDVI is low. However, in these ecoregions, the amount of vegetation has improved since 2000, with mean NDVI levels going from 0.08, 0.15, 0.08 and 0.11 in 2000 to 0.10, 0.18, 0.12 and 0.13 respectively in 2023.

Table 11: Classification of vegetation cover (NDVI) based on ecoregions divisions in 2000.

Name	Minimum	Maximum	Mean	Area of arenas with NDVI classify-cation (km^2)
Alashan Plateau semi-desert	0.020716	0.167403	0.066595	1.549515
Altai alpine meadow and tundra	–0.041297	0.8356	0.447685	1.847604
Altai montane forest and forest steppe	0.110255	0.859978	0.586297	2.038968
Altai steppe and semi-desert	0.24145	0.799791	0.521414	0.254039
Central Tibetan Plateau alpine steppe	0.0532	0.0789	0.069438	0.015808
Emin Valley steppe	0.055365	0.819484	0.290983	5.343731
Junggar Basin semi-desert	–0.171962	0.874815	0.152806	27.366403
Karakoram-West Tibetan Plateau alpine steppe	–0.062345	0.218932	0.031641	0.779973
North Tibetan Plateau-Kunlun Mountains alpine desert	–0.164422	0.513398	0.086163	19.851451
Pamir alpine desert and tundra	–0.054019	0.424546	0.119441	3.417256
Qaidam Basin semi-desert	–0.191100	0.278864	0.080643	2.209025
Rock and Ice	–0.075600	0.269455	–0.012968	1.099327
Taklimakan Desert	–0.181898	0.793929	0.086815	76.751566
Tarim Basin deciduous forests and steppe	0.016457	0.61935	0.089074	5.763608
Tian Shan foothill arid steppe	0.10338	0.789768	0.439169	0.972174
Tian Shan montane conifer forests	0.086819	0.885946	0.530611	1.425375
Tian Shan montane steppe and meadows	–0.093751	0.875281	0.353765	21.228148

Table 12: Classification of vegetation cover (NDVI) based on ecoregions divisions in 2005.

Name	Minimum	Maximum	Mean	Area of arenas with NDVI classify-cation (km^2)
Alashan Plateau semi-desert	0.024269	0.137483	0.063685	1.549515
Altai alpine meadow and tundra	–0.035260	0.83096	0.451796	1.847604
Altai montane forest and forest steppe	0.10491	0.863939	0.57805	2.038968
Altai steppe and semi-desert	0.267149	0.808383	0.544267	0.254039
Central Tibetan Plateau alpine steppe	0.0578	0.0776	0.069378	0.015808
Emin Valley steppe	0.064729	0.80623	0.317591	5.343731
Junggar Basin semi-desert	–0.192430	0.927757	0.168551	27.365448
Karakoram-West Tibetan Plateau alpine steppe	–0.064121	0.26982	0.026307	0.779973
North Tibetan Plateau-Kunlun Mountains alpine desert	–0.184302	0.550939	0.094414	19.846451
Pamir alpine desert and tundra	–0.054584	0.422466	0.13886	3.417256
Qaidam Basin semi-desert	0.171300	0.26967	0.082013	2.201525
Rock and Ice	–0.074800	0.344393	–0.021671	1.099327
Taklimakan Desert	–0.175655	0.78328	0.095594	76.756566
Tarim Basin deciduous forests and steppe	–0.122748	0.742965	0.101872	5.763608
Tian Shan foothill arid steppe	0.128404	0.761067	0.499164	0.972174
Tian Shan montane conifer forests	0.042952	0.872852	0.492354	1.425375
Tian Shan montane steppe and meadows	–0.108059	0.88735	0.342893	21.209103

Table 13: Classification of vegetation cover (NDVI) based on ecoregions divisions in 2010.

Name	Minimum	Maximum	Mean	Area of arenas with NDVI classify-cation (km^2)
Alashan Plateau semi-desert	0.0251	0.156013	0.069917	1.549515
Altai alpine meadow and tundra	–0.030100	0.8483	0.447748	1.847604
Altai montane forest and forest steppe	0.153305	0.864199	0.567695	2.038968
Altai steppe and semi-desert	0.238124	0.807561	0.587318	0.254039
Central Tibetan Plateau alpine steppe	0.066	0.0851	0.077617	0.015808
Emin Valley steppe	0.067906	0.798935	0.335793	5.343731
Junggar Basin semi-desert	–0.128363	0.820894	0.188803	27.378903
Karakoram-West Tibetan Plateau alpine steppe	–0.065062	0.195633	0.025916	0.779973
North Tibetan Plateau-Kunlun Mountains alpine desert	–0.163778	0.537248	0.102822	19.848951
Pamir alpine desert and tundra	–0.064005	0.415137	0.12624	3.417256
Qaidam Basin semi-desert	–0.187300	0.348592	0.098393	2.186525
Rock and Ice	–0.080600	0.261311	–0.019348	1.099327
Taklimakan Desert	–0.125400	0.7671	0.099849	76.726566
Tarim Basin deciduous forests and steppe	–0.011591	0.65088	0.101618	5.763608
Tian Shan foothill arid steppe	0.132332	0.795914	0.516423	0.972174
Tian Shan montane conifer forests	0.075842	0.876967	0.548598	1.425375
Tian Shan montane steppe and meadows	–0.190533	–0.878573	0.365406	21.240648

Table 14: Classification of vegetation cover (NDVI) based on ecoregions divisions in 2015.

Name	Minimum	Maximum	Mean	Area of arenas with NDVI classify-cation (km^2)
Alashan Plateau semi-desert	0.02805	0.152062	0.073175	1.549515
Altai alpine meadow and tundra	–0.014300	0.849298	0.46039	1.847604
Altai montane forest and forest steppe	0.1477	0.866951	0.571273	2.038968
Altai steppe and semi-desert	0.2203	0.808246	0.576432	0.254039
Central Tibetan Plateau alpine steppe	0.0643	0.0867	0.074508	0.015808
Emin Valley steppe	0.065934	0.830494	0.333953	5.343731
Junggar Basin semi-desert	–0.199042	0.83892	0.187073	27.371403
Karakoram-West Tibetan Plateau alpine steppe	–0.064099	0.218998	0.031506	0.779973
North Tibetan Plateau-Kunlun Mountains alpine desert	–0.199100	0.544989	0.098162	19.856451
Pamir alpine desert and tundra	–0.045398	0.469946	0.137724	3.417256
Qaidam Basin semi-desert	–0.185452	0.296632	0.091435	2.201525
Rock and Ice	–0.086180	0.290036	0.017878	1.099327
Taklimakan Desert	–0.167808	0.7579	0.10416	76.734066
Tarim Basin deciduous forests and steppe	0.030569	0.655555	0.111113	5.763608
Tian Shan foothill arid steppe	0.109939	0.825393	0.53483	0.972174
Tian Shan montane conifer forests	0.04382	0.858642	0.5565	1.425375
Tian Shan montane steppe and meadows	–0.085294	0.877921	0.368744	21.230648

The distinct topographical features found in the Tianshan and Altai mountains have resulted in the presence of abundant grassland and forest vegetation. Consequently, the ecoregions situated in this region, namely Tian Shan foothill arid steppe, Altai montane forest and forest steppe, Altai steppe and semi-desert, Tian Shan montane conifer forests, Altai alpine meadow and tundra, and Emin Valley steppe, exhibit substantial vegetation with high NDVI values. As can be seen, the revitalization and development of vegetation in these ecoregions is more prominent during the period under study. Only in 2020, NDVI decreased in these ecoregions, but it again has an upward trend and normal vegetation has increased. This revitalization and development of vegetation is more prominent in the Tian Shan foothill arid steppe ecoregion, so that its NDVI has increased from 0.48 in 2020 to 0.56 in 2023 (Fig. 13, Tabs. 15 and 16).

Table 15: Vegetation cover classification (NDVI) based on ecoregions divisions (2020).

Name	Minimum	Maximum	Mean	Area of arenas with NDVI classify-cation (km^2)
Alashan Plateau semi-desert	0.031	0.129193	0.066389	1.549515
Altai alpine meadow and tundra	–0.020200	0.8201	0.425986	1.847604
Altai montane forest and forest steppe	0.11874	0.848825	0.54862	2.038968
Altai steppe and semi-desert	0.20505	0.76781	0.560979	0.254039
Central Tibetan Plateau alpine steppe	0.0695	0.0887	0.080397	0.015808
Emin Valley steppe	0.068533	0.819078	0.324058	5.343731
Junggar Basin semi-desert	–0.141897	0.825483	0.184406	27.421403
Karakoram-West Tibetan Plateau alpine steppe	–0.042049	0.190949	0.036133	0.779973
North Tibetan Plateau-Kunlun Mountains alpine desert	–0.074712	0.614853	0.11043	19.873951
Pamir alpine desert and tundra	–0.051024	0.405781	0.13389	3.417256
Qaidam Basin semi-desert	–0.092845	0.535508	0.102987	2.241525
Rock and Ice	–0.076941	0.259547	–0.009148	1.099327
Taklimakan Desert	–0.127306	0.779886	0.107867	76.786566
Tarim Basin deciduous forests and steppe	0.034547	0.728055	0.124142	5.763608
Tian Shan foothill arid steppe	0.142023	0.859359	0.483168	0.972174
Tian Shan montane conifer forests	0.044904	0.845019	0.488253	1.425375
Tian Shan montane steppe and meadows	–0.102500	0.933632	0.34722	21.240648

Table 16: Vegetation cover classification (NDVI) based on ecoregions divisions (2023).

Name	Minimum	Maximum	Mean	Area of arenas with NDVI classify-cation (km^2)
Alashan Plateau semi-desert	0.031885	0.112891	0.06282	1.549515
Altai alpine meadow and tundra	–0.017536	0.813509	0.423099	1.847604
Altai montane forest and forest steppe	0.122865	0.83864	0.54210	2.038968
Altai steppe and semi-desert	0.21795	0.778232	0.53419	0.254039
Central Tibetan Plateau alpine steppe	0.0655	0.0856	0.078207	0.015808
Emin Valley steppe	0.060161	0.828862	0.301536	5.343731
Junggar Basin semi-desert	–0.182885	0.841734	0.18347	27.421403
Karakoram-West Tibetan Plateau alpine steppe	–0.047465	0.218858	0.046283	0.779973
North Tibetan Plateau-Kunlun Mountains alpine desert	–0.135032	0.557652	0.106581	19.873951
Pamir alpine desert and tundra	–0.057781	0.411547	0.13789	3.417256
Qaidam Basin semi-desert	–0.162868	0.353611	0.094669	2.241525
Rock and Ice	–0.076800	0.356202	–0.007643	1.099327
Taklimakan Desert	–0.145283	0.760485	0.106296	76.786566
Tarim Basin deciduous forests and steppe	0.031389	0.733905	0.12035	5.763608
Tian Shan foothill arid steppe	0.171138	0.870284	0.563711	0.972174
Tian Shan montane conifer forests	0.049584	0.864204	0.48319	1.425375
Tian Shan montane steppe and meadows	–0.060800	0.87388	0.353977	21.240648

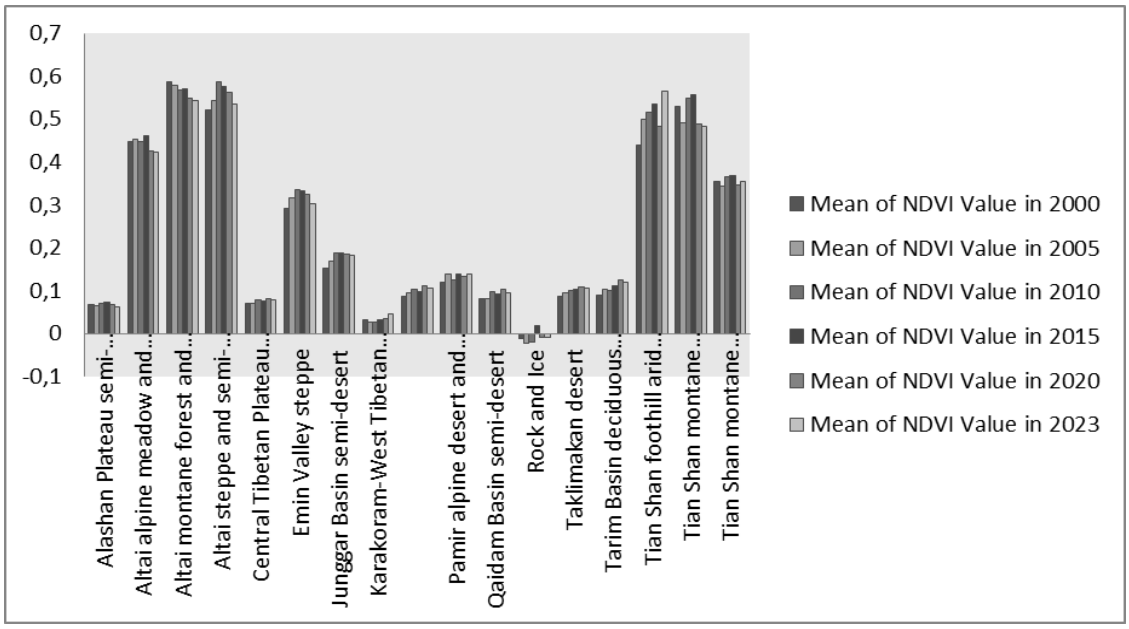

Figure 14: Column chart of average NDVI values (annual)
By ecoregion boundaries from 2000, 2005, 2010, 2015, 2020 and 2023.

Tables 11-16 as well as figure 14 show the NDVI values of different eco-origins during the studied years. As can be seen, the ecoregions located in the range of Tianshan and Altai mountains have the highest NDVI. According to the NDVI values in the mentioned tables, it can be said that there have been many changes in the vegetation of the region during different years. In 2000 and 2005, the Altai montane forest and forest steppe ecoregions had the highest NDVI values of 0.58 and 0.57 among the Xinjiang ecoregions, respectively. The highest NDVI value in 2010, 2015 and 2020 with values of 0.58, 0.57 and 0.56 belonged to Altai steppe and semi-desert ecoregion and in 2023 with value of 0.56 belonged to Tian Shan foothill arid steppe ecoregion.

Estimation of the area and percentage of afforestation and deforestation (2000 to 2022)

Changes in land use and land cover have significant impacts on ecology, the environment, and politics at both global and regional levels. Therefore, land cover monitoring and modeling is important in environmental planning and management. Figure 15 shows the spatial distribution of deforestation and afforestation in Xinjiang Province (Figure 15A), ecoregions (Fig. 15B) and counties of Xinjiang Province (Fig. 15C) from 2000 to 2022.

Additionally, the table show the changes in vegetation cover in Xinjiang Province between 2000 and 2022. Specifically, when examining the vegetation in the northern regions of Xinjiang Province, such as Altai montane forest and forest steppe, Altai steppe and semi-desert, Emin Valley steppe, and Tian Shan montane steppe and meadows ecoregions, no significant alterations have been observed. These regions collectively encompass an average area of approximately 1.665 million km² within Xinjiang Province. According to figure 15 and tables 17-18, most parts of Xinjiang Province lack vegetation (1,403,680.527 km^2). In figure 15, the areas without vegetation are highlighted with a yellow color, mainly representing the southern and central regions of Xinjiang Province. These areas include the Taklimakan Desert,

North Tibetan Plateau-Kunlun Mountains alpine desert, Central Tibetan Plateau alpine steppe, Karakoram-West Tibetan Plateau, as well as alpine steppe and Pamir alpine desert and tundra. It is worth noting that there has been no significant change in the vegetation status of these regions. From 2000 to 2022, approximately one percent of the land area in Xinjiang Province has experienced vegetation degradation.

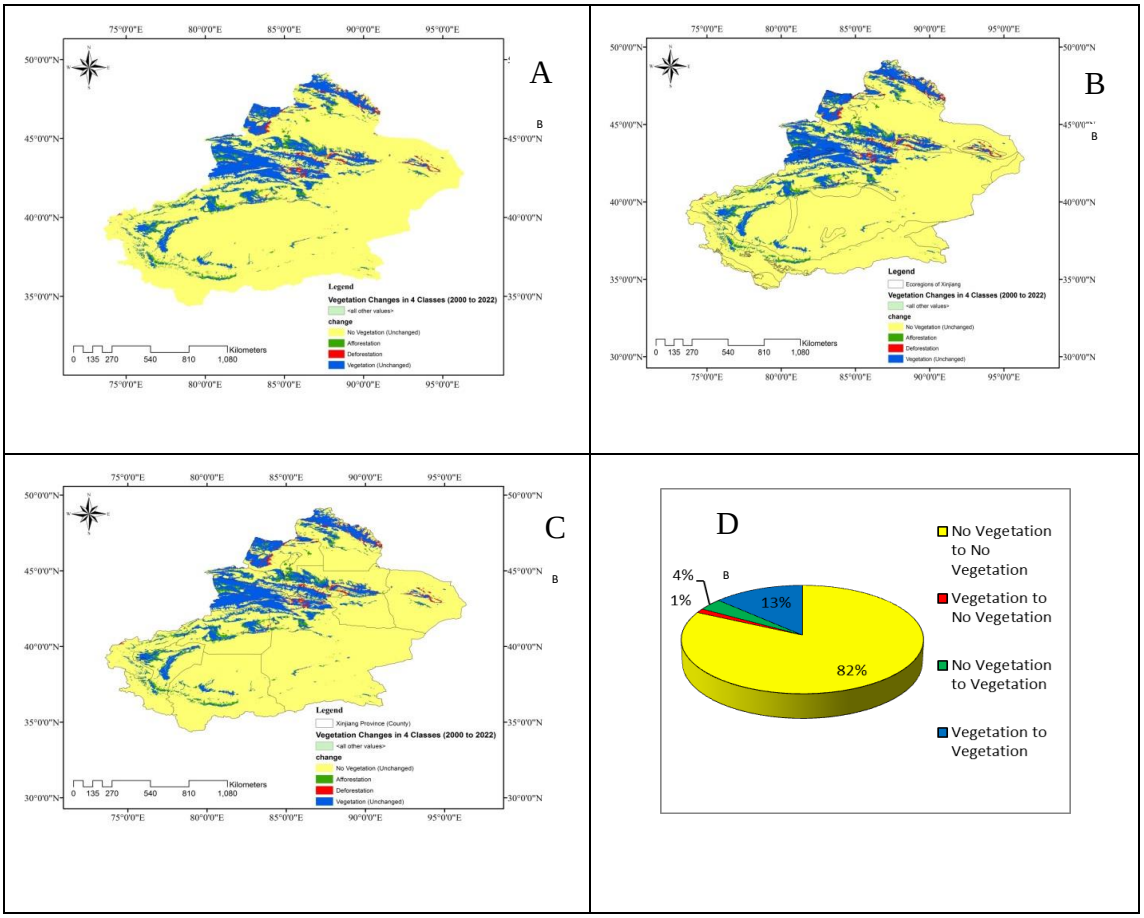

Figure 15: Visual patterns of forestry and deforestation, their area and percentage from 2000 to 2022 (Classification based on border of Xinjiang Province (A), the borders of eco-regions (B), the borders of the counties (C), the pie chart of the percentage changes in the area of afforestation and deforestation activities and other changes (D).

Deforestation and vegetation destruction have primarily occurred within the ecoregions of Tian Shan montane steppe and meadows, Emin Valley steppe, Tian Shan montane conifer forests, and Altai alpine meadow and tundra, covering an area of 21,749.34084 km^2. However, due to protective measures and efforts towards vegetation revitalization and development, significant positive ecological changes have taken place in various parts of Xinjiang Province. Notably, in an area of 59,743.718885 km^2, approximately 4% of the total area of Xinjiang Province, predominantly in the Junggar Basin semi-desert, Tian Shan foothill arid steppe, Tian Shan montane steppe and meadows, Taklimakan Desert, and North Tibetan Plateau-Kunlun Mountains ecoregions, there has been substantial restoration of alpine desert vegetation (Fig. 15).

Table 17: Area of revival and development activities and destruction of vegetation coverage in Xinjiang province from 2000 to 2022.

Vegetation changes	Area (km^2)
No Vegetation to No Vegetation	1,403,680.527142
Vegetation to No Vegetation (Deforestation)	21,749.340839
No Vegetation to Vegetation (Afforestation)	59,743.718885
Vegetation to Vegetation	223,681.424438

Figures 16 and 17 as well as table 18 show the changes in vegetation in 2022 compared to 2000. Figure 16 shows the vegetation cover has had a significant growing trend, with, 37988.61 km^2 of the target areas without vegetation cover being reduced. Also, vegetated areas in 2022 was 283,462.35 km^2, which has increased by an average of 37,988.467 km^2 compared to 2000.

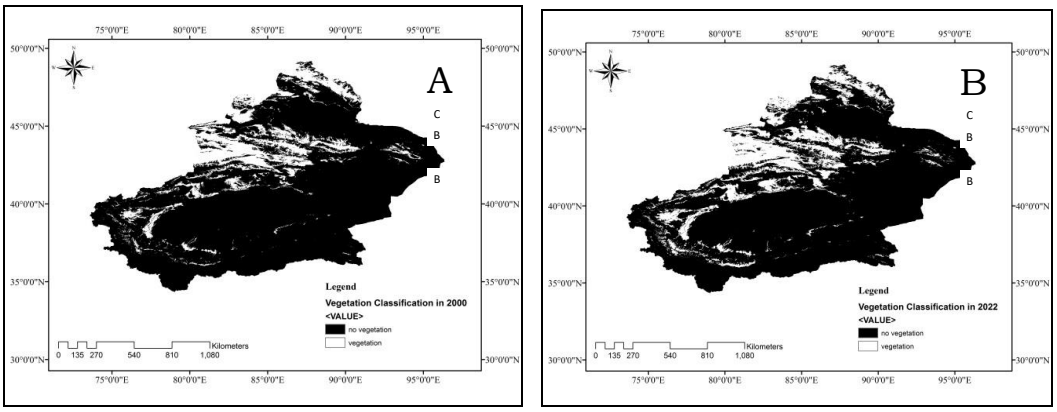

Figure 16: Visual patterns of vegetation changes based on the presence or absence of vegetation from 2000 (A) to 2022 (B).

Table 18: The area of vegetation changes in Xinjiang province from 2000 to 2022.

Vegetation changes in 2000	Area (km^2)
No Vegetation	1,463,463.10104
Vegetation	245,473.884643
Vegetation Changes in 2022	Area (km^2)
No Vegetation	1,425,474.48557
Vegetation	28,3462.351692

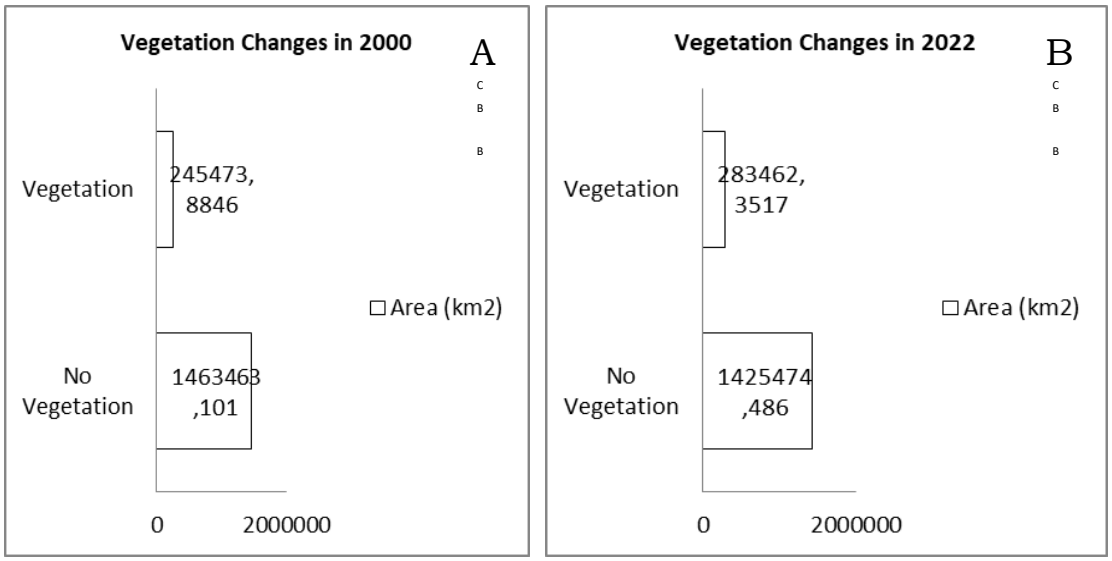

Figure 17: Models of changes in vegetation area based on the presence or absence of vegetation in square kilometers from 2000 (A) to 2022 (B).

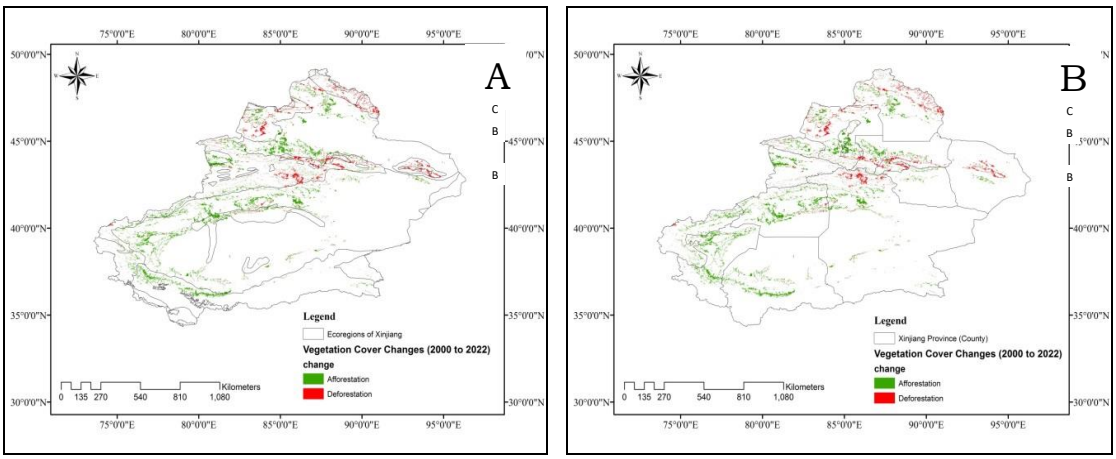

Figure 18: Visual patterns of afforestation and deforestation based on county boundaries and ecoregions in square kilometers from 2000 (A) to 2022 (B).

In contrast, deforestation has been observed in the northern and southeastern parts of Xinjiang Province, which account for only 27% of the total area. These regions correspond to the ecoregions of Altai montane forest and forest steppe, Altai alpine meadow and tundra, Emin Valley steppe, Tian Shan montane steppe and meadows, and Tian Shan montane conifer forests. In general, it can be said that vegetation has grown significantly and environmental protection measures and policies have had positive ecological effects. The area of afforestation and deforestation was 59,743.72 and 21,749.34 km^2, respectively, which means that the area of restored areas is on average 37,994.38 km^2 more than the destroyed areas (Tab. 19).

In contrast, deforestation has been observed in the northern and southeastern parts of Xinjiang Province, which account for only 27% of the total area. These regions correspond to the ecoregions of Altai montane forest and forest steppe, Altai alpine meadow and tundra, Emin Valley steppe, Tian Shan montane steppe and meadows, and Tian Shan montane conifer forests. In general, it can be said that vegetation has grown significantly and environmental protection measures and policies have had positive ecological effects. The area of afforestation and deforestation was 59,743.72 and 21,749.34 km^2, respectively, which means that the area of restored areas is on average 37,994.38 km^2 more than the destroyed areas (Tab. 19).

Table 19: Area of afforestation and deforestation in Xinjiang Province from 2000 to 2022.

Vegetation changes from 2000 to 2022	Area (km^2)
Deforestation	21,749.34084
Afforestation	59,743.71889

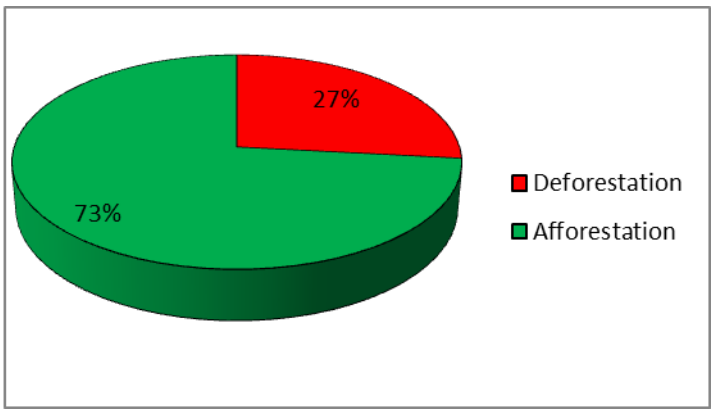

Figure 19. Circular graph percentage of afforestation and deforestation areas by percentage from 2000 to 2022.

Identifying the pattern of spatial distribution of vegetation within the study border using spatial autocorrelation (confidence level above 90% (Spatial) autocorrelation, Average Nearest Neighbor)

Tables 20-25 show clustering of the average distribution of NDVI in the ecoregions of Xinjiang Province during the years 2000-2023 respectively.

All outputs represent the same result. Hence the clusteriness of the mean distribution of NDVI at the border of the ecoregions of Xinjiang Province for 2000 which is as follows: Based on the z-score of 4.125841, it is highly improbable that this clustered pattern is due to random chance, with a probability of less than 1%.

Table 20: Clusteriness of the mean distribution of NDVI of the ecoregions of Xinjiang Province in 2000.

Moran's Index:	0/604016
Expected Index:	–0/062500
Variance:	0/026097
z-score:	4/125841
p-value:	0/000037
Global Moran's I Summary	
Input Feature Class:	Ecoregions of Xinjiang
Input Field:	Export of 2000 (Mean NDVI)
Conceptualization:	Invers Distance
Distance Method:	Euclidean
Row Standardization:	True
Distance Threshold:	628514/2532 m
Weights Matrix File:	None
Selection Set:	False

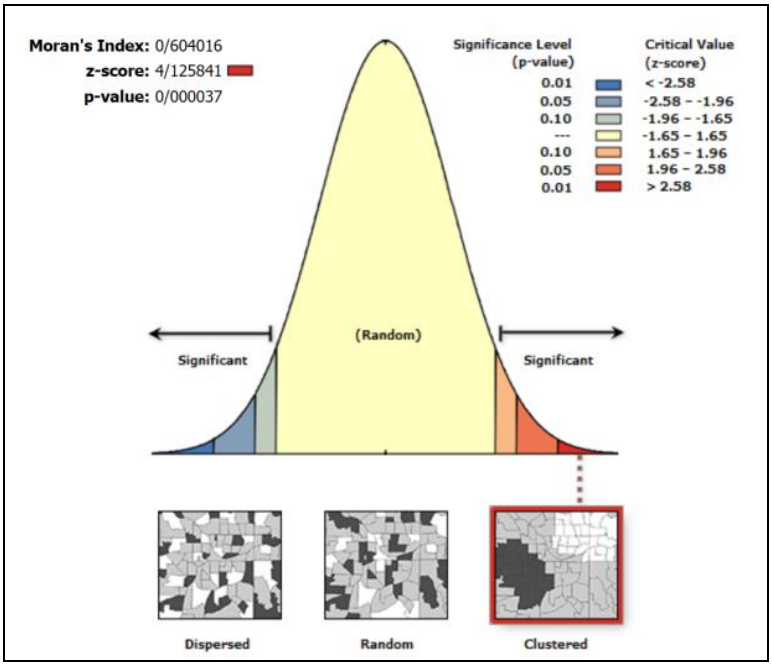

Figure 20: Moran's index for the year 2000 based on the mean NDVI distribution.

How can we interpret Moran's index? When the z-score or p-value indicates statistical significance, a positive value of Moran's I index suggests a tendency towards clustering, while a negative value of Moran's I index suggests a tendency towards dispersion. This tool calculates a z-score and p-value to determine whether the null hypotheses can be rejected. The expected value of Moran's I is –1/(N-1). Values of I that surpass –1/(N-1) indicate positive spatial autocorrelation, meaning that similar values, whether high or low, tend to cluster

together in space. Values of I below –1/(N-1) indicate negative spatial autocorrelation, where neighboring values are dissimilar (Figs. 20-24). Regarding the results in table 21 for the year 2005, the z-score of 4.202093 suggests that there is a less than 1% chance that the observed clustered pattern is due to random chance. Therefore, the result can be considered reliable. (**)

Table 21: Clusteriness of the mean distribution of NDVI of the ecoregions of Xinjiang Province in 2005.

Moran's Index:	0.617828
Expected Index:	–0.062500
Variance:	0.026212
z-score:	4.202093
p-value:	0.000026
Global Moran's I Summary	
Input Feature Class:	Ecoregions of Xinjiang
Input Field:	Export of 2005 (Mean NDVI)
Conceptualization:	Invers distance
Distance Method:	Euclidean
Row Standardization:	True
Distance Threshold:	628514.2532 m
Weights Matrix File:	None
Selection Set:	False

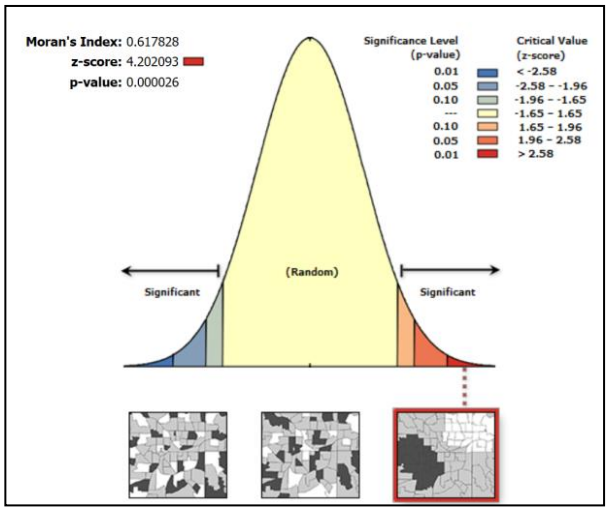

Figure 21: Moran's index for the year 2005 based on the mean NDVI distribution.

Table 22, which presents the clustering analysis of the average NDVI distribution in the ecological regions of Xinjiang Province in 2010, indicate the following: With a z-score of 4.176516, the probability of observing such a clustered pattern by random chance is less than 1%.

Table 22: Clusteriness of the mean distribution of NDVI of the ecoregions of Xinjiang Province in 2010.

Moran's Index:	0.614116
Expected Index:	-0.062500
Variance:	0.026246
z-score:	4.176516
p-value:	0.000030
Global Moran's I Summary	
Input Feature Class:	Ecoregions of Xinjiang
Input Field:	Export of 2010 (Mean NDVI)
Conceptualization:	Invers Distance
Distance Method:	Euclidean
Row Standardization:	True
Distance Threshold:	628514.2532 Meters
Weights Matrix File:	None
Selection Set:	False

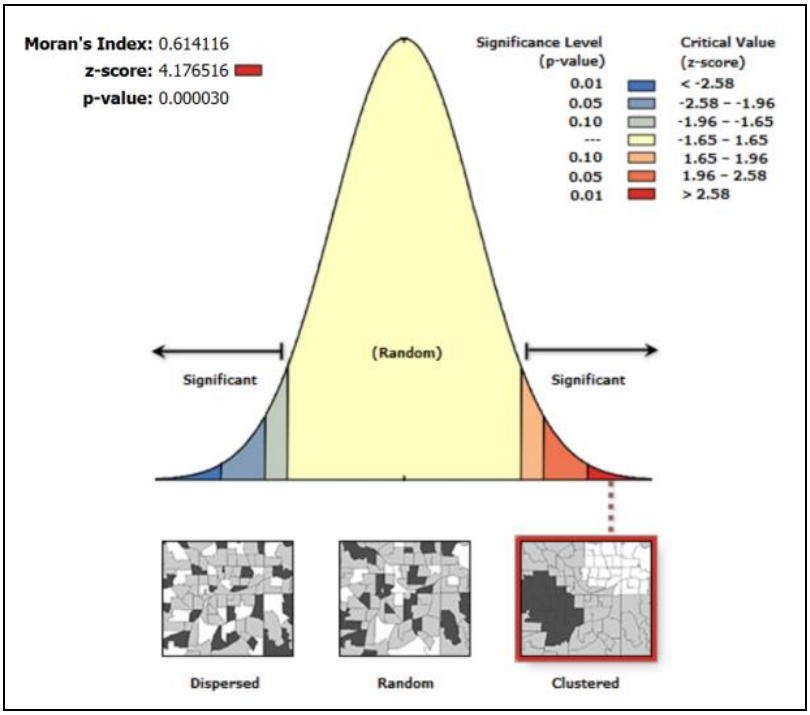

Figure 22: Moran's index for the year 2010 based on the mean NDVI distribution.

Table 23: which depicts the clustering analysis of the average NDVI distribution in the ecological regions of Xinjiang Province in 2015, reveal the following: With a z-score of 4.165062, the probability of this clustered pattern occurring by random chance is less than 1%.

Table 23: Clusteriness of the mean distribution of NDVI of the ecoregions of Xinjiang Province in 2015.

Moran's Index:	0.612921
Expected Index:	-0.062500
Variance:	0.026297
z-score:	4.165062
p-value:	0.000031
Global Moran's I Summary	
Input Feature Class:	Ecoregions of Xinjiang
Input Field:	Export of 2015 (Mean NDVI)
Conceptualization:	Invers Distance
Distance Method:	Euclidean
Row Standardization:	True
Distance Threshold:	628514.2532 Meters
Weights Matrix File:	None
Selection Set:	False

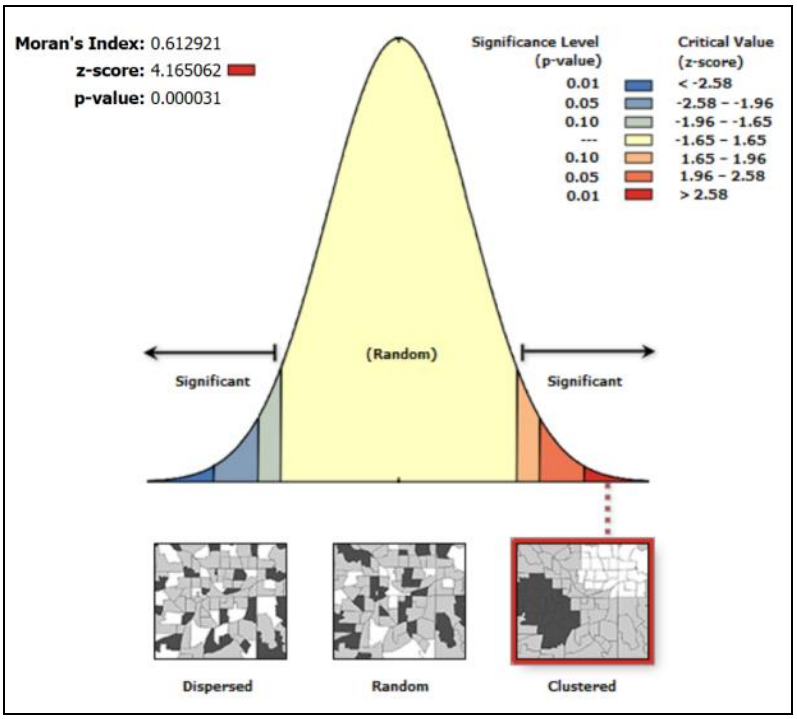

Figure 23: Moran's index for the year 2015 based on the mean NDVI distribution.

Table 24, depicting the clustering analysis of the average NDVI distribution in the ecological regions of Xinjiang in 2020, indicate the following: With a z-score of 4.232639, the probability of observing such a clustered pattern by random chance is less than 1%.

Table 24: Clusteriness of the mean distribution of NDVI of the ecoregions of Xinjiang Province in 2020

Moran's Index:	0.622168
Expected Index:	-0.062500
Variance:	0.026166
z-score:	4.232639
p-value:	0.000023
Global Moran's I Summary	
Input Feature Class:	Ecoregions of Xinjiang
Input Field:	Export of 2020 (Mean NDVI)
Conceptualization:	Invers Distance
Distance Method:	Euclidean
Row Standardization:	True
Distance Threshold:	628514.2532 Meters
Weights Matrix File:	None
Selection Set:	False

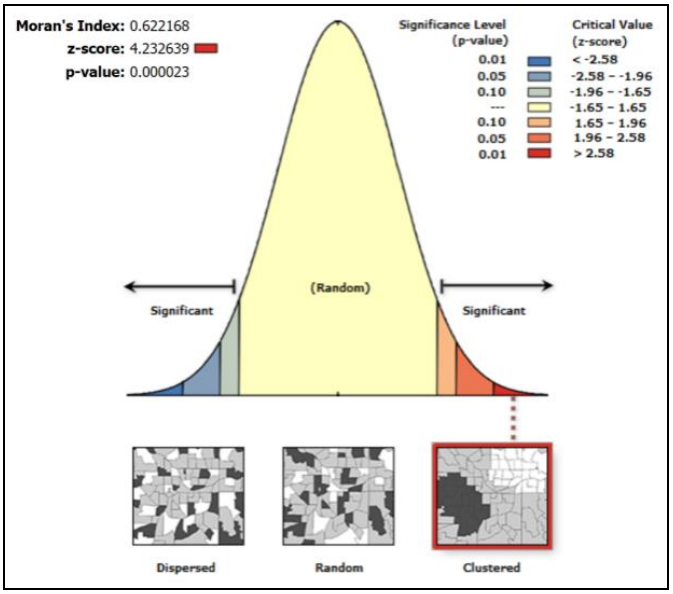

Figure 24: Moran's index for the year 2020 based on the mean NDVI distribution.

Lastly, table 25, illustrating the clustering analysis of the average NDVI distribution in the ecological regions of Xinjiang in 2023, suggest the following: With a z-score of 4.001364, the probability of observing such a clustered pattern due to random chance is less than 1%.

Table 25: Clusteriness of the mean distribution of NDVI of the ecoregions of Xinjiang Province in 2023.

Moran's Index:	0.584470
Expected Index:	-0.062500
Variance:	0.026143
z-score:	4.001364
p-value:	0.000063
Global Moran's I Summary	
Input Feature Class:	Ecoregions of Xinjiang
Input Field:	Export of 2023 (Mean NDVI)
Conceptualization:	Invers Distance
Distance Method:	Euclidean
Row Standardization:	True
Distance Threshold:	628514.2532 Meters
Weights Matrix File:	None
Selection Set:	False

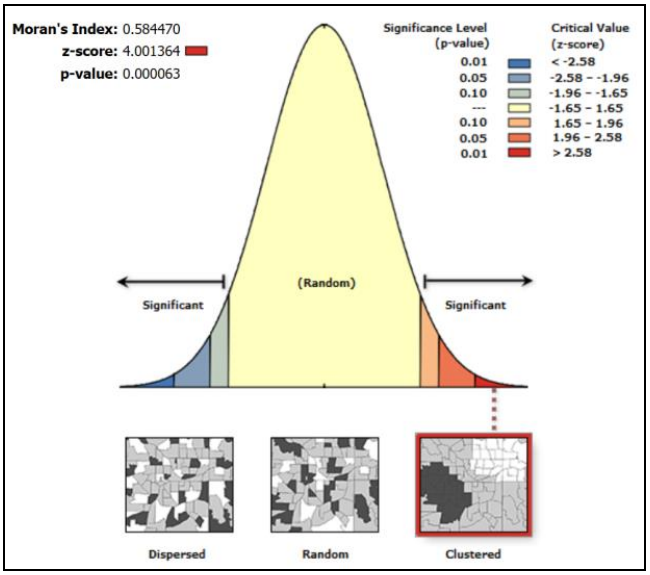

Figure 25: Moran's index for the year 2023 based on the mean NDVI distribution.

We found that z-score or p-value expressed statistical significance, as well as the Moran i-positive index value indicating a clustering tendency, while the Moran I-negative index value indicates a dispersion tendency. The tool utilizes a z-score and p-value to determine the possibility of rejecting null assumptions.

The expected value of Moran's I is -1/(N-1). I values exceeding –1/(N-1) indicate positive spatial correlation, where similar values, whether high or low, tend to cluster together in space. Conversely, I values below –1/(N-1) represent negative spatial correlation, indicating that neighboring values differ from each other (Fig. 25).

Estimation of hot spots and cold spots of vegetation within the border of the study area (confidence level > 90%) using hot spot analysis, clusters and outliers.

According to Moran outputs, for all the years studied 2000 to 2023, NDVI spatial distribution patterns were calculated in clusters (Figs. 26A,B).

One point that has caused this distribution to be clustered is how the ecoregions are distributed. If we look closely, the highest NDVI average is more common in the northern and northwestern parts, and it's actually more concentrated, and that shows the cluster distribution pattern, and it's been going the same way all year. Itis the same locally.

Hot spots and cold spots of NDVI, were calculated with confidence percentages of 90, 95 and 99 percent, which certainly increases the percentage of confidence. The following patterns show the north and northwest parts are definitely considered hot spots because there is the highest percentage of average NDVI in these areas (Figs. 26A,B).

Ecoregions include cold spots as well as not significant are also clearly marked which make up the southern and central parts of the ecoregions of Xinjiang Province.

The high high cluster relates to the hot spots that are available in the Tian Shan ecoregions and northwestern Xinjiang Province, and the high low outlier, which is red, and the low low outlier, which are blue, which are described as inconveniences. Low low cluster are clusters that express cold spots that spread in the southern parts, and clusters that have a very low confidence percentage are not significant, which are shown white (Figs. 26A,B).

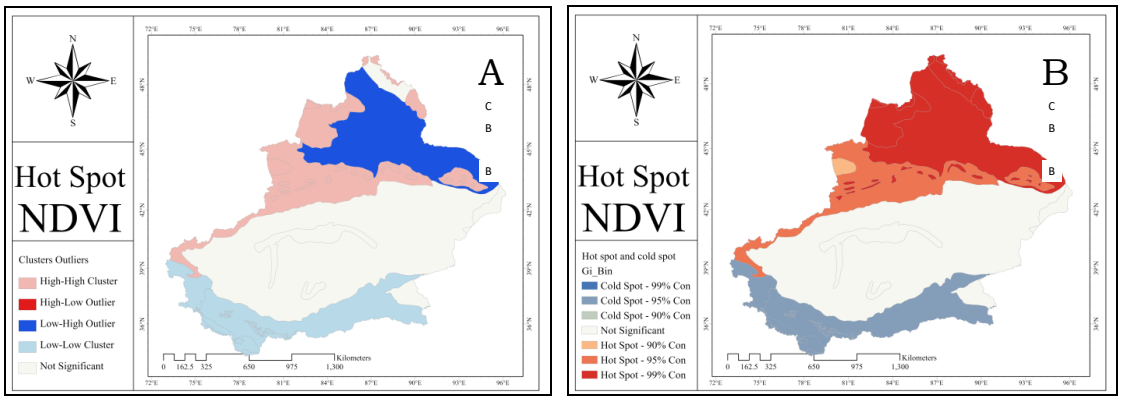

Figure 26: Spatial patterns of hot and cold spots changes in vegetation based on the boundaries of the ecoregions of Xinjiang Province (Clusters outliers is A, Hot Spot and Cold Spot is B).

Identification of factors affecting the distribution of vegetation within the study border (land use land cover, LST, rainfall, slope, elevation) by OLS

Ordinary Least Squares regression (OLS) is a widely used method for estimating the coefficient of linear regression equations. It helps describe the association between a dependent variable and one or more quantitative independent variables, whether it is a simple linear regression or multiple linear regression. In this calculation, NDVI is the dependent variable of the research and LULC, LST, Slope, Rainfall and Elevation are considered independent variables. The results are shown in figure 27.

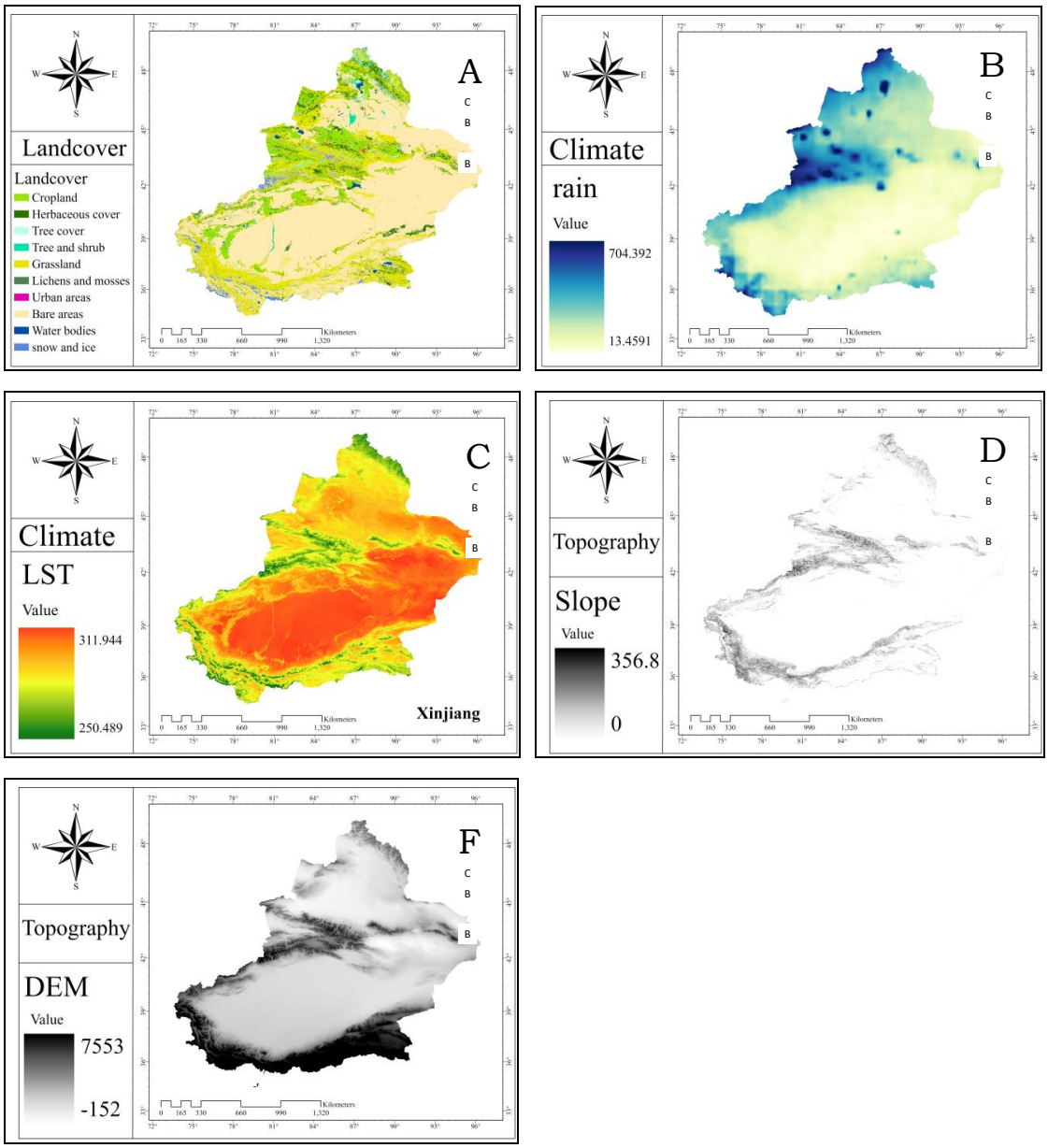

Figure 27: Spatial patterns of effective land use land cover (A), rainfall (B), LST (C), slope (D), elevation (E) drivers on vegetation distribution in Xinjiang Province.

Table 26: Summary of OLS results between NDVI and LULC model.

Variable	Coefficient [A]	Stderror	T-Statistic	Probability [B]	Robust_SE	Robust _T	Robust _Pr [B]
Intercept	–0/613850	0/129693	–4/733110	0/000268*	0/113681	–5/399769	0/000074*
LULC model	0/544243	0/080852	6/731360	0/000007*	0/069100	7/876157	0/000001*

In table 26, the column for Coefficient [a] shows the extent and manner of the relationship between LULC and NDVI. This relationship is strong (0.54) and it should have been predicted like this, and the relationship is also positive. For this connection to be meaningful, refer to the Probability [b] columns and Robust_Pr [b], we see that the numbers are less than 0.03 and are especially starred, the stars of the results indicate the significance of this relationship and we can calculate that LULC is a driver that has a complete impact on NDVI and has a positive relationship.

Table 27: Summary of OLS results between NDVI and LST model.

Variable	Coefficient [A]	Stderror	T-Statistic	Probability [B]	Robust_SE	Robust _T	Robust _Pr [B]
Intercept	1/104029	1/661837	0/664342	0/516554	1/564522	0/705665	0/491210
LST model	–0/003002	0/005791	–0/518356	0/611774	0/005384	–0/557562	0/585370

Table 27 shows the summary of OLS results between NDVI and LST models dedicate that they have a negative relationship with each other (Coefficient [a]) and this value is equal to –0.003002, in fact, areas covered with dense vegetation have low LST values and this relationship also argues this point. Unfortunately, the relationship between LST and NDVI is not very significant according to the Probability column [b] and Robust_Pr [b].

Table 28: Summary of OLS results between NDVI and rainfall model.

Variable	Coefficient [A]	Stderror	T-Statistic	Probability [B]	Robust_SE	Robust _T	Robust _Pr [B]
Intercept	–0/033441	0/107761	–0/310326	0/760585	0/052291	–0/639516	0/532133
Rainfall model	0/001301	0/000470	2/768490	0/014340*	0/000370	3/518273	0/003106*

Table 28 shows there is a statistically significant relationship between NDVI and rainfall. However, the impact of this relationship is not as strong as the influence of the LULC factor.

Table 29: Summary of OLS results between NDVI and elevation model.

Variable	Coefficient [A]	Stderror	T-Statistic	Probability [B]	Robust_SE	Robust _T	Robust _Pr [B]
Intercept	0/414286	0/078734	5/261874	0/000096*	0/085896	4/823133	0/000225*
Elevation model (DEM)	–0/000064	0/000025	–2/561612	0/021689*	0/000019	–3/423192	0/003775*

Focusing on the column Coefficient [a] and Probability [b] in table 29, the results show a meaningful and inverse relationship between NDVI and DEM with confidence level and value of –0.00006, although this relationship is not very strong, but this relationship can be trusted. It is interpreted as having more vegetation in areas where there is less height.

Table 30: Summary of OLS results between NDVI and slope model.

Variable	Coefficient [A]	Stderror	T-Statistic	Probability [B]	Robust_SE	Robust _T	Robust _Pr [B]
Intercept	0/253870	0/083998	3/022338	0/008573*	0/069781	3/638121	0/002430*
Slope model	–0/001246	0/007745	–0/160889	0/874325	0/006483	–0/192223	0/850144

The relationship between NDVI and slope is inverse but not a significant relationship (Tab. 30). Among the results, LULC factor is the most effective factor affecting NDVI and after LULC factor, the LST factor is not very significant, although it has indirect relationship and after LULC it can be the most effective factor on vegetation.

The dominant factor influencing NDVI is land use and land cover (LULC) driver, which has the strongest impact. Following the LULC driver, land surface temperature (LST) factor can also be considered significant, although its influence is not as pronounced. Despite having an indirect relationship, the LST factor becomes the most influential factor in the distribution and growth of vegetation within the counties and boundaries ecoregions of Xinjiang Province after the LULC driver.

DISCUSION

Many research studies claims that vegetation is an important part of the Earth's ecosystem and biosphere, which, in addition to affecting biogeochemical cycles, carbon balance regulation and maintaining climate stability, water and soil protection, is responsible for an important part of completing the energy cycle as well. On the other hand, monitoring and modeling the time and place changes in vegetation cover and predicting the processes affecting it are considered an integral part of ecological resource and reserve management. Recently, understanding dynamics of vegetation patterns, mainly caused by various natural and human factors such as climate and soil changes, land use changes, wildfires, and mining measures, has become widespread. Therefore, this article attempts to revise a model of changes in vegetation and natural and human drivers affecting the temporal spatial distribution process and dynamics of vegetation at the scale of the counties and ecoregions in Xinjiang Province from 2000 to present. Satellite platforms such as Modis/Terra, CHIRPS, Sentinel 1-2 and GTOPO30 platforms were used to extract the NDVI, LST, precipitation (rainfall), global land cover product and DEM data respectively. NDVI was inserted into the dependent variable and effective drivers were also listed as LULC, LST, precipitation (rainfall), elevation and slope. Methods of calculating and zoning vegetation, predicting mean, minimal and maximum values, temporal and spatial patterns of vegetation, distribution and changes in their area in km^2, kernel density and point density, estimation of afforestation and deforestation, spatial distribution patterns with confident level, identification of hot and cold spots and prediction of drivers affecting the development and distribution of vegetation were considered the most important methodological elements of the study. Terrain factors, such as altitude, play a role in influencing vegetation coverage. Changes in effective accumulated temperature and soil moisture caused by altitude variations can impact vegetation growth (Liu et al., 2023). The output findings from this research argue that; interpretation of the digital elevation model (DEM) and slope argues the study boundaries have expanded between altitude levels –152 m and 7,553 m and fluctuations of 0 to 356 degrees that, in conjunction with patterns of average annual precipitation 0 to 704 mm and average annual LST 250 to 311 K, have created a wide range of herbaceous plant species, shrubs, and broadleaf and coniferous trees. In a study conducted by Wang et al. (2022) in Southeast Tibet, it was observed that vegetation patterns

exhibit noticeable spatial variations with changes in elevation. The impact of slope and aspect on NDVI change was found to be relatively less significant compared to elevation. Similarly, Xianghong et al. (2015) found in their research in China that elevation plays a crucial role in determining local-scale land use spatial patterns. Areas below 400 m in elevation tend to have higher land use intensity, and it decreases significantly as the elevation increases. LULC driver alignment also assessed that the highest amount of area is related to the bare area class, which is 139,433.7 km^2, which occupies almost 61.49% of the study area, and the lowest amount of area is related to the lichens and mosses class, which accounts for 41.8 km^2, or 0.018% of the total studied area. The grassland and crop land occupy 21.2% and 7.17%, and were calibrated in second and third place after bare land respectively.

When studying the spatio-temporal dynamics of vegetation, the Normalized Difference Vegetation Index (NDVI) serves as a vital indicator to assess the state and distribution patterns of plant growth at both global and regional scales. It also enables the observation of long-term vegetation changes over time (Zhuang et al., 2020; Gadiga, 2015). We utilized the NDVI of natural vegetation to track vegetation dynamics. Our analysis revealed that the highest NDVI value, reaching 0.933, was observed in July for 2020, indicating vigorous vegetation growth. This predicted value represents areas with dense vegetation which were occupied western, northwestern and north regions likewise Tian Shan and Altai ecoregions, whereas findings represented the lowest NDVI value of –0.199 corresponded to 2010, which has the presence of abundant sand, rocks such as Taklimakan Desert in the central, east and southern ecoregions in fact.

2015 had the highest area of the regions, with NDVI value of more than 0.5, (149,450.6 km^2), and 2000 also experienced the largest area corresponding to areas with a NDVI value ofless than 0.5 (1614503.6 km^2). Therefore, 2015 has experienced the highest level of dense vegetation, and 2000 is also covered with sporadic and vast vegetation community.

Overall, the findings argued that areas where NDVI value has decreased to less than 0.5, their area also declined from 2000 to 2023, or the area NDVI value more than 0.5 increased, which indicates the existence of suitable conditions for the development of vegetation as well as the correct management of the areas studied by humans. The rising number of positive NDVI values indicates a growth in the extent of green vegetation.

Interpretation of visual patterns and robust statistical parameters proved that afforestation activities have increased by 4% from 2000 to 2022 that covers an area of 59,743.71 km^2 in all the studied boundaries, which is very commendable. Areas that had a diversity of vegetation cover have also benefited from the process of restoration, development and proper management of vegetation cover during the same period, with the area reaching 13%, which occupies approximately 223,681.42 km^2 of the total studied area in Xinjiang Province.

Countries and international organizations worldwide are slowly but surely acknowledging the threats and risks accompanying the deteriorating and declining vegetation coverage and are implementing various complex measures to safeguard vegetation (Wang et al., 2023). Over the past five decades, the Chinese government has actively promoted the implementation of multiple environmental protection initiatives, resulting in significant positive changes in vegetation cover. Noteworthy projects include the Grain for Green Project, the establishment of the Three-North Shelterbelt Program, and the conservation of natural forest resources.

Amendments and enhancements to the "Forest Law of the People's Republic of China" have been implemented alongside ecological programs aimed at curbing deforestation and increasing forest area. Since 2000, one such ecological restoration initiative is the "Returning Cultivated Land to Forests and Grasses Project" (Wang et al., 2023; He et al., 2023; Han et al., 2022; Yin et al., 2018). Based on the results of various studies, this set of measures has had an effective role in the growth of vegetation, in this regard, the results of the studies of Zhuang et al. (2020), in Xinjiang and Zhong Bao et al. (2008), Xuemei et al. (2016), Karnieli et al. (2014), Shan et al. (2022), He et al. (2023) in other parts of China, indicates that the vegetation cover has an upward trend.

Also, cluster distribution and hot and cold spot processors calculated at 90, 95 and 99 percent confidence levels that the borders of the ecoregions in the northern and northwestern regions of Xinjiang Province certainly formed the high percentage of the average value of the NDVI. The central and southern ecoregions were found to have minor values of NDVI. The results of the OLS estimate show a strong link between NDVI and LULC valued at 0.54, which is significant. Vegetation is very sensitive to climate change (Wang et al., 2023) hence, it becomes vital to examine the spatio-temporal vegetation changes and how it responds to long-term climate changes. The findings reveal a weak relationship between NDVI and LST, with a value of –0.003. This lack of significance is evident in both the probability and robust probability analyses. Notably, areas characterized by dense vegetation exhibit lower LST values, which aligns with this relationship. Similarly, a study of Gang et al. (2016) in Central Asia yielded similar results, indicating a weak negative correlation between annual NDVI and temperature. The relationship between precipitation and NDVI was significant with a value of 0.001, although precipitation drivers are not as effective as LULC. In this particular context, various studies conducted by Liu et al. (2006) and Sun et al. (2001) in the Yellow River Basin, China, Zhong Bao et al. (2008) in the Loess Plateau, China, and Xuemei et al. (2016) in the Hexi region of Northwest China have revealed a positive correlation between NDVI and precipitation. Precipitation is identified as the primary driver of vegetation growth, while temperature plays a moderating role in this process (Li et al., 2022). Additionally, it has been observed that there are time lags in the response of NDVI to changes in precipitation (Gang et al., 2016).

There is a meaningful and inverse relationship between NDVI and DEM with confidence level and value of –0.00006, showing that vegetation is more present at lower altitudes. The OLS model also showed a negative relationship between NDVI and slope with the confidence level –0.0012 which was not very noticeable. Henceforth, the LULC driver is the most effective factor affecting NDVI, and the LST driver can be practically emphasized after the LULC, but it is not strongly meaningful, although it has an indirect relationship, and after the LULC driver, LST can be the most effective driver in the distribution and development of vegetation within the counties and ecoregions boundaries of Xinjiang Province. As a consequence, NDVI is an important vegetation indicator that reflects the state of the regional climate and the environment drivers, which are significantly affected by precipitation, temperature, topographic complications, and human activities.

CONCLUSIONS

Vegetation holds great significance within the ecosystem, and any form of destruction can have detrimental consequences for the environment. Hence, it is crucial to actively monitor, conserve, and sustainably utilize this vital resource. The dynamics of vegetation patterns involve complex processes influenced by a range of biological and human-induced factors, including climate change, changes in land use, and ecological engineering practices. The findings of this study indicate that the dynamics of vegetation cover are impacted by various environmental factors, notably land use and land cover (LULC), land surface temperature (LST), rainfall, elevation, and slope. Moreover, the implementation of diverse vegetation protection policies has proven effective in rejuvenating and fostering vegetation growth. Utilizing the Normalized Difference Vegetation Index (NDVI) to examine vegetation dynamics facilitates a better comprehension of how vegetation responds to different natural and human variables.

ACKNOWLEDGEMENTS

This research was supported by Xinjiang Institute of Ecology and Geography, Chinese Academy of Sciences, Urumqi 830011, China, Tianchi Talents Project of Xinjiang (E3350107); National Natural Science Foundation of China (No.42107084); Key Research and Development Program of Xinjiang (2022B01032-4). Professor YU Ruide is also given special gratitude that provided insight, support and expertise that greatly assisted the research.

REFERENCES

1. Cao K., Gao J., 2022 – Assessment of climatic conditions for tourism in Xinjiang, China, *Open Geosciences*, 14, 382-392.
2. Duan H., Xue X., Wang T., Kang W., Liao J and Liu, S., 2021 – Spatial and temporal differences in alpine meadow, alpine steppe and all vegetation of the Qinghai-Tibetan Plateau and their responses to climate change, *Remote Sensing*, 13, 669, DOI: 10.3390/rs13040669.
3. Elsu C. A., Ramesh K. V. and Sridevi H., 2017 – Quantification and understanding the observed changes in land cover patterns in Bangalore, *International Journal of Civil Engineering and Technology (IJCIET)*, 8, 4, 597-603.
4. Gadiga B. L., 2015 – Monitoring the spatio-temporal dynamics of vegetation cover in Mubi Region, Adamawa State, Nigeria, *Journal of Geographic Information System*, 7, 598-606, DOI: 10.4236/jgis.2015.76048.
5. Gang Y., Zengyun H., Xi C. and Tashpolat T., 2016 – Vegetation dynamics and its response to climate change in Central Asia, *Journal of Arid Land*, 8, 3, 375-388, DOI: 10.1007/s40333-016-0043-6.
6 Han Z., Wu Q., Lai R, Soomro S., Hou D and Hu C., 2022 – Spatio-temporal variations of vegetation cover and its influence on surface air temperature change over the Yellow River Basin China, *Journal of Water and Climate Change*, 13, 9, 3239, DOI: 10.2166/wcc.2022.037.
7. He Z., Yue T., Chen Y., Mu W., Xi M. and Qin F., 2023 – Analysis of spatial and temporal changes in vegetation cover and driving forces in the Yan River Basin, Loess Plateau, *Remote Sensing*, 15, 4240, DOI: 10.3390/rs15174240.
8. Hu Y. and Nacun, B., 2018 – An analysis of land-use change and grassland degradation from a policy perspective in inner Mongolia, 1990-2015, *Sustainability*, 10, 4048, DPO: 10.3390/su10114048.
9. Hu, Y and Hu, Y., 2019 – Land cover changes and their driving mechanisms in Central Asia from 2001 to 2017 supported by Google Earth Engine, *Remote Sensing,* 11, 554, DOI: 10.3390/rs11050554.
10. Jiang M., Tian S., Zheng Z., Zhan Q and He, Y., 2017 – Human activity influences on vegetation cover changes in Beijing, China, from 2000 to 2015, *Remote Sensing*, 9, 271, DOI: 10.3390/rs9030271.
11. Jiapaer G., Liang S., Yi Q. and Liu J., 2015 – Vegetation dynamics and responses to recent climate change in Xinjiang using leaf area index as an indicator, *Ecological indicators,* 58, 64-76.
12. Karnieli A., Qin Z., Wu B., Panov N and Yan F., 2014 – Spatio-temporal dynamics of land-use and land-cover in the Mu Us Sandy Land, China, Using the change vector analysis technique, *Remote Sensing*, 6, 9316-9339; DOI: 10.3390/rs6109316.
13. Li M., Yan Q., Li G., Yi M and Li J., 2022 – Spatio-temporal changes of vegetation cover and its influencing factors in northeast China from 2000 to 2021, *Remote Sensing*, 14, 5720, DOI: 10.3390/rs14225720.
14. Li Z., Deng X., Yin F and Yang C., 2015 – Analysis of climate and land use changes impacts on land degradation in the North China Plain, *Hindawi Publishing Corporation Advances in Meteorology*, 2015, 976370, 1-11, DOI: 10.1155/2015/976370.
15. Liu Y., Haohong H. H., Meng L., Liu M., Wu Z., Liu T and Labatt D., 2023 – Spatial temporal evolution of vegetation coverage and its relationship with terrain and human factors in the upper reaches of Ganjiang River Basin, China, *Frontiers in Earth Science*, 10:1043403, DOI: 10.3389/feart.2022.1043403.
16. Liu X., Hong Z., Zhou L., Liu J., Guo X. and Li S., 2022 – Past and future of land use change in the middle reaches of the Yellow River Basin in China, *Research Square*, DOI: DOI: 10.21203/rs.3.rs-2144585/v1.
17. Liu L. Z. and Xiao J. F., 2006 – Spatial-temporal correlations of NDVI with precipitation and temperature in Yellow river basin, *Chinese Journal of Ecology*, 25, 5, 477-481. (in Chinese)

18. Lovland T. and Merchant J., 2004 – Ecoregions and ecoregionalization: geographical and ecological perspectives, *Environmental Management*, 34, 1-13, DOI: 10.1007/s00267-003-5181-x.
19. Luo M., Liu T., Meng F., Duan Y., Bao A., Xing W., Feng X., De Maeyer P. and Frankl A., 2019 – Identifying climate change impacts on water resources in Xinjiang, China, *Science of the Total Environment*, 676, 613-626.
20. Meng X., Gao X., Li S and Lei J., 2020 – Spatial and temporal characteristics of vegetation NDVI changes and the driving forces in Mongolia during 1982-2015, *Remote Sensing*, 12, 603, DOI: 10.3390/rs12040603.
21. Miao L., Feng Z., Sun Z., Moore J and Cui X., 2016 – China's land-use changes during the past 300 years: a historical perspective, *International Journal of Environtal Research and Public Health*, 13, 847, DOI: 10.3390/ijerph13090847, Posted on *Authorea* 17 Aug (2020): The copyright holder is the author/funder, All rights reserved, No reuse without permission, DOI: 10.22541/au.159769328.83108985, This a preprint and has not been peer reviewed, Data may be preliminary.
22. Sun R., Liu C. M. and Zhu Q. J., 2001 – Relationship between the fractional vegetation cover change and rainfall in the Yellow River basin, *Acta Geografica Sinica*, 56, (6), 667-672. (in Chinese)
23. Shan Y., Dai X., Li W., Yang Z., Wang Y., Qu G., Liu W., Ren J., Li C., Liang S. and Zeng B., 2022 – Detecting spatial-temporal changes of urban environment quality by remote sensing-based ecological indices: a case study in Panzhihua City, Sichuan Province, China, *Remote Sensing*, 14, 4137, DOI: 10.3390/rs14174137.
24. Tahir A. A., Quazi K. H., Sana I., Maleeha B., Hira Jannat B. and Hira J., 2019 – Investigative spatial distribution and modelling of existing and future urban land changes and its impact on urbanization and economy, *Remote Sensing*, 11, 2, 105.
25. Wang C., Wang J., Naudiyal N., Wu N., Cui X., Wei Y. and Chen Q., 2022 – Multiple effects of topographic factors on spatio-temporal variations of vegetation patterns in the three parallel rivers region, Southeast Tibet, *Remote Sensining*, 14, 1, 151, DOI: 10.3390/rs14010151.
26. Wang M., Wang Y., Li Z and Zhang H., 2023 – Analysis of spatial-temporal changes and driving factors of vegetation coverage in Jiamusi City, *Forests*, 14, 1902, DOI: 10.3390/f14091902
27. Xianfeng L., Jinshui Z., Xiufang Z., Pan Yaozhong P., Yanxu L., Donghai Z. and Lin Z. L., 2014 – Spatiotemporal changes in vegetation coverage and its driving factors in the Three-River headwaters region during 2000-2011, *Journal of Geographical Sciences*, 2014, 24, 2, 288-302. DOI: 10.1007/s11442-014-1088-0.
28. Xianghong D., Xiyong H., Yuandong W. and Li W., 2015 – Spatial-temporal characteristics of land use intensity of coastal zone in China during 2000-2010, *China Geographcal Sciences*, 25, 1, 51-61, DOI: 10.1007/s11769-014-0707-0.
29. Xuemei Y., Shizeng L., Taibao Y., Xianying X., Caizhou K., Jinnian T., Huaidong W., Ghebrezgabher M. and Zhiqi L., 2016 – Spatial-temporal dynamics of desert vegetation and its responses to climatic variations over the last three decades: a case study of Hexi region in Northwest China, *Journal Arid Land*, 8, 4, 556-568, DOI: 10.1007/s40333-016-0046.
30. Xiaoa H. and Weng Q., 2007 – The impact of land use and land cover changes on land surface temperature in a karst area of China, *Journal of Environmental Management*, 85, 245-257, DOI: 10.1016/j.jenvman.2006.07.016.
31. Xue J., Wang Y., Teng H., Wang N., Li D., Peng J., Biswas A. and Shi Z., 2021 – Dynamics of vegetation greenness and its response to climate change in Xinjiang over the past two decades, *Remote Sensing*, 13, 4063, DOI: 10.3390/rs13204063.
32. Yao B., Ma L., Si H., Li S., Gong X. and Wang X., 2023 – Spatial pattern of changing vegetation dynamics and its driving factors across the Yangtze River basin in chongqing: a geodetector-based study, *Land*, 12, 269.

33. Yin H., Pflugmacher D., Lib A., Lic Z. and Hostert P., 2018 – Land use and land cover change in Inner Mongolia – understanding the effects of China's re-vegetation programs, *Remote Sensing of Environment*, 204, 918-930, DOI: 10.1016/j.rse.2017.08.030.
34. Yu H., Bian Z., Mu S., Yuan J. and Chen F., 2020 – Effects of climate change on land cover change and vegetation dynamics in Xinjiang, China, *International Journal of Environmental Research and Public Health*, 17, 1-24.
35. Zhang X., She D., Huang X. and Wang G., 2020 – Identifying the effects of land use changes and check dams on sediment yield in a watershed of the Loess Plateau, China, *Authorea*, 17, DOI: 10.22541/au.159769328.83108985.
36. Zhao H., Li X., Ezizi M. and Yao J., 2022 – Changes in the characteristics of dry-wet periods in Xinjiang, China based on the SPEI index, *Atmósfera*, 35, 3, 483-496.
37. Zhu Z., Zhang Z ., Zhao X., Zuo L and Wang X., 2022 – Characteristics of land use change in China before and after 2000, *Sustainability*, 14, 14623, DOI: 10.3390/su142114623.
38. Zhuang Q., Wu S., Feng X. and Niu Y., 2020 – Analysis and prediction of vegetation dynamics under the background of climate change in Xinjiang, China, *PeerJ*, 8:e8282, DOI: 10.7717/peerj.8282.
39. Zhong B. X., Jiong X. X. and Zheng W. Z., 2008 – Spatiotemporal variations of vegetation cover on the Chinese Loess Plateau (1981-2006): Impacts of climate changes and human activities, *Science in China Series D: Earth Sciences*, 51, 1, 67-78.
40. * https://www.usgs.gov/special-topics/remote-sensing-phenology/science/ndvi-foundation-remote-sensing-phenology
41. ** https://pro.arcgis.com/en/pro-app/latest/tool-reference/spatial-statistics/spatial-autocorrelation.htm#:~:text=When%20the%20z%2Dscore%20or, can%20reject%20the%20null%20hypotheses
42. *** https://earthobservatory.nasa.gov/features/MeasuringVegetation

THE FIRST CULICIDAE INVENTORY IN THE REGION OF GUELMA (NORTHEAST ALGERIA)

Abdelhakim ROUIBI *,
Amna ROUIBI ** and *Adem ROUIBI* ***

* The 8 Mai 1945 University, Laboratory of Biology, Water and Environment (LBEE), Guelma Street, P.O. Box 401, DZ-24000, Algeria, rouibi.ah@gmail.com, ORCID: 0000-0002-5978-5645.
** Badji Mokhtar University, Faculty of Sciences, Department of Biology, Annaba Street, P.O. Box 12, DZ-23000, Algeria, rouibiam23@gmail.com, ORCID: 0000-0002-9962-1995.
*** Badji Mokhtar University, Faculty of Sciences, Department of Biology, Annaba Street, P.O. Box 12, DZ-23000, Algeria, rouibiadem00@gmail.com, ORCID: 0009-0009-9000-5852.

DOI: 10.2478/trser-2024-0004

KEYWORDS: Culicidae, inventory, associations, Guelma, Algeria.

ABSTRACT

Multiple studies about mosquitoes were carried out in several regions in northeastern Algeria, but the region of Guelma was not among them; therefore, the current study came to fill this void. Our inventory offered us a close knowledge of the biodiversity of Culicidae taxa in the region of Guelma that helped us define the presence of 12 species belonging to four genera (*Culex, Culiseta, Aedes,* and *Anopheles*). *Culex pipiens* (52.25%) was the most abundant species known in the north-east of Algeria. As well as *Aedes albopictus* being second (22.58%), after its new appearance in the region. Notably, results showed the first record of both *Anopheles multicolour* and *Aedes geniculatus* in the north-east of Algeria.

RÉSUMÉ: Le premier inventaire des Cuculidae dans la region de Guelma nord-est de l'Algerie.

Plusieurs études sur les moustiques ont été réalisées dans les régions du nord-est de l'Algérie, mais la région de Guelma n'en faisait pas partie; par conséquent, la présente étude est donc venue combler ce vide. Notre inventaire nous a offert une connaissance approfondie de la biodiversité des taxons Culucidae dans la région de Guelma, qui nous a permis de définir la présence de 12 espèces appartenant à quatre genres (*Culex, Culiseta, Aedes* et *Anopheles*). *Culex pipiens* (52,25%) était l'espèce la plus abondante connue dans le nord-est de l'Algérie. Ainsi qu' *Aedes albopictus* étant deuxième (22,58%), après sa nouvelle apparition dans la région. Les résultats ont notamment montré le premier enregistrement d'*Anophèles multicolor* et *Aedes geniculatus* dans le nord-est de l'Algérie.

REZUMAT: Primul inventar de Culicidae în regiunea Guelma (nord-estul Algeriei).

Mai multe studii despre țânțari au fost efectuate în mai multe regiuni din nord-estul Algeriei, dar regiunea Guelma nu a fost printre ele; prin urmare, studiul actual a venit să acopere acest gol. Inventarul nostru ne-a oferit o cunoaștere aprofundată a biodiversității taxonilor de Culicidae din regiunea Guelma, care ne-a ajutat să definim prezența a 12 specii cuprinse în patru genuri (*Culex, Culiseta, Aedes* și *Anopheles*). *Culex pipiens* (52,25%) a fost cea mai abundentă specie cunoscută în nord-estul Algeriei. La fel și *Anopheles albopictus* fiind a doua (22,58%), după noua sa apariție în regiune. În special, rezultatele au arătat prima înregistrare atât a *Anopheles multicolor*, cât și a *Aedes geniculatus* în nord-estul Algeriei.

INTRODUCTION

Insects are one of the most important classes of the arthropod phylum and have attracted great interest among ecologists in terms of their large numbers, diversity, economic importance, and health threats (Hubálek and Halouza, 1999). Mosquito-borne diseases are flourishing worldwide and are the most common of all arboviruses: malaria, dengue, West Nile fever, chikungunya, yellow fever, Japanese encephalitis, Western equine encephalitis, La Crosse encephalitis, and Zika fever (Armstrong et al., 2017; Krow-Lucal et al., 2017; Mathew et al., 2017; Aréchiga-Ceballos and Aguilar-Setién, 2015; Harris et al., 2015; Mari and Peydró, 2012; Gubler, 1998). These are a global health threat for both humans and animals. Knowing and understanding these species is necessary to implement a effective control programs. Therefore, these taxa are worth studying.

The surveillance should be designed to detect diseases and provide relevant field-based data for developing and implementing effective control measures to prevent outbreaks before significant public health consequences can occur (Bamou et al., 2021). However, the first and most important step of the control process is to identify the level of numerical density and diagnose the dominant species, because having the proper information about the insects is the key to providing an accurate scientific recommendation. In other words, effective control against mosquitoes depends on the species' life cycle (James et al., 2018).

Mosquitoes are poorly known in Algeria for two reasons: the first is that at every study we discover new distributions of mosquito species, and second, there are regions that have never been the subject of Culicidae inventory, such as the Wilaya of Guelma. Based on that, we don't have a complete picture of the populations that exist in this country.

There were inventoried in all six wilayas in the proximity to Guelma: Annaba (Boulares et al., 2023; Arroussi et al., 2021), El Tarf (Serradj et al., 2018; Houmani et al., 2017; Amara et al., 2016); Souk Ahras (Hamaidia and Soltani, 2021; Hafsi et al., 2021; Hamaidia and Berchi, 2018; Benmalek et al., 2018); Oum El Bouaghi (Messai, 2017); Constantine (Berchi, 1996); and Skikda (Rouari et al., 2022; Chahed et al., 2021; Matoug et al., 2018).

Based on data collected in the region of Guelma, which was treated using different ecological indexes, we came close to understanding the biodiversity and the distribution of Culicidae fauna in that region and its surrounding areas.

MATERIAL AND METHODS

Study area

Guelma is an inland mountain region bordered by the wilayas of Skikda, Annaba, and El Tarf in the north, Constantine in the west, Souk Ahras in the east, and finally, Oum El Bouaghi in the south (Fig. 1). It occupies a major agricultural region at 290 m a.s.l. and has multiple mountains, mainly Mahouna, Dbegh, Houara, Salaoua, and Marmoura. It is very fertile due to large and long rivers, which are oued Seybouse, that extend over 45 km from south to north. Oued Bouhamdane, which has its source in the commune Bouhamdane in the west of the wilaya, Oued Mellah is coming from the south-east. Oued Charef, which takes its source in the south of the wilaya. Guelma also has two dams: Hammam Debagh Dam on Oued Bouhamdane with a capacity of 220 HM^3 and Medjez Beggar Dam (Ain-Makhlouf) with a capacity of 2,8 HM^3.

The climatic conditions characterizing this region were predominantly distinguished by a sub-humid climate (hot summer and warm winter) with an average annual temperature between 7.7°C and 26.4°C and an annual rainfall of 0 to 623 mm according to climate data (*).

Mosquito sampling

Mosquitoes are a group of insects that, in their early stages of development, develop in a high diversity of aquatic ecosystems, including permanent and temporary habitats that can include any receptacle that accumulates water (Rueda, 2008), including the artificial ones. That's why we relied in our inventory on collecting samples of larvae from both natural and artificial aquatic habitats.

This entomological research took place in the breeding season of the year 2022, from April to November, searching for potential breeding habitats for mosquitoes. The inventory has been made by the authors by collecting larvae of mosquitoes at different sites covering the entire wilayas of Guelma (Fig. 1). For that we used the dipping method (Silver, 2008).

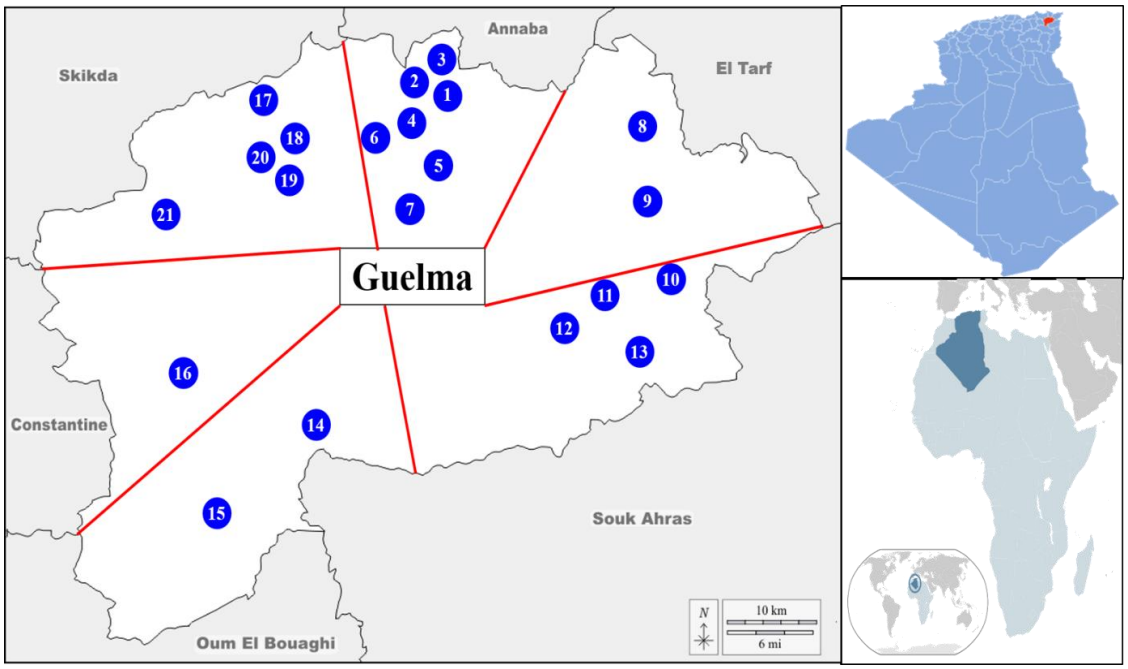

Figure 1: The location of the wilayas of Guelma and the sampling sites.

Overall, 2,435 specimens were collected from 21 stations that were organized into districts according to their closeness to the surrounding regions (Skikda Annaba, El Tarf, Souk Ahras, Oum El Bouaghi, and Constantine).

The purpose was to comparing the collected data with previous studies about the surrounding regions of Guelma.

The details and the geographical characteristics (latitude and longitude) of localities and the type of breeding sites were presented in table 1.

Table 1: Types and characteristics of sampling sites.

Communes	Stations		Type of breeding site	Coordinates	
Nechmaya	Boulekbech	S1	Grass-land pools	36°36.427'N	007°30.090'E
	Merah	S2	Tank	36°36.705'N	007°30.466'E
	Bateh	S3	Bucket	36°36.895'N	007°30.877'E
Heliopolis	Oued chiha	S4	Oued	36°34.998'N	007°25.377'E
	Hammam Bradaa	S5	Swamp	36°32.022'N	007°25.388'E
	Hammam Oulad Ali	S6	Oued	36°33.912'N	007°22.193'E
Guelma	Bourouaih	S7	Ditch	36°28.455'N	007°24.247'E
Oued Fragha	Mogsibaya	S8	Stream	36°33.828'N	007°41.736'E
	Brahmia	S9	Bucket	36° 29.902'N	007° 43.060'E
Bouchegouf	Kraimia	S10	Stream	36°26.252'N	007°41.008'E
Djeballah Khemissi	Layaicha	S11	Swamp	36°27.337'N	007°34.976'E
Boumahra	Douakha	S12	Irrigated pastures	36°26.449'N	007°34.979'E
Hammam N'Bail	Oued Helia	S13	Oued	36°23.739'N	007°36.853'E
Ain Laabi	Hammam bel hachani	S14	Bucket	36°14.196'N	007°20.152'E
Tamlouka	CCLS	S15	Swamp	36°08.987'N	007°08.536'E
Oued Zenati	Saaidia	S16	Bucket	36°19.103'N	007°09.726'E
Roknia	Chtaibi	S17	Oued	36°36.975'N	007°15.546'E
	Roknia I	S18	Well	36°33.281'N	007°14.955'E
	Roknia II	S19	Tank	36°33.412'N	007°15.875'E
	Belmars	S20	Swamp	36°32.466'N	007°14.270'E
Bouhamdane	Bouhamdane	S21	Oued	36°27.971'N	007°06.773'E

Mounting and identification of specimens

The samples collected were taken to the lab and prepared for identification. Larvae were sorted by station and date than stored in labeled tubes containing 70% ethanol. For the identification, we used both the software of the European identification key for mosquitoes (Schaffner et al., 2001), and the African identification key for mosquitoes (Brunhes et al., 2000).

Data analysis

To define the Culicidae fauna diversity in the region of Guelma, we used different statistical tools, graphs, and indices in the present study to assess the diversity between different habitats. The species richness (S) and the number of individuals (Abundance) of each species present were recorded at the study sites. We calculated the relative abundance (RA%). Shannon diversity index (H') to determine the population distribution and each community's diversity value. Also, the equitability (E), which is the relation between the population distribution and the stand structures in the study site, was calculated. In order to get the data set, we used XLStat 2014.

RESULTS

It is worth mentioning that we checked 30 aquatic habitats in the Guelma Region, but we found 21 with for mosquito larvae.

Four genera comprising 12 species, of which over 50% of samples belong to the genus *Culex*. *Aedes* comes secondly with 23.71%, followed by *Culiseta* with 15.82%, and lastly, *Anopheles* with only 3.86% (Fig. 2). As for the species, *Culex pipiens* (52.25%) was the most abundant species. *Aedes albopictus* has 22.58% of the specimens, followed by *Culiseta longiareolata* (15.82%), the only species representative of the *Culiseta* genera. On the other hand, the species accounted for the lowest percentage is *Anopheles multicolor* with only 0.12% (Fig. 3).

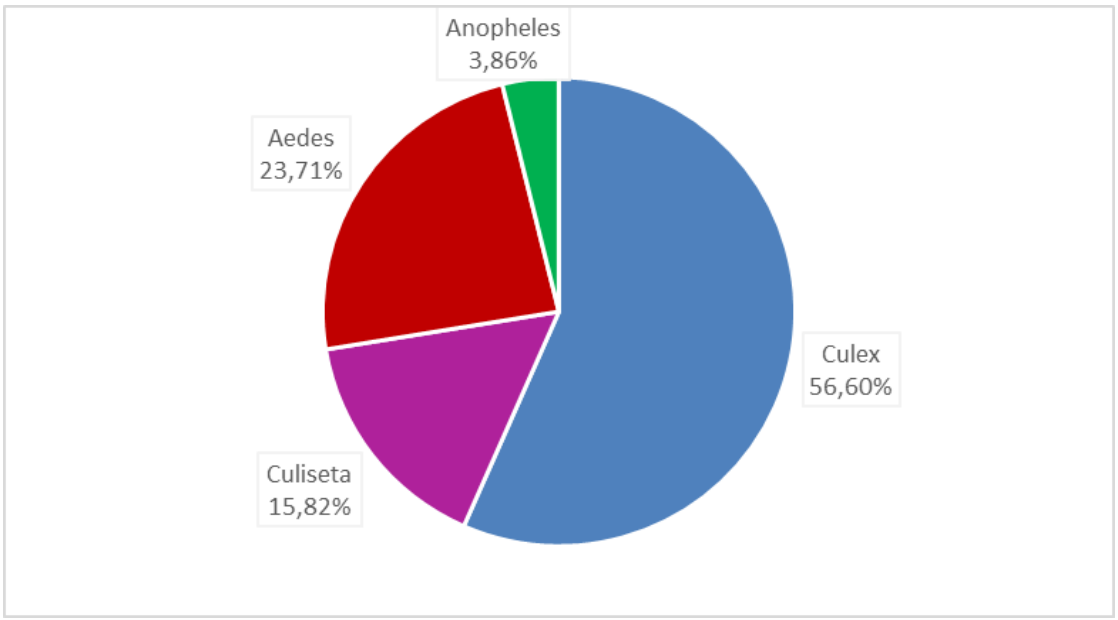

Figure 2: Frequencies of the genera collected in the region of Guelma.

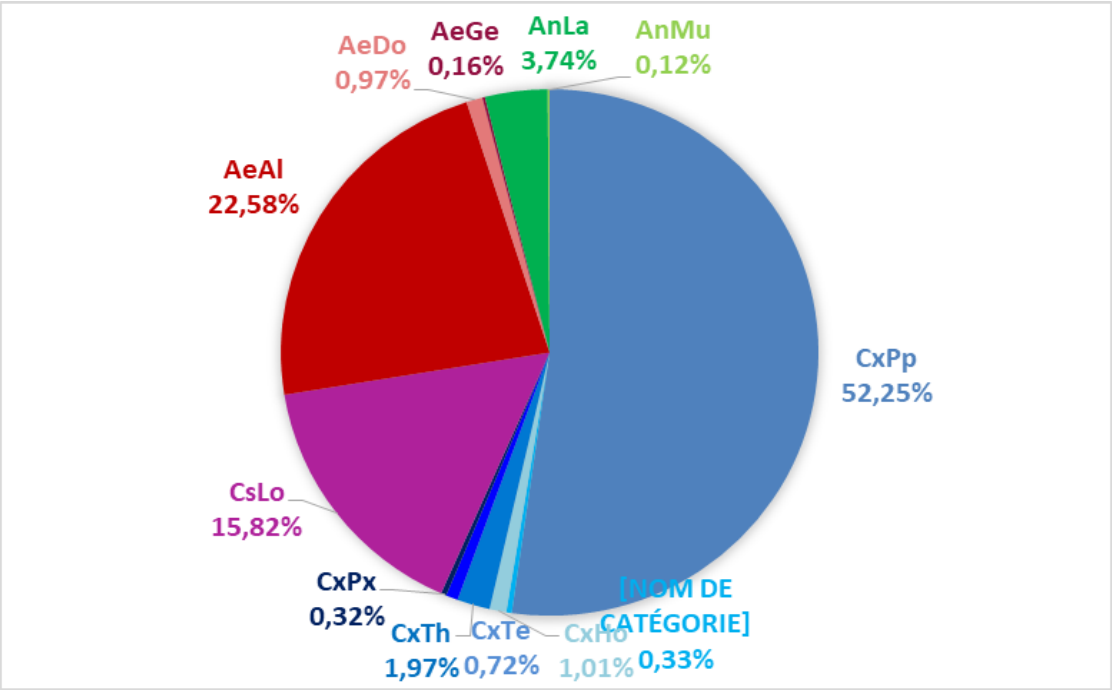

Figure 3: The frequencies of the species collected in the region of Guelma.

Samples collection sites were selected in such a way that they were close to the proximities of the wilayas in order to compare the results with previous studies conducted in those wilayas.

It was found that in the sites near Souk Ahras and Skikda, *Culex pipiens* was the most abundant species (67.59% and 73.02%, respectively), while *Aedes albopictus* species was the most abundant in the sites near Annaba (51.3%) and Tarf (38.49%), and especially Oum El Bouaghi (80.28%) and Constantine (100%). As for the Shannon index, high values were registered in the east of Guelma (Annaba, El Tarf, and Souk Ahras), while in the west (Oum El Bouaghi, Constantine, and Skikda), the lowest values were registered, as shown in table 2. As a remark, in table 2, the area near Constantine is without values for H' and E indexes because we found only one species (*Aedes albopictus*).

Most types of mosquitoes (nine species) were found only in natural breeding sites, and one species (*Aedes albopictus*) was found only in artificial sites, while two species (*Culex pipiens* and *Culiseta longiareolata*) were observed in both habitats.

Figure 4 shows the association between different mosquito species in natural breeding sites where *Culex pipiens* is present with four species: *Culiseta longiareolata*, *Anopheles labranchiae*, *Culex hortinsis* and *Culex martini*. While *Anopheles labranchiae* is frequent with eight species: *Culex pipiens*, *Culiseta longiareolata*, *Culex theileri*, *Anopheles multicolor*, *Culex territans*, *Culex hortinsis*, *Culex perexiguus*, and *Aedes geniculatus*. Besides, *Culex martinii* being found with *Culex pipiens*, it was also found with *Culex territans*. The only species found alone in natural sites is *Aedes dorsalis*.

Table 2: Spatial distribution and diversity indexes and the dominance of mosquito species recorded in the study areas. H': Shannon index, E: Equitability, RA: Relative Abundance (%). (Ae. – Aedes; An. – Anopheles; Cx. – Culex; Cs. – Culiseta).

Sites	H'	E	Species Abundance (RA%)
Near Annaba	1.37	0.66	*Cx. pipiens* (14.94%), *Cx. martinii* (0.65%), *Cx. theileri* (0.65%), *Cx. territans* (2.6%), *Cs. longiareolata* (21.1%), *Ae. albopictus* (51.3%), *Ae. dorsalis* (7.79%), *An. labranchiae* (0.97%).
Near El Tarf	1.33	0.75	*Cx. pipiens* (36.82%), *Cx. perexiguus* (3.35%), *Cs. longiareolata* (17.15%), *Ae. albopictus* (38.49%), *Ae. geniculatus* (1.67%), *An. labranchiae* (2.51%).
Near Souk Ahras	1.02	0.52	*Cx. pipiens* (67.59%), *Cx. hortinsis* (0.64%), *Cx. theileri* (9.38%), *Cx. territans* (2.13%), *Cs. longiareolata* (1.92%), *An. labranchiae* (17.7%), *An. multicolor* (0.64%).
Near Oum El Bouaghi	0.6	0.55	*Cx. pipiens* (15.14%), *Cs. longiareolata* (4.58%), *Ae. albopictus* (80.28%).
Near Constantine	–	–	*Ae. albopictus* 100%.
Near Skikda	0.7	0.39	*Cx. pipiens* (73.02%), *Cx. martinii* (0.54%), *Cx. hortinsis* (2%), *Cx. theileri* (0.27%), *Cs. longiareolata* (24.07%), *An. labranchiae* (0.09%).

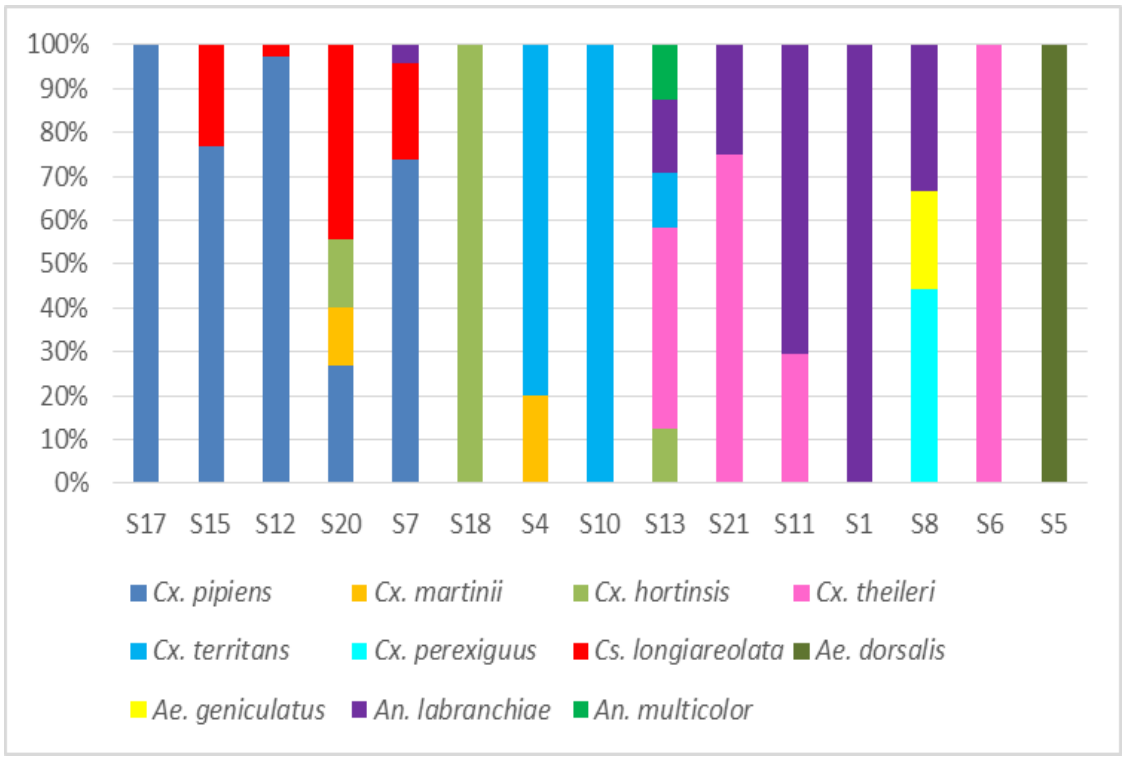

Figure 4: The association of the different species sampled in natural habitats; S-station).

Figure 5 represents the artificial sites species associations, that illustrates the presence of *Aedes albopictus* the species that only resides in artificial habitats in association with both *Culex pipiens* and *Culiseta longiareolata*.

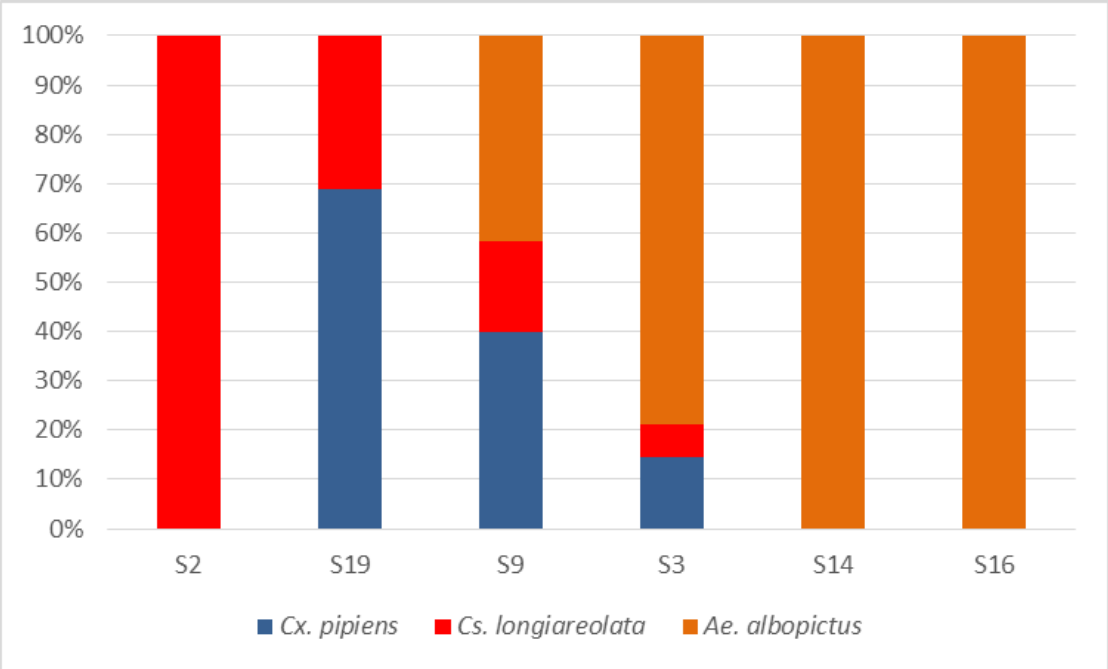

Figure 5: The association of the different species sampled in artificial habitats; S-station.

DISCUSSION

Mosquitoes have been the subject of numerous studies in Algeria, but they have been unorganized, discontinued, and without follow-up. There are areas that have been continuously the subject of Culicidae studies, while there are places that have been discarded and their mosquito populations undiscovered like the region of Guelma till now. This is illustrated by the checklist of mosquitoes by (Merabti et al., 2021).

The Culicidae populations found in the region of Guelma in this study are divided into two subfamilies, Culicinae, which are also composed of the genera *Aedes*, represented by *Aedes albopictus*, *Aedes dorsalis*, and *Aedes geniculatus*. The genus *Culex* is represented by *Culex pipiens* with the highest numbers, *Culex theileri* being the second, followed by *Culex hortinsis* and *Culex territance*, and as accessory species, *Culex martinii* and *Culex perexiguus*. And finally, the genus *Culiseta* is represented only by *Culiseta longiareolata*. For the subfamily Anophelinae with *Anopheles labranchiae* and *Anopheles multicolor*.

According to the studies conducted in the neighboring wilayas of Guelma: Annaba (Boulares et al., 2023; Rouibi et al., 2023; Arroussi et al., 2021); El Tarf (Rouibi et al., 2023; Serragd et al., 2018; Houmani et al., 2017; Amara Korba et al., 2026); Souk Ahras (Hamaidia and Soltani, 2021; Hafsi et al., 2021; Hamaidia and Berchi, 2018; Benmalek et al., 2018); Oum El Bouaghi (Messai, 2017); Constantine (Berchi, 1996); and Skikda (Rouari et al., 2022; Chahed et al., 2021; Matoug et al., 2018), the species that were found are species that are characteristic for the northeastern region of Algeria, except for two species *Aedes geniculatus* and *Anopheles multicolor* that are specific to the state of Guelma.

Natural breeding sites are most diverce habitats for Culicidae larvae in our inventory (11 out of 12 species found) even though artificial habitats have only three species (*Culex pipiens*, *Culiseta longiareolata*, and *Aedes albopictus*) 63% of samples were collected.

Mosquitoes lay their eggs at diverse sites (Machault et al., 2009), and this is related to the quantity and quality of water and the environmental characteristics of the habitat. The data we have is evidence of the difference between species oviposition, where some of them frequent only natural sites and others artificial ones, and some can be found in both.

Culex pipiens is present in most districts, known for its great ecological valence, it is present in about 90% of the prospected lodgings of Guelma which is confirmed by Himmi (2007) in Moroco and Berchi et al. (2012) in Algeria. This was confirmed in the works carried out in the wilayas neighboring Guelma. These results can only confirm this species has great ecological plasticity allowing it to colonize different types of breeding sites (F.A.O., 2009), capable of withstanding the abiotic conditions of different environments (Brunhes et al., 2000).

Anopheles multicolor has been reported from arid areas in Africa north of the Sahara Desert, from Morocco to Egypt, extending further south in the African continent along the Nile River valley and the Red Sea coast (Trari et al., 2017; Hammadi et al., 2009; Ramsdale, 1990; Kenawy et al., 1986). In sub-Saharan Africa, its presence was reported only in Niger, at the extreme northern limit of the country (Coetze, 2020). Therefore, its appearance in our data was expected due its being reported in other regions of Algeria and neighboring countries. The peculiarity of this species in our work is that we found it only in running water.

It is worth nothing that, *Aedes albopictus*, as known as the Asian tiger mosquito, was found in stations close to Annaba, where its presence had already been confirmed (Rouibi et al., 2023; Arroussi et al., 2021), as well as at El Tarf (Rouibi et al., 2023), Souk Ahras (Hafsi et al., 2021; Hamaidia and Berchi, 2018) but this species hasn't been found in both Oum El Bouaghi and Constantine yet, but our data of Guelma makes finding it there possible.

Meanwhile *Aedes geniculatus* was only found in one studied site in the wilaya of Guelma, and the studies carried out in all neighboring wilayas did not record it. Knowing that this species can be found in forest areas and moves a little (Wagner and Mathis, 2016).

The results showed a difference between the eastern and the western regions of Guelma, this is dependent on their biogeographical characteristics. When comparing the results with near wilayas, we concluded: 1. The biodiversity in the east of Guelma is richer in species than the west; east has 12 species and west seven). 2. Prior studies in the near wilayas on the west of Guelma have not found *Culex martinii*. As for *Aedes albopictus* that we found with large abundance is only declared in the wilaya of Skikda (Chahed et al., 2021). 3. The prior studies in the neighboring wilaya on the east of Guelma have not found *Aedes dorsalis. Culiseta longiareolata* was not noted in references in the Wilaya of El Tarf and *Culex martini* was not declared in El Tarf and Annaba. 4. *Anopheles multicolor* and *Aedes geniculatus* are among the species that lives in Algeria (Robert et al., 2019; Benhissen et al., 2018, 2017; Merabti et al., 2017; Merabti, 2016; Lafri et al., 2014; Hammadi et al., 2009; Brunhes et al., 2000), but they have never been found in the north east of the country. So, this is the first detection of both of them in the wilayas of Guelma and therefore in northeastern Algeria which make their appearance in neighboring wilayas possible.

The species present with low proportions are: *Culex theileri* (1.97%), *Culex martinii* (0.32%), *Culex hortinsis* (1.01%), *Culex territans* (0.72%), *Culex perexiguus* (0.32%), *Aedes dorsalis* (0.97%), *Aedes geniculatus* (0.16%), *Anopheles multicolor* (0.12%). These

percentages may reflect the beginning of the presence of these species in the region or their decline from previous high percentages, which will be confirmed in later works.

In natural sites *Culex pipiens* and *Anopheles labranchiae* are mostly present, so they are more tolerant. While we came across *Culex pipiens* with *Culiseta longieriolata* in the natural sites as proved by Moslov (1989), and these two species are also found in artificial sites with *Aedes albopictus* where the later exists only in artificial sites.

The importance of this study lies in identifying the distribution of mosquitoes in Guelma and its environs and thus identifying the extent of the spread of disease vectors, as some of the species that we found, according to Moslov (1989) and Zeller and Schuffenecker (2004), are carriers of mosquito-borne pathogens such as the West Nile.

CONCLUSIONS

In this first study of Culicidae species inventory in the wilayas of Guelma, and after selecting collection points in diverse areas of the wilaya, we conclude that: the Culicidae populations in our study area is divided into Culicinae and Anophelinae. These species have preferences when it comes to their breeding habitats some prefer natural sites and others artificial sites depending on quantity and quality of water and the environmental characteristics of the habitat. Both *Culex pipiens* and *Culiseta longiareolata* can live in natural and artificial habitats due to their great ecological valences. *Anopheles multicolor* might need more study to realize if its presence in here was due to climate change or due to the need of a new habitat. We have to highlight the possibility of finding *Aedes albopictus* in other areas close to Guelma. Meanwhile *Aedes geniculatus* could be picky about its breeding habitat therefore it wasn't found in many sites. The diversity in the east of Guelma is richer in species than in west, due to climatic factors and geographic characteristics. *Anopheles multicolor* and *Aedes geniculatus* presence in the north east of Algeria needs to be explained in deeper studies.

REFERENCES

1. Amara K. R., Boukraa S., Alayat M. S., Bendjeddou M. L., Francis F., Boubidi S. C. and Bouslama Z., 2016 – Preliminary report of mosquitoes survey at Tonga Lake (North-East Algeria), *Advances in Environmental Biology*, 9, 27, 288-294.
2. Aréchiga Ceballos N. and Aguilar-Setién A., 2015 – Alphaviral equine encephalomyelitis (Eastern, Western and Venezuelan), *Revue Scientifique et Technique*, 34, 2, 491-501.
3. Armstrong N., Hou W. and Tang Q., 2017 – Biological and historical overview of Zika virus, *World Journal of Virology*, 6, 1, 1-8.
4. Arroussi D. E. R., Bouaziz A. and Boudjelida H., 2021 – Mosquito survey reveals the first record of Aedes (Diptera: Culicidae) species in urban area, Annaba District, Northeastern Algeria, *Polish Journal of Entomology*, 90, 1, 14-26.
5. Bamou R., Mayi M. P. A., Djiappi-Tchamen B., Nana-Ndjangwo S. M., Nchoutpouen E., Cornel A. J., Awono-Ambene P., Parola P., Tchuinkam T. and Antonio-Nkondjio, C., 2021 – An update on the mosquito fauna distribution in Cameroon, *Parasit Vectors*, 14, 1, 527.
6. Benhissen S., Habbachi W. and Ouakid M.-L., 2017 – Biodiversite et repartition des moustiques (Diptera: Culicidae) dans les oasis de la region de Biskra (Sud-Est Algerien) – Biodiversity and Distribution of Mosquitoes (Diptera: Culicidae) in the Oasis of Biskra Region (South-East Algeria), *Algerian Journal of Arid Environment*, 96**,** 1-96.
7. Benhissen S., Habbachi W., Rebbas K. and Masna F., 2018 – Entomological and typological studies of larval breeding sites of mosquitoes (Diptera: Culicidae) in Bousaâda area (Algeria), *Bulletin de la Société Royale des Sciences de Liège*, 87, 112-120.
8. Benmalek L., Bendali-Saoudi F. and Soltani N., 2018 – Inventory and distribution of mosquitoes of the Burgas lakes, *Journal of entomology and zoology studies*, 6, 1, 838-843.

9. Berchi S., 1996 – Bioecologie de Culex pipiens L. (Diptera) dans la region de Constantine et perspectives de lutte, PhD Thesis, Universite Mentouri Constantine, Algeria, 1-133. (in French)
10. Berchi S., Aouati A. and Louadi, K., 2012 – Typologie des gîtes propices au développement larvaire de Culex pipiens L. 1758 (Diptera-Culicidae), source de nuisance à Constantine (Algérie), *Ecologia mediterranea*, 38, 2, 5-16. (in French)
11. Boulares M., Rehimi N., Houhamdi I., Baaloudj A., Soltani N. and Houhamdi M., 2023 – Systematic and ecological study of mosquitoes (Diptera: Culicidae) at lake Fetzara (Annaba, Northeast Algeria), *Ukrainian Journal of Ecology*, 13, 1, 1-7.
12. Brunhes J., Rhaim A., Geoffroy B., Angel G. and Hervy J.-P., 2000 – Les moustiques de l'Afrique méditerranéenne: logiciel d'identification et d'enseignement, Paris, Tunis, Institut de Recherche pour la Développment, IPT, ISBN 2-7099-1446-8. ISSN 1142-2580. (in French)
13. Rubén Bueno M. and Jiménez Peydró R., 2012 – Re-emergence of malaria and dengue in Europe, in Current Topics in Tropical Medicine, Alfonso J. R.-M. (ed.). IntechOpen, 483-512.
14. Chahed S., Nabti I., Brahmia K. and Djouaher T., 2021 – Confirmation de la présence de l'Aedes (Stegomiya albopictus (Skuse 1894)) dans deux régions littorales: Jijel et Skikda (Nord-est d'Algérie), *Entomologie faunistique - Faunistic Entomology*, 74, 66-72. (in French)
15. Coetzee M., 2020 – Key to the females of Afrotropical Anopheles mosquitoes (Diptera: Culicidae), *Malaria Journal*, 19, 1, 70.
16. F.A.O, 2009 – Renforcement de la surveillance et des systemes d'alerte pour la fievre catarrhale ovine,la fievre du nil occidental et la rage au maroc, en Algerie et en Tunisie Algeria: Food and Agriculture Organization. 14. (in French)
17. Gubler D. J., 1998 – Dengue hemorrhagic fever, *Clinical Microbiology Review*, 11, 3, 480-96.
18. Hafsi N.-E. H., Hamaidia K., Barour C. and Soltani N., 2021 – A survey of Culicidae (Diptera) in some habitats in Souk-Ahras province (Northeast Algeria), *Biodiversity Journal*, 12, 1, 3-16.
19. Hamaidia H. and Berchi, S., 2018 – Systematic and biotypical study of the family Culicidae in the region of Tebessa (Algeria), *International Journal of Mosquito Research*, 5, 2, 39-46.
20. Hamaidia K. and Soltani, N., 2021 – Short communication: New report of Aedes albopictus in Souk Ahras, Northeast Algeria, *Biodiversitas Journal of Biological Diversity*, 22, 7.
21. Hammadi D., Boubidi S. C., Chaib S. E., Saber A., Khechache Y., Gasmi M. and Harrat Z., 2009 – Malaria in Sahara, *Bulletin de la Societe de pathologie exotique*, 102, 3, 185-192.
22. Harris M. C., Dotseth E. J., Jackson B. T., Zink S. D., Marek P. E., Kramer L. D., Paulson S. L. and Hawley D. M., 2015 – La Crosse Virus in Aedes japonicus japonicus mosquitoes in the Appalachian Region, United States, *Emerging Infectious Diseases*, 21, 4**,** 646-9.
23. Himmi O., 2007 – Les Culicides (Insectes, Dipteres) au Maroc: systématique, écologie et études épidémiologiaues pilotes, These de Doctorat, Université Mohammed V, 1-295. (in French)
24. Houmani M., Bendali-Saoudi F. and Soltani N., 2017 – Inventory of Culicidae in the region of El Taref (North-east Algeria), *Journal of Entomology and Zoology Studies*, 5, 6, 263-267.
25. Hubálek Z. and Halouzka J., 1999 – West Nile fever – a reemerging mosquito-borne viral disease in Europe, *Emerging Infectios Diseases*, 5, 5, 643-50.
26. James S., Collins F. H., Welkhoff P. A., Emerson C., Godfray H. C. J., Gottlieb M., Greenwood B., Lindsay S. W., Mbogo C. M., Okumu F. O., Quemada H., Savadogo M., Singh J. A., Tountas K. H. and Touré Y. T., 2018 – Pathway to deployment of gene drive mosquitoes as a potential biocontrol tool for elimination of malaria in Sub Saharan Africa: Recommendations of a Scientific Working Group, *American Journal of Tropical Medicine and Hygiene*, 98, 6, 1-49.
27. Kenawy M. A., Beier J. C. and El Said S., 1986 – First record of malaria and associated Anopheles in El Gara Oasis, *Journal of the American Mosquito Control Association*, 2, 1, 101-103.
28. Krow-Lucal E., Lindsey N. P., Lehman J., Fischer M. and Staples J. E., 2017 – West Nile Virus and other nationally notifiable arboviral diseases – United States, 2015, *MMWR Morbidityand Mortality Weekly Report*, 66, 2, 51-55.
29. Lafri I., Bitam I., Beneldjouzi A. and Ben Mahdi M. H., 2014 – An inventory of mosquitoes (Diptera: Culicidae) in Algeria, *Bulletin de la Société zoologique de France*, 139, 1-4, 255-261.

30. Machault V., Gadiaga L., Vignolles C., Jarjaval F., Bouzid S., Sokhna C., Lacaux J. P., Trape J. F., Rogier C. and Pages F., 2009 – Highly focused anopheline breeding sites and malaria transmission in Dakar, *Malaria Journal*, 8, 138.
31. Mathew A. J., Ganapati A., Kabeerdoss J., Nair A., Gupta N., Chebbi P., Mandal S. K. and Danda D., 2017 – Chikungunya Infection: a Global Public Health Menace, *Current Allergy and Asthma Reports*, 17, 2, 13.
32. Matoug H., Merabti B., Elbah D., Tadjer W., Adjami Y. and Ouakid M. L., 2018 – Study of a culicidian stand in the El Marsa wetlands of the Skikda Region, *World Journal of Environmental Biosciences*, 7, 1, 15-18.
33. Merabti B., 2016 – Identification, composition et structure des populations Culicidiénne de la région de Biskra (Sud-est Algérien). Effets des facteurs écologiques sur l'abondance saisonnière. Essais de lutte, University of Kasdi Merbah Ouargla, Algerie, PhD Thesis, 1-175. (in French)
34. Merabti B., Boumaza M., Ouakid M. L., Carvajal T. M. and Harbach R. E., 2021 – An updated checklist of the mosquitoes (Diptera: Culicidae) present in Algeria, with assessments of doubtful records and problematic species, *Zootaxa*, 5027, 4, 515-545.
35. Merabti B., Lebouz I., Adamou A. E., Kouidri M. and Ouakid, M. L., 2017 – Effects of certain natural breeding site characteristics on the distribution of Culicidae (Diptera) mosquito species in southeast Algeria, *African Entomology*, 25, 2, 506-514.
36. Messai N., 2017 – Etude de la bioecologie et de la structure du peuplement des moustiques (Diptera: Culicidae) dans les zones humides des hautes plaines du sud Constantinois, Thèse de Doctorat, Université Frères Mentouri – Constantine, 1-126. (in French)
37. Moslov A. V., 1989 – Blood-sucking mosquitoes of the subtribe Culisetina (Diptera, Culicidae) in world fauna,Washington D. C., Smithsonian Institution Libraries, 1-248.
38. Ramsdale C. D., 1990 – Anopheles mosquitoes and imported malaria in Libya, *Mosquito systematics*, 22, 1, 34-40.
39. Robert V., Günay F., Le Goff G., Boussès P., Sulesco T., Khalin A., Medlock J. M., Kampen H., Petrić D. and Schaffner F., 2019 – Distribution chart for Euro-Mediterranean mosquitoes (western Palaearctic region), *Journal of the European Mosquito Control Association*, 37, 1-28.
40. Rouari L., Gouzi H., Ghermaoui M., Benaceur F., Kemassi A., Merabti B., Messahli I., Rezzoug A., Rouari A. and Chaibi R., 2022 – First study of larvicidal activity of Algerian Oudneya africana extracts against Culex pipiens larvae, *Ukrainian Journal of Ecology*, 12, 1, 65-70.
41. Rouibi A., Adjami Y., Merabti B., Boumaza M., Khamsa K., Rouibi A., Ramdani, K. and Ouakid M. L., 2023 – Update on the distribution and the status of the Asian tiger mosquito on the population of Culicidae in the north-east of Algeria, *Ukrainian Journal of Ecology*, 13, 1, 17-27.
42. Rueda L. M., 2008 – Global diversity of mosquitoes (Insecta: Diptera: Culicidae) in freshwater, *Hydrobiologia*, 595, 477-487.
43. Schaffner F., Angel G., Geoffroy B., Hervy J.-P., Rhaiem A. and Brunhes J., 2001 – The mosquitoes of Europe. An identification and training programme. IRD Editions & EID Méditerranée, ISBN: 2-7099-1485-9.
44. Serradj N., Bendali-Saoudi F. and Soltani N., 2018 – Inventory of the invertebrate fauna at the level of the lake of Birds (Algeria), *Journal of Entomology and Zoology Studies*, 6, 5, 98-106.
45. Silver J. B., 2008 – Mosquito ecology: field sampling methods, 3rd ed. ed, Dordrecht, the Netherlands: Springer Dordrecht, the Netherlands, 1-1477.
46. Trari B., Dakki M. and Harbach R. E., 2017 – An updated checklist of the Culicidae (Diptera) of Morocco, with notes on species of historical and current medical importance, *Journal of Vector Ecology*, 42, 1, 94-104.
47. Wagner S. and Mathis A., 2016 – Laboratory colonisation of Aedes geniculatus, *Journal of the European Mosquito Control Association*, 34, 1-4.
48. Zeller H. G. and Schuffenecker I., 2004 – West Nile Virus: an overview of its spread in Europe and the Mediterranean Basin in contrast to its Spread in the Americas, 23, 147-156.
49. * – fr.climate-.data.org

HISTOLOGICAL STUDY OF THE NERVOUS SYSTEM OF *RUTILUS FRISII KUTUM* KAMENSKY, 1901 FINGERLINGS

Zahra KHOSHNOOD *

* Islamic Azad University, Department of Biology, Dezful Branch, Dezful, Iran. Zkhoshnood@gmail.com, ORCID: 0000-0001-6340-6997.

DOI: 10.2478/trser-2024-0005

KEYWORDS: Histology, nervous system, Caspian Kutum, Caspian Sea.

ABSTRACT

The nervous system and its development play a crucial role in fish survival, locomotion and adaptation. *Rutilus frisii kutum* is one of the ecologically and economically important fish species of the Caspian Sea which is annually cultured and released in the Caspian Sea as millions of fingerlings. In order to investigate the nervous system structure of the Caspian Kutum, *Rutilus frisii kutum*, fingerlings were studied through histology technique. Results showed that the nervous system of the fingerlings is well developed, and composed of central (brain and spinal cord) and peripheral (nerves and ganglia) nervous tissue. The brain showed the normal structure of a ray-finned bony fish as in other teleosts, which shows that the fingerlings have the complete nervous system for facing and adapting to the new environment after release to the sea.

RÉSUMÉ: Étude histologique du système nerveus de *Rutilus frisii kutum* Kamensky, 1901 doigts.

Le système nerveux et son développement jouent un rôle crucial dans la survie, la locomotion et l'adaptation des poissons. *Rutilus frisii kutum* est l'une des espèces de poissons écologiquement et économiquement importantes de la mer Caspienne qui est cultivée et relâchée chaque année dans la mer Caspienne sous forme de millions d'alevins. Afin d'étudier la structure du système nerveux du Kutum caspien, *Rutilus frisii kutum*, des alevins ont été étudiés par la technique histologique. Les résultats ont montré que le système nerveux des alevins est bien développé, composé de tissu nerveux central (cerveau et moelle épinière) et périphérique (nerfs et ganglions). Brain a montré la structure normale d'un poisson osseux à nageoires rayonnées comme les autres téléostéens, ce qui montre que les alevins disposent du système nerveux complet pour faire face et s'adapter au nouvel environnement après leur libération à la mer.

REZUMAT: Studiu histologic al sistemului nervos la alevinii de *Rutilus frisii kutum* Kamensky, 1901.

Sistemul nervos și dezvoltarea lui joacă un rol crucial în supraviețuirea, locomoția și adaptarea peștilor. *Rutilus frisii kutum* este una dintre speciile de pești importante din punct de vedere ecologic și economic din Marea Caspică, care este cultivată și eliberată anual în Marea Caspică ca milioane de pui. Pentru a investiga structura sistemului nervos al speciei *Rutilus frisii kutum*, puieții au fost studiati prin tehnica histologică. Rezultatele au arătat că sistemul nervos al alevinilor este bine dezvoltat, compus din țesut nervos central (creier și măduva spinării) și periferic (nervi și ganglioni). Creierul a arătat structura normală a unui pește osos cu aripioare raze ca și alți teleostei, ceea ce arată că puieții au sistemul nervos complet pentru a se confrunta și a se adapta la noul mediu după eliberarea în mare.

INTRODUCTION

The nervous system is considered as the basis of the structural and functional mechanisms of living beings in response to environmental and internal stimuli, for this reason, the extent of the nervous system is in all parts of the body (Macdonald and Montgomery, 2003). The nervous system in fish is generally divided into two parts: the central and the peripheral nervous systems. The brain is the most specific location of the community of nerve cells in fish, and the control of different parts of the body is considered its main and primary function (Abdelnaeim Hussein and Cao, 2018).

The fish brain is relatively simple compared to the brains of mammals, but it is still capable of processing sensory information, controlling movement, and regulating basic bodily functions. The brain of a fish is divided into different regions, each responsible for specific functions such as processing visual information, regulating behavior, and controlling motor movements (Abrahão et al., 2015).

Fish also have a network of nerves that extend from the brain and spinal cord to the rest of the body, forming the peripheral nervous system. This network of nerves allows fish to sense their environment, respond to stimuli, and coordinate movements (Butler, 2011).

Water is in general under the permanent high impact of numerous stressors all over the world (Bănăduc et al., 2022, 2023).

The Caspian Sea is one of the largest enclosed seawater bodies in the world, located in the northern region of Iran. The Caspian Sea ecosystem is home to many ecologically and economically important fish species such as the Caspian Kutum, *Rutilus frisii kutum* (Khoshnood et al., 2013).

For maintenance and protection of the fish population in such an endangered ecosystem, millions of fingerlings are produced and released annually into the sea by the Iranian Fisheries Organization, These fingerings face different environmental factors and need to be prepared and capable of coping with them, therefore, having a complete and functional nervous system would be one of the key factors for such situation (Khoshnood, 2017). In order to know the optimum age for releasing the fingerlings into the sea for maximum survival, this study focused on the structure of the nervous system of *R. frisii kutum* at the age of release.

MATERIAL AND METHODS

Caspian Kutum, *Rutilus frisii kutum*, larvae and fingerlings were obtained from Shahid Ansari Fish Proliferation and Culture Center, Rasht, Iran. The mean total length and mean body weight of fingerlings were 3.5 cm and 2.6 g respectively. For histological studies, fish were euthanased in 100 mg/l of MS222 and 100 mg/l of sodium bicarbonate and immediately immersed into Bouin's fixative for 24 hours, washed and dehydrated in an ascending series of ethanol for embedding in Paraffin (Merck). Following embedding in Paraffin (Merck), transversal and longitudinal sections of 6 µm were cut on a Leica RM2255 microtome, collected on glass slides, and stained with Haematoxylin and Eosin and finally observed by light microscopy (Khoshnood et al., 2015; Khoshnood, 2015).

RESULTS AND DISCUSSION

The brain, which is the prominent part of the beginning of the spinal cord, is composed of three main parts: the anterior brain or Prosencephalon, the middle brain or Mesencephalon, and the posterior brain or Rhombencephalon. The forebrain itself is divided into two parts, telencephalon and diencephalon. Therefore, the five sub-sections of the brain structure are respectively: telencephalon, diencephalon, mesencephalon, metencephalon and myelencephalon.

The cerebrum is composed of attached neurones; the diencephalon or midbrain is devided into two regions: dorsal epithalamus which contains pineal gland, habenular ganglion and thalamus itself, and the hypothalamus at ventral region. The hypothalamus consists of infundibulum and two inferior lobes which is the strict feature of the diencephalon and its role is the regulation of pituitary gland.

The mesencephalon is large and covered by optic tectum layers and the tegmentum is located at its inferior part. The optic tectum is devided into two optic lobes (Fig. 1).

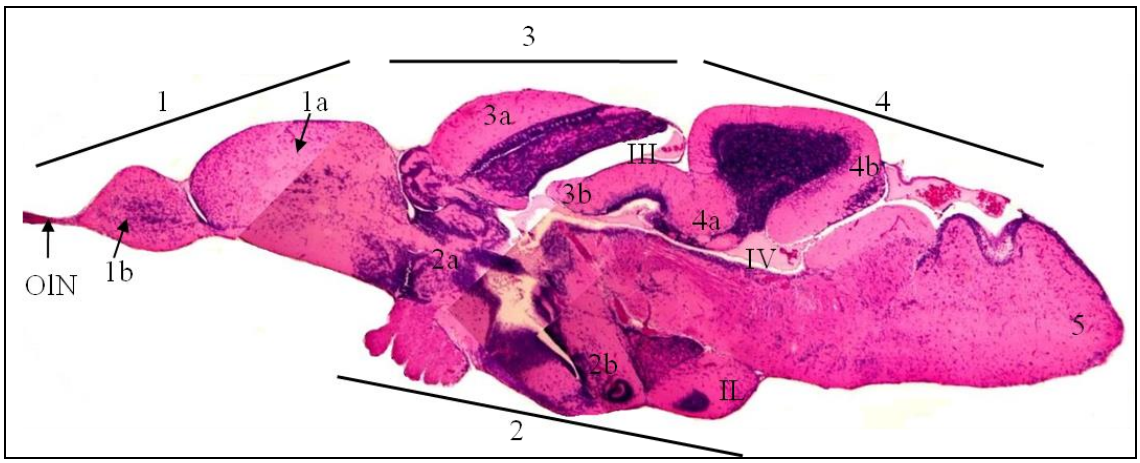

Figure 1: Histological micrograph of the brain in *R. frisii kutum* fry (H&E). The general structure of the brain (Fig. 1) is illustrated from the snout part (left) to the caudal part (right). The brain is devided into 5 distinct section: 1) Telencephalon or cerebrum is at the anterior part of the brain and is composed of two cerebral hemispheres (1a) and a pair of olfactory lobes (1b); 2) Diencephalon, which is composed of epithalamus and one thalamus at the dorsal part (2a) and one hypothalamus at the ventral part (2b) and some other parts such as pineal and pituitary glands; 3) Mesencephalon composed of optic lobes at the dorsal part (3a: optic tectum) and tegmentum (3b) at the ventral part; 4) Metencephalon composed of cerebellum with valvula cerebelli (4a) and corpus cerebelli (4b); 5) Medulla oblongata is the final part of the brain and is continued to the spinal cord. III: third ventricle; IV: fourth ventricle; OlN: Olfactory Nerve; IL: Inferior Lobe.

The cerebellum is the most important part of the dorsal metencephalon. The role of this part is to regulate coordination between motor responses as seen in other vertebrates. The cerebellum is well developed in Caspian kutum fingerlings (Fig. 1). Medulla oblongata is the main part of the hindbrain, from the caudal portion of it, the spinal cord is formed. This part contains nuclei of some cerebral nerves (5 to 10) and is the formation center for Mauthnerian system which is a well-developed nervous-muscular system in teleost fish. Stimulation of mauthnerian cells causes rapid and strong movements of the fish tail during stress and flight (Fig. 1).

The brain and the spinal cord consist of neurones and neuroglial cells. The myelinated axons of the neurons are making the white matter of the brain and spinal cord while the gray matter is made up of neuron cell bodies (Fig. 2).

Along the length of the spinal cord, some aggregations of the neurons are visible, named spinal ganglions (Fig. 2). Ganglial neurons are large and the ganglia are covered with connective tissue.

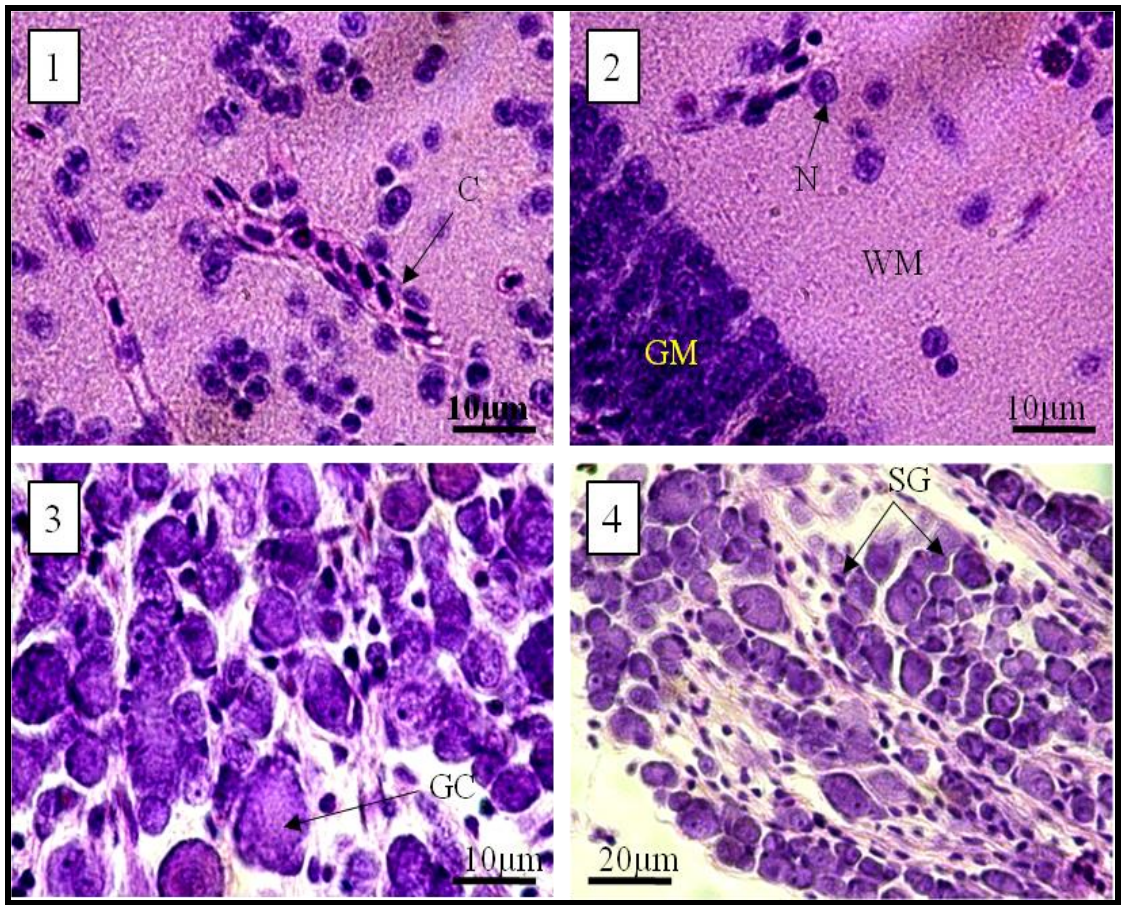

Figure 2: Histological micrograph of the nervous tissue in *R. frisii kutum* fry (H&E). The brain tissue consists of two parts: white matter (consisting of myelinated nerve fibers) and gray matter (consisting of the cell bodies of neurones) (2); In the nervous tissue, delicate capillaries are seen, in which there are nucleated red blood cells (1); Spinal ganglion is seen on the side of the spinal cord (4) which consists of neurones with large cell bodies that have large basal nuclei (3). C: Capillary; N: Nucleus; WM: White Matter; GM: Grey Matter; GC: Ganglionic Cell; SG: Spinal Ganglion.

The brain in Caspian Kutum fingerlings is composed of forebrain or Prosencephalon, midbrain or Mesencephalon and hindbrain or Rombencephalon, the forebrain consisting of telencephalon and diencephalon. Therefore five parts are distinguishable as follows: telencephalon, diencephalon, mesencephalon, metencephalon, and myelencephalon.

The telencephalon consists of olfactory lobes and cerebral hemispheres; diencephalon consists of epithalamus, thalamus and hypothalamus; mesencephalon consists of optic lobes and tegmentum; metencephalon consists of cerebellum; and myelencephalon consists of

medulla oblongata. Medulla oblongata becomes wider at the end, followed by the spinal cord. In the middle of the spinal cord a fine canal is visible which is connected to the cerebral ventricles. The telencephalon is reduced compared to the same area in mammals and consists of olfactory lobes and cerebral hemispheres (cerebrum). Cerebral ventricles are partially visible in this part. The diencephalon or midbrain consists of dorsal epithalamus (including pineal gland, habenular ganglion and thalamus) and ventral hypothalamus. Mesencephalon is large and covered by optic tectum layers with the tegmentum at the inferior part. Optic tectum is divided into two optic lobes and is made up of layers. The cerebellum is the most important part of the dorsal metencephalon. The role of this part is to regulate coordination between motor responses, and as is seen in other vertebrates, the cerebellum is well developed.

The medulla oblongata is the main part of the hindbrain, and the spinal cord is formed in its caudal part. In the spinal cord, the grey matter is different from what is seen in higher vertebrates, in this part the horns of this matter are very close to each other in such a way that white matter can hardly be seen between them, and the gray matter is seen as an Y letter.

Neurons and neuroglia cells form the cellular part of the brain and spinal cord. Lateral ventricles are either absent or surrounded by nervous tissue. In 1893, Gage stated that the unusual arrangement of the forebrain is due to the fact that its lateral walls fold outward during development, while in other vertebrates, these parts curve inward. In 1896, Studnička also confirmed this idea based on the folding of the side walls of the forebrain, and finally this idea was known as the inversion theory and was studied in diverse fish species (Butler, 2000).

Newly, it has been shown that there are two regions in the dorsal and temporal parts of the telencephalon in teleost fishes: the dorsal inverted region and the ventral region, which grew laterally and was not involved in inversion. Thus, the inversion theory can be ended in the form of local temporal inversion (Mueller and Wullimann, 2009; Wullimann and Mueller, 2004; Wullimann and Rink, 2002; Wullimann, 2009). Most of the studies on the brain and nervous system of fishes are in the field of studying the details of diverse parts of the brain, and few studies have been done in the field of comparing the brains of different fish species with each other (Nieuwenhuys, 2011; Ferreiro-Galve et al., 2008; Wullimann and Rink, 2002).

There are differences between the fish brains that live in different ecosystems, which depends on the neurological needs of each fish in its own environment. There are differences between the relative size of the telencephalon, and the relative size and external morphology of the cerebral hemispheres between sharks and teleost fishes (Lisney and Collin, 2006).

The reason why these regions are more widespread in the brain of sharks compared to teleost fishes is not well known, because many of the functions of these parts in the brains of both groups are still unknown (New, 2001; Smeets, 1998; Meek and Nieuwenhuys, 1998).

In both groups of sharks and teleost fishes, pelagic species have relatively smaller sizes compared to coastal species or related to coral reefs (Northcutt, 1978; Huber et al., 1997).

This shows the role of the brain in fish that live in complex milieus with multiple structures. Still, the brain in pelagic fish such as *Carcharhinus falciformis* shark and *Coryphaena hippurus* teleost fish is visibly large and significant, this can be referred to the life behavior of them; for example, it has been determined that sharks of the Carcharhinidae family are social animals and form herds of ten to more than thousands of individuals and have very complex social and reproductive behaviors, including reproductive dances and social hierarchy (Ritter and Godknecht, 2000; Gruber and Myrberg, 1977; Johnson and Nelson, 1973).

Terrain size may not be related to habitat complexity, but instead to complex social behaviors and intra- and inter-species interactions, especially seen in coral reef fishes (Kotrschal et al., 1998). It can be proportional and instead, it should match the complex social behaviors and intra- and inter-species interactions that are especially seen in coral reef fishes. For example, the relative size of *C. falciformis* and *C. hippurus* can be credited to their complex social behavior in their community (Kotrschal et al., 1998; Bshary et al., 2002).

For a long time, the size of the cerebellum has been attributed to the complexity of the movement behaviors of fish (New, 2001; Bauchot et al., 1977).

But despite little information about this part of the fish brain, it is generally accepted that this part of the brain obviously plays a very important role in neuro-motor behaviors (New, 2001; Meek and Nieuwenhuys, 1998; Nieuwenhuys et al., 1998; Smeets, 1998).

For example, the size of the cerebellum and the amount of its folds are very significant in *Alopias superciliosus* and *C. falciformis* sharks, and these species have high swimming power (Compagno, 1984). Brain growth has an inverse allometric relationship with body growth (Northcutt et al., 1978), because, both ontogenically and phylogenically, smaller fish have relatively larger brains (and vice versa) (Brandstaètter and Kotrschal, 1990; Ridet and Bauchot, 1990a; Bauchot et al., 1982).

The brains of fish show the typical arrangement of the brain of most vertebrates. The existence of a small number of exit routes from the brain has caused a large part of the motor system in fishes to be controlled by the spinal cord (Davis and Northcutt, 1983; Northcutt and Davis, 1983; Nieuwenhuys et al., 1998).

Mattner's system, which is seen for sudden escapes in the brain, is an exception to this. Sensory signals received from different parts of the body reach the brain through cranial nerves, these nerves include the trigeminal (V), facial (VII), vagal (X) and three lateral line nerves (two front and one posterior). In the front part, the spinal cord is connected to the brain stem and the cerebellum. The cerebellum protrudes from the upper front part of the spinal cord and a pair of visual lobes cover the cerebellum. The cephalopod brain is made up of a pair of brain hemispheres, in front of which there are olfactory lobes. The brain stem is the main center of all bodily sensory structures except smell and vision (Webb and Northcutt, 1997; Northcutt, 1996; Ariens Kappers et al., 1967; Herrick, 1906; Johnston, 1901; Allis, 1897).

The roof of the fourth ventricle is also covered by the choroid network, which shows different degrees of differentiation in different fishes (Weiger, et al., 1988).

CONCLUSIONS

Results of the present study showed that the nervous system of the Caspian Kutum, *Rutilus frisii kutum*, fingerlings at the size and age of releasing to the sea is fully developed and potentially capable of performing normal nervous functions to cope with the environmental challenges and survival behaviors.

REFERENCES

1. Abrahão V. P., Shibatta O. A., Abrahão V. P. and Shibatta O.A., 2015 – Gross morphology of the brain of Pseudopimelodus bufonius (Valenciennes, 1840) (Siluriformes: Pseudopimelodidae), *Neotropical Ichthyology*, 13, 2.
2. Allis E. P., 1897 – The cranial muscles and cranial and first spinal nerves in Amia calva, *Journal od Morphology*, 12, 487-807.
3. Ariens Kappers C. U., Huber G. C. and Crosby E. C., 1967 – The comparative anatomy of the nervous system of vertebrates including man, I-III, New York, NY, Hafner.
4. Bauchot R., Bauchot M. L., Platel R. and Ridet J. M., 1977 – Brains of Hawaiian tropical fishes; brain size and evolution, *Copeia*, 19, 42-46.

5. Bauchot R., Diagne M. and Ridet J. M., 1982 – The brain of Photoblepharon palpebratus steinitzi (Pisces, Teleostei, Anomalopidae), *Journal of Hirnforsch*, 23, 399-404.
6. Bănăduc D., Simić V., Cianfaglione K., Barinova S., Afanasyev S., Öktener A., McCall G., Simić S. and Curtean-Bănăduc A. 2022 – Freshwater as a sustainable resource and generator of secondary resources in the 21st century: stressors, threats, risks, management and protection strategies, and conservation approaches, *International Journal of Environmental Research and Public Health*, 19, 16570, 1-30, DOI: 10.3390/ijerph192416570.
7. Bănăduc D., Barinova S., Cianfaglione K. and Curtean-Bănăduc A., 2023 – Editorial: Multiple freshwater stressors – Key drivers for the future of freshwater environments, *Frontiers in Environmental Science*, 11, 1143706, 1-3, 10.3389/fenvs2023.1143706.
8. Brandstaètter R. and Kotrschal K., 1990 – Brain growth patterns in four European cyprinid fish species (Cyprinidae, Teleostei): roach (Rutilus rutilus), bream (Abramis brama), common carp (Cyprinus carpio) and sabre carp (Pelecus cultratus), *Brain Behaviour and Evolution*, 35, 195-211.
9. Bshary R., Wickler W. and Fricke H., 2002 – Fish cognition: a primate's eye view, *Animal Cognition*, 5, 1-13.
10. Butler A. B., 2000 – Topography and topology of the teleost telencephalon: a paradox resolved, *Neuroscience Letters*, 293, 95-98.
11. Butler A. B., 2011 – Brain and nervous system, Functional morphology of the brains of ray-finned fishes, *Encyclopedia of Fish Physiology*, 37-45.
12. Compagno L. J. V., 1984 – Sharks of the world, An annotated and illustrated catalogue of sharks species to date, FAO Fisheries Synopsis, 125, 4, 1-2.
13. Davis R. E., and Northcutt R. G., 1983 – Fish neurobiology, II. Ann Arbor: The University of Michigan Press.
14. Ferreiro-Galve S., Carrera I., Candal E., Villar-Cheda B., Anadón R., Mazan S. and Rodríguez-Moldes I., 2008 – The segmental organization of the developing shark brain based on neurochemical markers, with special attention to the prosencephalon, *Brain Research Bulletin*, 75, 236-240.
15. Gruber S. H. and Myrberg A. A. J., 1977 – Approaches to the study of the behavior of sharks, *American Zoologist*, 17, 471-486.
16. Herrick C. J., 1906 – On the centers of taste and touch in the medulla oblongata in fishes, *Journal of Comparative Neurology and Psychology*, 16, 403-439.
17. Huber R., van Staaden M. J., Kaufman L. S., Liem K. F., 1997 – Microhabitat use, trophic patterns, and the evolution of brain structure in African cichlids, *Brain, Behavior and Evolution*, 50, 167-182.
18. Macdonald J. and Montgomery J., 2005 – The nervous system, *Fish Physiology*, 22, 351-383.
19. Johnson R. H. and Nelson D. R., 1973 – Agonistic display in the gray reef shark, Carcharhinus menisorrah, and its relationship to attacks on man, *Copeia*, 45, 76-84.
20. Johnston J. B., 1901 – The brain of Acipenser. A contribution to the morphology of the vertebrate brain, 15, 59-260.
21. Khoshnood Z., 2017 – Histopathological alterations in digestive system of the Caspian Kutum, Rutilus frisii kutum (Kamensky 1901) fry after exposure to atrazine herbicide, *Romanian Journal of Biology and Zoology*, 62, 1-2, 73-86.
22. Khoshnood Z. 2015 – Histopathological alterations in the kidney of Caspian Kutum, Rutilus frisii kutum, larvae and fingerlings exposed to sublethal concentration of atrazine, *Bulletin of environmental contamination and toxicology*, 94, 2, 58-163.
23. Khoshnood Z., Jamili S. and Khodabandeh S., 2015 – Histopathological effects of atrazine on gills of Caspian kutum Rutilus frisii kutum fingerlings, *Diseases of aquatic organisms*, 113, 3, 227-234.

24. Khoshnood Z., Khoshnood R. and Ghobeitihasab M., 2013 – Effects of the invasive ctenophore species, Mnemiopsis leidyi, on the Caspian Sea, *Transylvanian Review of Systematical and Ecological Research*, 15, 1, 117-126.
25. Kotrschal K., van Staaden M. J. and Huber R., 1998 – Fish brains: evolution and environmental relationships, *Reviews in Fish Biology and Fisheries*, 8, 373-408.
26. Lisney T. J., and Collin S. P., 2006 – Brain morphology in large pelagic fishes: a comparison between sharks and teleosts, *Journal of Fish Biology*, 68, 532-554.
27. Meek J. and Nieuwenhuys R. 1998 – Holosteans and teleosts, in The central nervous system of vertebrates (Nieuwenhuys R., ten Donkelaar H. J. and Nicholson C., eds), Berlin: Springer-Verlag, 759-938.
28. Abdelnaeim Hussein M. N. and Cao X., 2018 – Brain anatomy and histology in Teleosts, *Benha Veterinary Medical Journal*, 35, 2, 446-463.
29. Mueller T. and Wullimann M. F., 2009 – An evolutionary interpretation of teleostean forebrain anatomy, *Brain Behaviour and Evolution*, 74, 30-42.
30. New J. G., 2001 – Comparative neurobiology of the elasmobranch cerebellum; theme and variations on a sensorimotor interface, *Environmental Biology of Fishes*, 60, 93-108.
31. Nieuwenhuys R., 2011 – The development and general morphology of the telencephalon of actinopterygian fishes: synopsis, documentation and commentary, *Brain Structure and Function*, 215, 141-157.
32. Nieuwenhuys R. H., ten Donkelaar H. J. and Nicholson C., 1998 – The meaning of it all, in The central nervous system of vertebrates (Nieuwenhuys R., ten Donkelaar H. J. and Nicholson C., eds), Berlin, Springer-Verlag, 2135-2195.
33. Nieuwenhuys R., ten Donkelaar H. J. and Nicholson C. 1998 – The central nervous system of vertebrates, 1-3, Berlin, Springer Verlag, 2219.
34. Northcutt R. G., 1978 – Brain organization in the cartilaginous fishes, in Sensory biology of sharks, skates and rays (Hodgson E. S. and Mathewson R. F., eds), 117-193, Arlington, VI, Office of Naval Research.
35. Northcutt R. G., 1996 – The agnathan ark: The origin of craniate brains, *Brain Behaviour and Evolution*, 48, 237-247.
36. Northcutt R. G. and Davis R. E., 1983 – Fish neurobiology, I. Ann Arbor, The University of Michigan Press.
37. Ridet J.-M. and Bauchot R., 1990 – Analyse quantitive de l'encéphale des Téléostéens: caractéres evolutifs et adaptatifs de l'encéphalisation, I, Généralités et analse globale, *Journal of Hirnforsch*, 31, 51-63. (in French)
38. Ritter E. K. and Godknecht A. J., 2000 – Agonistic displays in the blacktip shark (Carcharhinus limbatus), *Copeia*, 2, 282-284.
39. Smeets W. J. A. J., 1998 – Cartilaginous fishes, in The central nervous system of vertebrates (Nieuwenhuys R., ten Donkelaar H. J. and Nicholson C., eds). 551-654, Berlin, Springer-Verlag.
40. Webb J. F. and Northcutt G., 1997 – Morphology and distribution of pit organs and canal neuromasts in non-teleost bony fishes, *Brain Behaviour Evolution*, 50, 139-151.
41. Weiger T., Lametschwandtner A., Kotrschal K. and Krautgartner W. D., 1988 – Vascularization of the telencephalic chorioid plexus of a ganoid fish [Acipenser ruthenus (L.)], *American Journal of Anatomy*, 182, 33-41.
42. Wullimann M. F., 2009 – Secondary neurogenesis and telencephalic organization in zebrafish and mice: a brief review, *Integrated Zoology*, 4, 123-133.
43. Wullimann M. F., and Rink E., 2002 – The teleostean forebrain: A comparative and developmental view based on early proliferation, Pax6 activity and catecholaminergic organization, *Brain Research Bulletin*, 57, 3/4, 363-370.
44. Wullimann M. F. and Mueller T., 2004 – Teleostean and mammalian forebrains contrasted: evidence from genes to behavior, *Journal of Comparative Neurology*, 475,143-162.

BIOMETRICS OF THE COMMON SMOOTH-HOUND SHARK, *MUSTELUS MUSTELUS* FROM LANDING SITES OF LAGOS AND ONDO COASTS (NIGERIA)

Omolara Opeyemi FOLA-MATTHEWS *, *Olufemi Olukolajo SOYINKA* ** and *Aderonke Omolara LAWAL-ARE* *** *(c.a.)*

* Nigerian Institute for Oceanography and Marine Research, P.M.B. 12729, V. I., Lagos, Nigeria, tunjimoruf@yahoo.com, ORCID: 0000/0002/7800/7558.

** University of Lagos, Department of Marine Sciences, University Road, Akoka, Lagos, Nigeria, awarushs@yahoo.com, ORCID: 0000-0002-5776-2757.

*** University of Lagos, Department of Marine Sciences, University Road, Akoka, Lagos, Nigeria, alawalare@gmail.com, ORCID: 0000-0001-7656-6930.

DOI: 10.2478/trser-2024-0006

KEYWORDS: biometrics, morphometrics, truss morphometrics, sharks, Nigeria.

ABSTRACT

This study investigates the biometrics of the common smooth-hound shark, *Mustelus mustelus*, from fish landing sites of the Lagos and Ondo Coasts. Morphometric measurements and meristic counts were used on 1,018 specimens to analyze morphometric differentiations. Significant sex-based differences were found across various morphometric traits, with phenotypically separable populations observed between locations. Bray-Curtis analysis categorized morphometrics into four groups based on similar characteristics. Principal component analysis identified three components, with PC1 dominated by chondrocranium and gill slit measurements, PC2 by gill slit and fin origin measurements, and PC3 by snout and fin origin measurements.

RÉSUMÉ: Biométrie de l'Émissole lisse, *Mustelus mustelus*, provenant des sites de débarquement au large des côtes de Lagos et d'Ondo (Nigeria).

Cette étude examine la biométrie de l'Émissole lisse, *Mustelus mustelus*, sur les sites de débarquement de poissons au large de Lagos et de la côte d'Ondo. Des mesures morphométriques et des comptages méristiques ont été effectués sur 1.018 spécimens pour analyser la différenciation morphométrique. Des différences significatives basées sur le sexe ont été constatées entre les traits morphométriques, avec des populations distinctes observées entre les différents sites. L'analyse de Bray-Curtis a permis de classer les caractéristiques morphométriques en quatre groupes sur la base de caractéristiques similaires. L'analyse en composantes principales a identifié trois composantes, la PC1 étant dominée par les mesures du chondrocrâne et de la fente branchiale, la PC2 par les mesures de la fente branchiale et de l'origine de la nageoire, et la PC3 par les mesures du museau et de l'origine de la nageoire.

REZUMAT: Biometria rechinului mustel, *Mustelus mustelus* din locurile de acostare costieră din Lagos și Ondo (Nigeria).

Aceast studiu investighează biometria rechinului mustel, *Mustelus mustelus*, din locurile de acostare a bărcilor pescărești de pe coastele Lagos și Ondo. Măsurătorile morfometrice și numărătorile meristice au fost utilizate pe 1.018 indivizi, pentru a se analiza diferențierile morfometrice. S-au găsit diferențe semnificative bazate pe sex în diferite trăsături morfometrice, cu populații separabile fenotipic observate între locații. Analiza Bray-Curtis a clasificat morfometria în patru grupuri pe baza unor caracteristici similare. Analiza componentelor principale a identificat trei componente, cu PC1 dominat de măsurătorile condrocraniului și a fantei branhiale, PC2 prin măsurarea originii fantei branhiale și a aripioarelor și PC3 prin măsurătorile originii botului și a aripioarelor.

INTRODUCTION

There are numerous approaches that can be taken into consideration to determine the stock or population structure of any fish species including among others genetic analyses, phenotype analyses to detail the growth rates, age composition, morphometrics, and micro constituents in calcified structures, together with parasite loads, and tagging returns. Biometrics is an old science concerning the documentation of the bio-measurements or identification characteristics of the targets which could be humans, animals, and even fossils. Biometric measurements include morphometrics and meristics which has various applications in taxonomy, species identifications, pollution monitoring, species abnormalities, environmental changes, growth variation, feeding behaviour, ecological strategies, stock management, and aquaculture.

Generally, fish demonstrate greater variances in morphological traits within and between populations than other vertebrates and are more susceptible to environmentally induced morphological variations. Meristic counts provide quantitative data and information about the number of certain specific structures in a fish's body. Studies on meristic features are also important in fisheries because it is necessary to understand fish population dynamics and growth patterns in fish stocks (Najmudeen et al., 2019). According to Sidiq et al. (2021), information on meristic features can be valuable for various reasons, including taxonomy, ecological studies, and population assessments. Morphometrics helps to indicate differences in growth and maturity patterns which are sensitive to environmental fluctuations and show little variation in the gene pool. It also provides the relationship between body parts (Carpenter et al., 1996) and to know the origin of stock, separation of stocks, or identification of the commercially important species of fish (Narejo et al., 2000; Kohinoor et al., 1995; Devi et al., 1991).

Morphological relationships (based on descriptive assessment of individual characters, functional morphology, and multivariate analyses of multiple anatomical characters) is directly related to species life history and specific habitat use. Thus, fish morphometrics analysis represents an important tool for determining their systematic, growth variation, population parameters, and environmental relationships (Pathak et al., 2013; Sampaio et al, 2013). Despite the presence of molecular biology techniques, the study of morphometric traits is still one frequently employed by many biologists and taxonomists as it provides faster and cost-effective methods (Abbas et al., 2016; Farrag et al., 2015; Mekkawy and Mohammed, 2011; Nayman, 1965).

Standard morphometric measurements concentrate along the specific locus of the fish i.e., from the head/tip of the snout to the posterior end of the vertebral column, and it is largely dependent on the size of the fish and highly correlated with the total length of the fish. In advancement of this, the Truss Network morphometric system, a landmark-based technique system, can capture information about the shape of an organism with no restrictions on the direction of variation or localization of shape changes (Cavalcanti et al., 1999). The Truss Network technique is also important in species identification when more intensive measurements are required due to the loss of some biometric characters of the fish during fishing, sampling, and handling. A Truss Network measures a series of distances calculated between landmarks that form a regular pattern of connected quadrilaterals or cells across the body form (Strauss and Bookstein, 1982). The tope shark, *Galeorhinus galeus* and the common smooth-hound shark *Mustelus mustelus*, are the two representatives from the family Triakidae identified in Nigeria and the Gulf of Guinea (Tobor, 1993; FAO, 1990). There are presently no occurrences of any other species of the genus *Mustelus* recorded. The common smooth-hound shark, *Mustelus mustelus* represents an important fishery resource of the

Southwestern Nigerian Coast caught mainly as bycatches in both artisanal and industrial fleets while the tope shark was not observed throughout the study period at all sampling locations. In this study, observation on the biometric measurements of the common smooth-hound shark, *Mustelus mustelus* was taken to collect taxonomic data of the species that would serve as a guide to differentiate amongst other *Mustelus* species that may be sighted around the Southwestern coast of Nigeria. Variations in morphometric and sex-related characteristics were also compared between species of *Mustelus mustelus* collected around the Coast of Lagos and Ondo.

MATERIAL AND METHODS

Ethical statement

This study was carried out with strict commendations and approval of the Health Research Ethics Committee of the College of Medicine of the University of Lagos, Nigeria, Registration number: CMUL/ACUREC/09/21/1094.

Study area

Samples of *Mustelus mustelus* were collected randomly at landing sites off the Lagos Coast (OLC) and off the Ondo Coast (ONC) as well as two fish markets in Lagos state between March 2018 and September 2021. The landing sites were located between 5°57'N-6°27'N and 3°23'E-4°54'E.

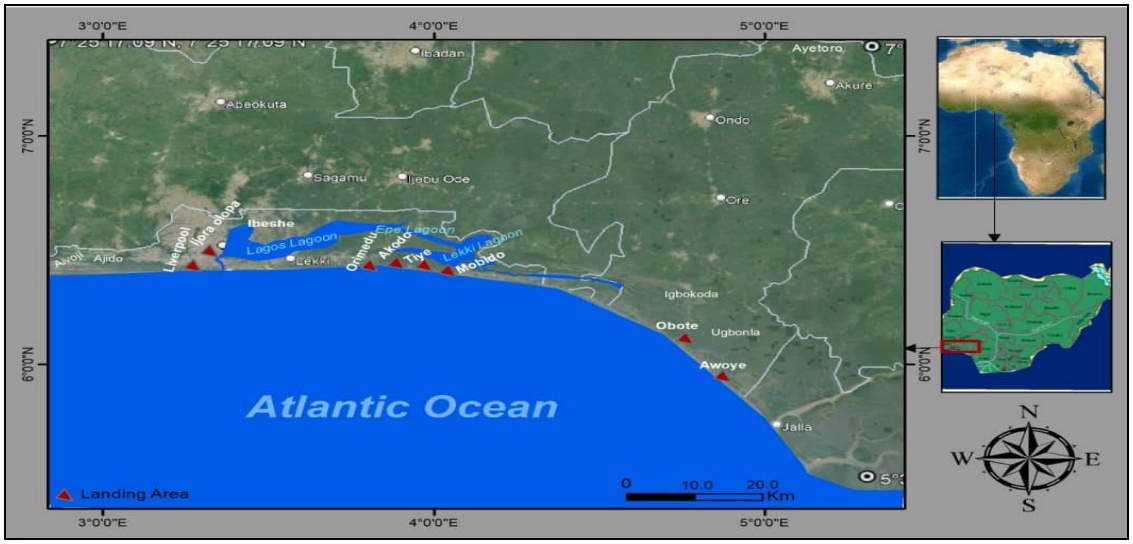

Figure 1: Map of the study area showing the location of fish landing sites of Lagos and Ondo Coasts, Nigeria (Google Earth Pro).

Sample collection

1,018 samples of *Mustelus mustelus* were collected in this study. All specimens were transported to the laboratory and persevered in an ice chest freezer. Length and weight measurements were taken after each specimen was properly thawed. Total Length (TL) was measured to the nearest centimeter with a tape measure; TL- distance from the tip of the snout to the end of the upper caudal lobe while the Total Weight (TW) was measured to the nearest gram on a digital balance.

Biometric measurements

The meristic features counted were the number of dorsal fins, gill slits, and vertebrae (monspondylous precaudal vertebrae, diplospondylous precaudal vertebrae, diplospondylous caudal vertebrae) (Fig. 2).

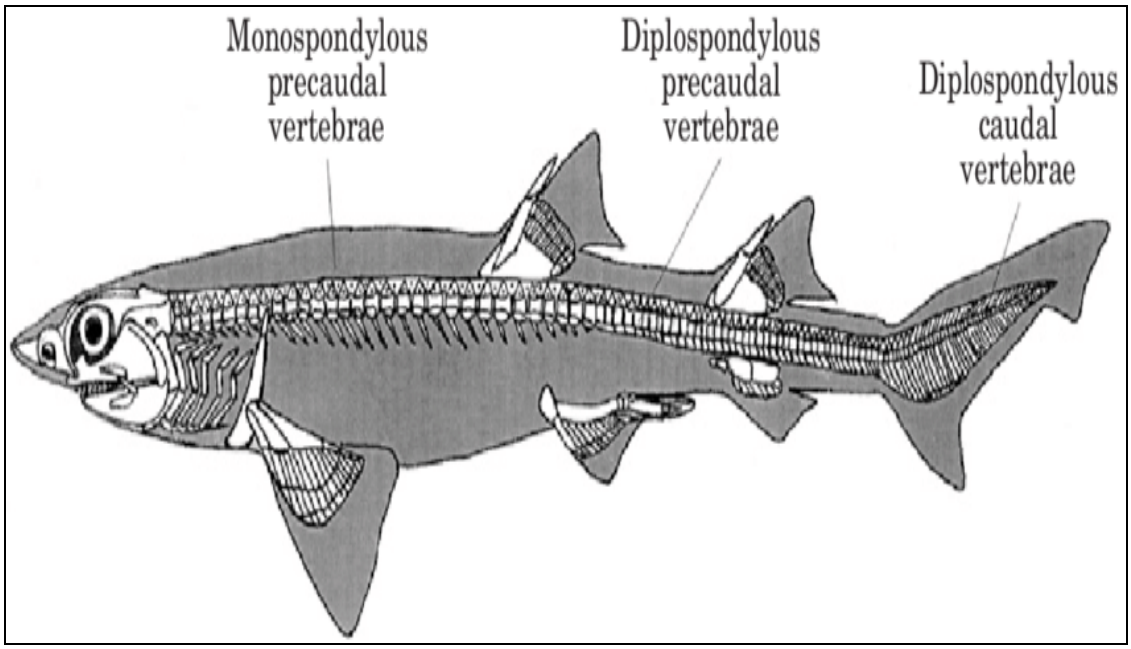

Figure 2: The location of caudal and precaudal vertebrates in sharks (Compagno, 1999).

One hundred and one selected conventional morphometric characters were measured for each studied specimen. The samples were measured using a measuring board and a measure tape to the nearest centimeter. The measurements of all the body parts were made first with the head of each specimen pointed to the left on the measuring board. The weight (g) of each specimen was measured using an electronic weighing balance (Satorius-Werke GMBH model).

The following conventional morphometric characters were measured for each fish: Total Length (TOT), Pre-pelvic Length (PP2), Fork Length (FOR), Snout-Vent Length (SVL) Precaudal Length (PRC), Preanal Length (PAL), Pre-Second Dorsal Length (PD2), Interdorsal Space (IDS), Pre-First Dorsal Length (PD1), Dorsal-Caudal Space (DCS), Head Length (HDL), Pectoral-Pelvic Space (PPS), Peribranchial Length (PG1), Pelvic-Anal Space (PAS), Prespiracular Length (PSP), Anal-Caudal Space (ACS), Preorbital Length (POB), Pelvic-Caudal Space (PCA), Prepectoral Length (PPL), Vent-Caudal Length (VCL), Prenarial Length (PRN), Por Preoral Length (POR), Eye Length (EYL) Eye Height (EYH), Intergill Length (ING), First Gill Slit Height (GS1), GS2 Second Gill Slit Height (GS2), Third Gill Slit Height (GS3), Fourth Gill Slit Height (GS4), Fifth Gill Slit Height (GS5), Sixth Gill Slit Height (GS6), Seventh Gill Slit Height (GS7), Pectoral Anterior Margin Pectoral Radial Length (PLR), Pectoral Base (PLB), Pectoral Inner Margin (PLI), Pectoral Posterior Margin (PIP), Pectoral Height (PIH), Subocular Pocket Depth (SOD), Dorsal Caudal Margin (DCM) Preventral Caudal Margin (CPV), Upper Postventral Caudal Margin (CPU), Lower Postventral Caudal Margin (CPL), Caudal Fork Width (CFW), Caudal Fork Length (CFL), Subterminal Caudal Margin (CST),

Subterminal Caudal Margin (CSW), Terminal Caudal Margin (CTR), Terminal Caudal Lobe (CTL), First Dorsal Length (D1A), First Dorsal Anterior Margin (D1B), First Dorsal Base (D1H), First Dorsal Height (DLI), First Dorsal Inner Margin (DIP), First Dorsal Posterior Margin (D2L), Second Dorsal Length (D2A), Second Dorsal Anterior Margin (D2B), Second Dorsal Base (D2H), Second Dorsal Height (D2I), Second Dorsal Inner Margin (D2P), Second Dorsal Posterior Margin (P2L), Pelvic Length (P2A), Pelvic Anterior Margin (P2A), Pelvic Base (P2B), Pelvic Height (P2H), Pelvic Inner Margin Length (P2I), Pelvic Posterior Margin Length (P2P), Anal Length (ANL), Anal Anterior Margin (ANA), Anal Base (ANB), Anal Height (ANH), Anal Inner Margin (ANI), Anal Posterior Margin (ANP), Head Height (HDH), Trunk Height (TRH), Abdomen Height (ABH), Tail Height (TAH), Caudal Peduncle Height (CPH), First Dorsal Midpoint-Pelvic Origin (DPO), Pelvic Midpoint-First Dorsal Insertion (PDI), Pelvic Midpoint-Second Dorsal Origin (PDO), Second Dorsal Origin-Anal Origin (DAO), Second Dorsal Insertion-Anal Insertion (DAI), Mouth Length (MOL), Mouth Width (MOW), Upper Labial Furrow Length, Lower Labial Furrow Length (LLA), Nostril Width (NOW), Internarial Space (INW), Anterior Nasal Flap Length (ANF), Clasper Outer Length (CLO), Clasper Inner Length (CLI), and Clasper Base Width (CLB).

The Truss Network illustrated by Bookstein (2018), Bookstein et al. (1985), Strauss and Bookstein (1982), for fish morphometrics was applied to construct a network of measurements on *Mustelus mustelus* species studied specimens. Fourteen selected anatomical landmarks were taken for two hundred and fifty randomly selected specimens from the fish samples.

Points of these fourteen selected landmarks used on the specimens for constructing the truss system on *Mustelus mustelus* are explicitelly shown in figure 1. The number of distances on the body described by and Bookstein et al., (1985) and Strauss and Bookstein (1982) were:

$$N = \left(\frac{5n}{2}\right) - 4$$

where: *N* = number of distances on the body;
n = number of homologous anatomical landmarks.

The fourteen landmarks (n) compared to thirty-one distances (N) determined on the samples are shown in table 1. The fish were positioned on their side with the head to the left on water-resistant graph sheets, the body positioned with the fins spread into a natural state. Measurements of all the thirty-one distances were taken on one side with a measuring tape for each fish specimen. Moreover, to avoid likely bias generated from size results on the morphometric features, all the morphometric character data were standardized using the ratio transformation method (i.e., Log ratio) by Turan (1999) and Reist (1985) which is efficient in eliminating such size-dependent disparity as:

$$\mathrm{M}_{adj} = \left({}^{\mathrm{logM}}/_{\mathrm{logSL}}\right)$$

where: M_{adj} = size adjusted truss measurement;
M = original truss measurement;
SL= standard length of fish based on size -djusted morphological and landmark distance data.

Table 1: 31 distances measured on the body of each sampled shark; dist. – distance.

S/N	Distance	Truss morphometric measurements
1.	1_2	Dist. between anterior tip of snout on upper jaw and chondrocranium end point
2.	1_3	Dist. between the anterior tip of snout on upper jaw and the first gill slit
3.	1_4	Dist. between the anterior tip of snout on upper jaw and pectoral fin origin
4.	2_3	Dist. between the chondrocranium and the first gill slit
5.	2_4	Dist. between the chondrocranium and the pectoral fin origin
6.	2_5	Dist. between the chondrocranium and the first dorsal fin origin
7.	3_4	Dist. between the first gill slit and the pectoral fin origin
8.	3_5	Dist. between the first gill slit and the first dorsal fin origin
9.	4_5	Dist. between pectoral fin origin and first dorsal fin origin
10.	4_6	Dist. between pectoral fin origin and the pectoral fin insertion
11.	4_7	Dist. between pectoral fin origin and the first dorsal fin insertion
12.	5_6	Dist. between first dorsal fin origin and the pectoral fin insertion
13.	5_7	Dist. between first dorsal fin origin and the first dorsal fin insertion
14.	6_7	Dist. between pectoral fin insertion and the first dorsal fin insertion
15.	6_8	Dist. between the pectoral fin insertion and the pelvic fin origin
16.	6_9	Dist. between the pectoral fin insertion and second dorsal fin origin
17.	7_8	Dist. between the first dorsal fin insertion and the pelvic fin origin
18.	7_9	Dist. between the first dorsal fin insertion and the second dorsal fin origin
19.	8_9	Dist. between the pelvic fin origin and the second dorsal fin origin
20.	8_10	Dist. between the pelvic fin origin and the anal fin origin
21.	9_10	Dist. between the second dorsal fin origin and the anal fin origin
22.	9_11	Dist. between the second dorsal fin origin and second dorsal fin insertion
23.	10_11	Dist. between the anal fin origin and the second dorsal fin insertion
24.	10_12	Dist. between the anal fin origin and the lower precaudal pit
25.	10_13	Dist. between the anal fin origin and the upper precaudal pit
26.	11_12	Dist. between the second dorsal fin insertion and the lower precaudal pit
27.	11_13	Dist. between the second dorsal fin insertion and the upper precaudal pit
28.	11_14	Distance between the second dorsal fin insertion and the terminal lobe
29.	12_13	Dist. between the lower precaudal pit and the upper precaudal pit
30.	12_14	Dist. between the lower precaudal pit and the terminal lobe
31.	13-14	Dist. between the upper precaudal pit and terminal lobe

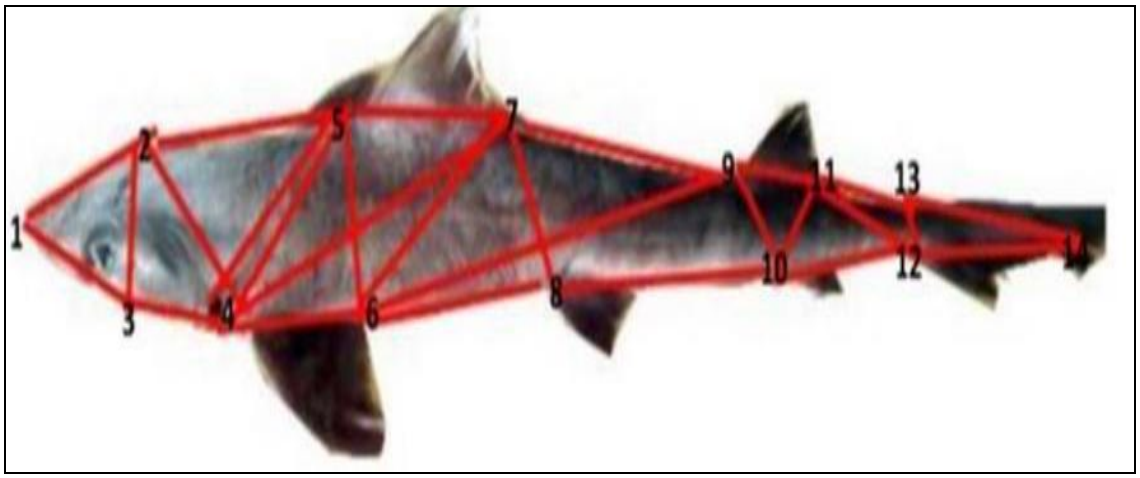

Figure 3: Location of the 14 anatomical landmarks used for Truss morphometrics on *Mustelus mustelus*; 1. anterior tip of the snout on the upper jaw; 2. most posterior aspects of chondrocranium; 3. first gill slit; 4. origin of pectoral fin; 5. origin of first dorsal fin; 6. insertion of pectoral fin; 7. insertion of first dorsal fin; 8. origin of pelvic fin; 9. origin of second dorsal fin; 10. origin of anal fin; 11. insertion of second dorsal fin; 12. lower precaudal pit; 13. upper precaudal pit; 14. terminal lobe.

RESULTS AND DISCUSSION

Meristic features

The meristic counts for *Mustelus mustelus* recorded are dorsal fins counts (first dorsal fin and second dorsal fin). Gill slits counts were five. There were variations in the number of vertebrae. Monospondylous, pre-caudal centra ranged from 24-30, diplospondylous pre-caudal centra ranged from 40-65 and diplospondylous caudal vertebrae ranged from 43-68. Meristic counts for *Mustelus mustelus* recorded in this present study showed variations in the number of vertebrae. The range of the diplospondylous pre-caudal centra was higher than the range of the monospondylous, pre-caudal centra. The result of meristic features consolidates the report of Cordova and Ebert (2021) on *Apristurus manocheriani*, a new species of catshark from the Southwest Indian Ocean.

Standard morphometrics

The result of the standard morphometrics using ANOVA revealed significant differences ($p < 0.05$) across the morphometric traits in the sexes of *Mustelus mustelus*, except for the Eye Height (EYH) which showed no significant difference. For location, ANOVA revealed significant differences ($p > 0.05$) in weight (WT), fork length (FOR), pre-pelvic length (PP2), pectoral inner margin (P1I), first dorsal length (D1L), first dorsal height (D1H), second dorsal length (D2L), second dorsal anterior margin (D2A), pelvic base (P2B), Anal height (ANL), abdomen height (ABH), and girth (GIR) of *Mustelus mustelus* from both sampling stations (OLC and ONC). This result is similar to the study from Grunow et al., (2022) on the morphological characters of the Small-Spotted Catshark, *Scyliorhinus canicula* with an optimal model organism. The maximum lengths of the same species were reported as 162 cm from the North-Eastern Mediterranean Sea (Ozcan and Başusta, 2018). Morphometric variations for female and male *Mustelus mustelus* from OLC and ONC are illustrated in figures 3 and 4.

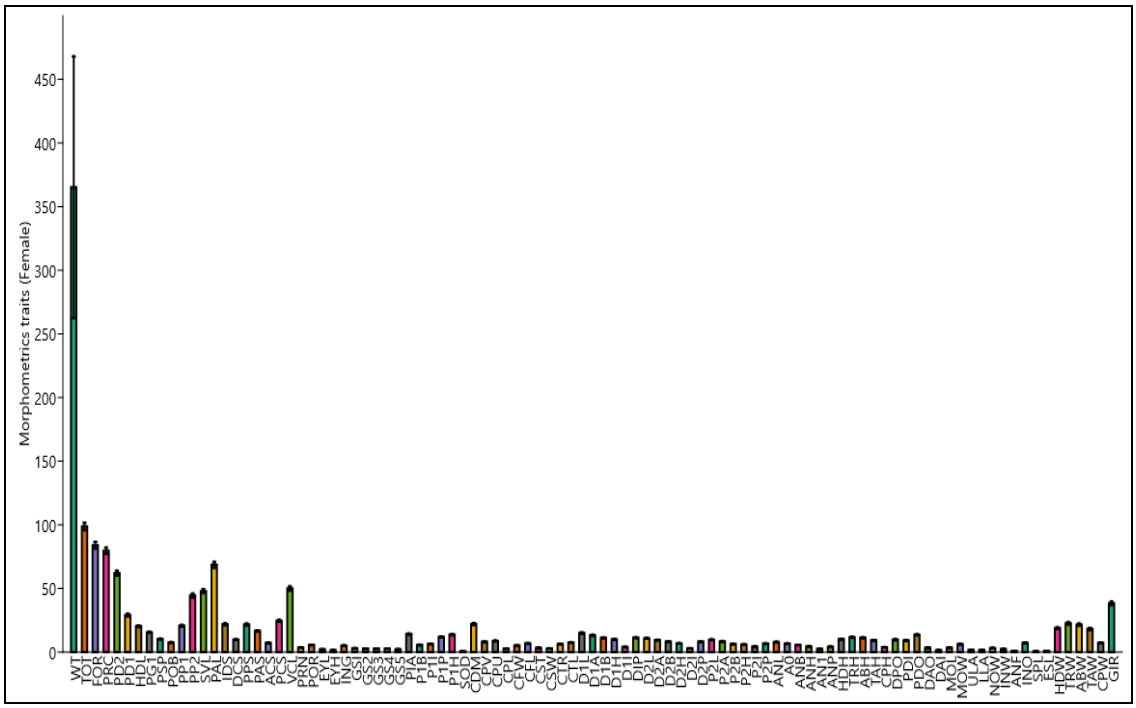

Figure 4: Morphometric variations for female *Mustelus mustelus*.

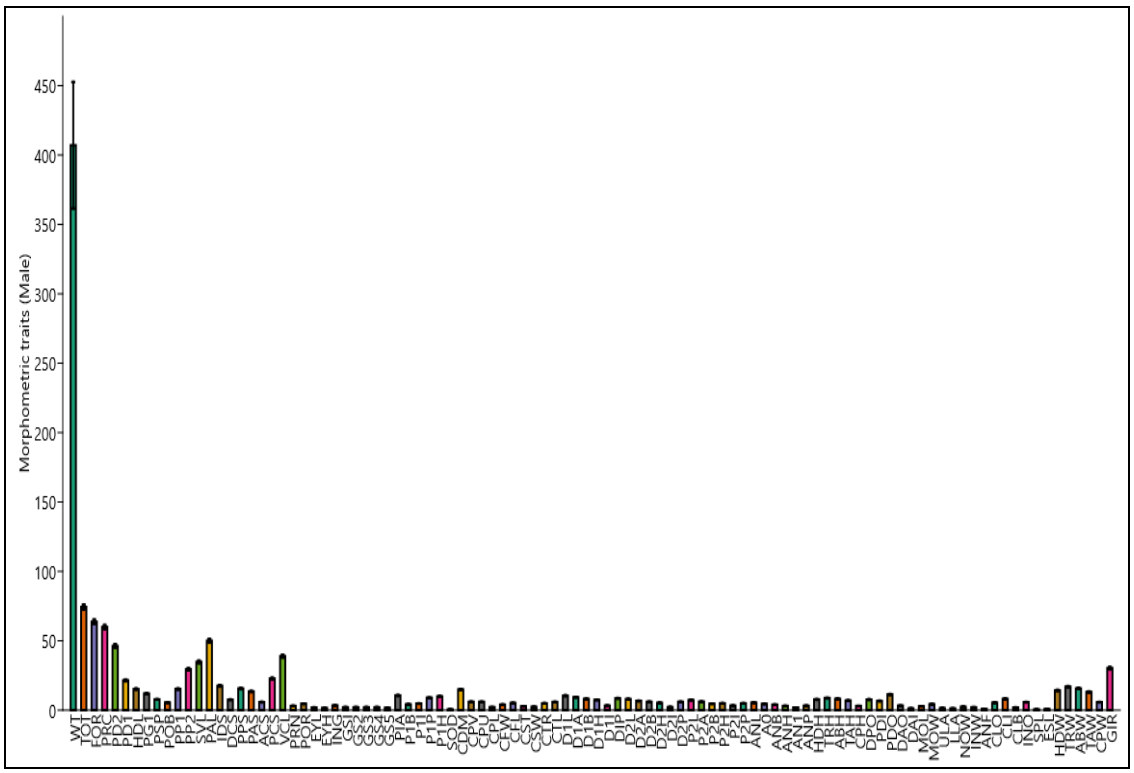

Figure 5: Morphometric variations for male *Mustelus mustelus*.

Using Bray-Curtis analysis, the interrelationships of the morphometric characteristics in relation to the sexes of the sharks across two locations are categorized into two subsets from the biplots; the sex of sharks was grouped into two (2): group 1 (male of OLC and male of ONC) and group 2 (female of OLC and female of ONC). Bray-Curtis analysis statistically grouped the morphometrics into four (4) categories based on similar characteristics; category 1 (Total weight of the OLC- male and female, ONC-male and female); category 2 (SOD, SPI, ANF and ESL); category 3a (PRN, CPH, CST, MOL, DAO, D1I, ANP, P2I, ANH, EYI, GS5, GS1, GS2. GS3, GS4, CPI, CSW, D2I, AN1, INW, NOW, EYH, ULA, DAI, LLA, and CLB); category 3b (CLO and CLI); category 3c (POB, ANL, ACS, INO, CPW, CTL, CPV, D2B, D2P, P2A, CPU); category 3d (POR, P2H, P1I, CTR, P2P, ANA, P2B, MOW, CFL, D2H, ING, P1B, ANB, and CFW); category 3e (PG1, PIA, D1I, PDO, P1H, D1A); category 3f (PSP, HDH, DCS, DPO, D1H, P2L, D2A, PDI, TAH, P1P, TRH, D1B, ABH, DIP, and DLL); category 3g (HDL, PP1, PPS, ABW, CDM, IDS, TEW, PAS, HDW, and TAW), category 3h (PD1 and PCS); and category 4a (TL, FOR, PRC, PD2 and PP2), category 4b (PP2, GIR, SVL, and VCL); figure 1 indicating that morphometric parameters clustered in the same category showing similar characteristics (Notarbartolo di Sciara et al., 2020) on biological notes and records and conservation of the long horned pygmy devil ray, *Mobula eregoodoo*.

The T-Test analysis on standard morphometrics showed that there were significant differences ($p < 0.05$) between the morphometric variables of the male and female *Mustelus mustelus* across the sampling period. As for location; the T-Test indicated that there were no significant differences ($p < 0.05$) between the morphometric variables acquired off Lagos and Ondo Coast of the sampled *Mustelus mustelus* sharks across the sampling period. Kousteni (2021) also recorded significant differences among the morphometric characters in the description and biological notes of the rare kitefin shark *Dalatias licha*.

Truss morphometrics

In this study, the contribution of the three principal components generated from truss morphometric data with the eigenvalues accounted for approximately 94% of the variation. There was very little difference in the percentage of variance of PC 1, PC 2, and PC 3, with low scores occurring. Negative and positive loading of morphometric measurements with different magnitudes in all the PCs signified that the size effect on the morphometric measurements had been totally removed before analysis (Tab. 2).

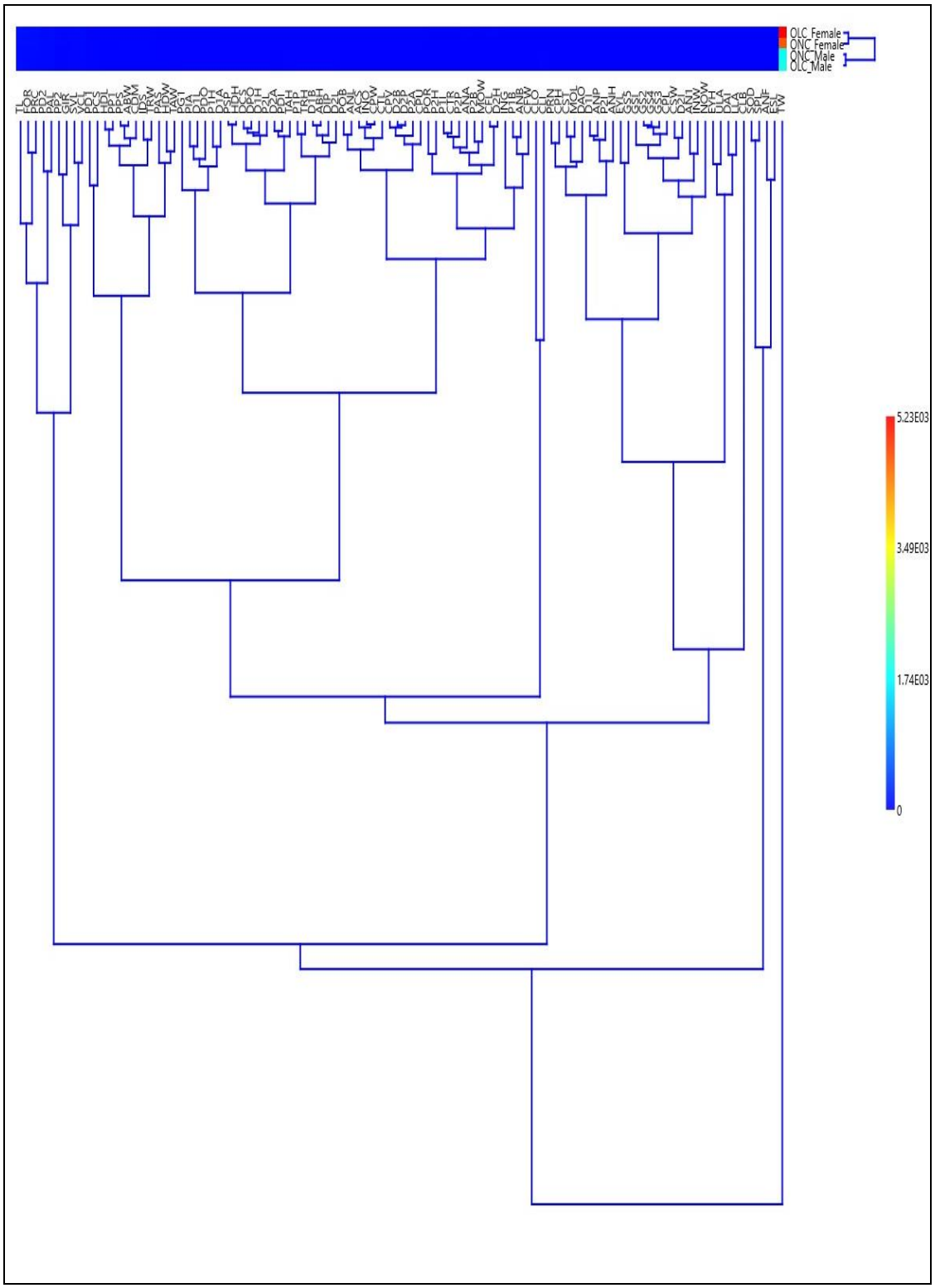

Figure 6: Hierarchical clustering (Bray-Curtis Similarities Index) of the sex-related morphometric characteristics of *Mustelus mustelus* across Lagos and Ondo Coasts.

Table 2: Relative contribution of the first three Principal Components (PC 1-3) generated from the truss morphometric data of *Mustelus mustelus*.

S/N	Distances	PC1	PC2	PC3
1.	1–2	0.1872	–0.1045	–0.00961
2.	1–3	0.177	0.04924	0.1035
3.	1–4	0.1709	0.08453	0.05093
4.	2–3	0.1624	0.09291	–0.01289
5.	2–4	0.1373	0.09861	0.02013
6.	2–5	0.2627	–0.1257	0.09192
7.	3–4	0.1107	0.5713	–0.03607
8.	3–5	0.1534	0.06837	0.05274
9.	4–5	0.1866	0.04342	–0.0403
10.	4–6	0.1549	0.06939	0.00774
11.	4–7	0.207	–0.1956	0.05386
12.	5–6	0.1796	0.05917	–0.04456
13.	5–7	0.1772	0.009683	0.1322
14.	6–7	0.2197	–0.1406	0.04204
15.	6–8	0.1931	0.1267	–0.0236
16.	6–9	0.254	–0.1405	0.03003
17.	7–8	0.1989	0.08497	–0.05471
18.	7–9	0.1654	0.1267	0.008822
19.	8–9	0.215	–0.02711	–0.9367
20.	8–10	0.1699	0.02255	0.04684
21.	9–10	0.1896	0.09933	0.1026
22.	9–11	0.1705	–0.01468	0.09519
23.	10–11	0.1827	0.1937	0.1292
24.	10–12	0.04635	0.383	–0.00818
25.	10–13	0.2113	0.09006	0.07337

The first PC which accounted for 66.17% of the total variability had the largest contributions from mainly the chondrocranium and first gill slit (0.2627), pectoral fin insertion, and pelvic fin origin (0.254). Principal Component 2 which accounted for 26.32% of the variability had high contributions from the first gill slit and pectoral fin origin (0.5713) and the distance between anal fin origin and lower precaudal pit (0.383). Principal component 3 accounted for 1.43% of the variability with high contributions from the anterior tip of the snout and the pectoral fin origin (0.1035). Rasheeq et al. (2023) investigated the stock structure of the white-spotted spine foot fish (*Siganus canaliculatus*) along the Indian coast using Truss morphometry. The PCA results demonstrated that the first two components (PC1 and PC2) accounted for over 52.6% of the total morphometric variance (PC1%-37% and PC2%-14%). PC1 and PC2 represented the posterior abdomen and the caudal peduncle region of the fish, and both components exhibited a positive correlation. Standard morphometric traits and truss measurements could both justify the differentiation among the stocks, as well as the ultimate scenario of the *M. mustelus* stock structure. The statistical analysis of this study is sufficient to distinguish among the stocks. Furthermore, if a large enough sample size is used, this study recommends that standard and truss morphometric characters can be a trustworthy method for

stock-identification research (Mahfuj et al., 2023, 2022). Research projects on fish stocks conducted in the Bay of Bengal and the Arabian Sea revealed significant alterations due to environmental differences (Bostancı and Yedier, 2018). According to a different study conducted by Ramya et al. (2021), geographic segregation and gene-pool interchange resulted in the segregation of horse mackerel stocks. Another concern is abiotic influence, which plays a vital role in stock adjustment (Kern and Langerhans, 2018). The morphological characteristics of various stocks or populations belonging to the same species may also vary widely. Based on the body depth of *N. japonicus*, a distinction was presented between the east and west coasts by Bostancı and Yedier (2018).

REFERENCES

1. Abbas E. M., Abdelsalam K. M., Geba K. M., Ahmed H. O. and Kato M., 2016 – Genetic and morphological identification of some crabs from the Gulf of Suez, Northern Red Sea, Egypt, *Egyptian Journal of Aquatic Research*, 42, 319-329.
2. Bookstein F. L., 2018 – A course in morphometrics for biologists; Geometry and statistics for studies of organismal form, Cambridge, Cambridge University Press, 556.
3. Bookstein F. L., Chernoff B. C., Elder R. L., Humphries, J. M., Smith, G. R. and Strauss, R.E., 1985 – Morphometrics in evolutionary biology, *Academy of Natural sciences of Philadelphia Special Publication*, 15, 277-289.
4. Bostancı D. and Yedier S., 2018 – Discrimination of invasive fish Atherina boyeri (Pisces: Atherinidae) populations by evaluating the performance of otolith morphometrics in several lentic habitats, *Fresenius Environmental Bulletin*, 27, 6, 4493-4501.
5. Carpenter K., Sommer E. H. J. and Marcus L. F, 1996 – Converting truss interlandmark distances to Cartesian Coordinates, in Marcus L. F., Corti Loy A., Naylor G. and Slice D. E., (eds), Advances in Morphometrics, New York Plenum Publications, 103-111, 284.
6. Cavalcanti M. J., Monteiro L. R and Lopez P. R. D, 1999 – Landmark based morphometric analysis in selected species of Serranid fishes (Perciformes: Teleostei), *Zoological Studies*, 38, 287-294.
7. Compagno L. J. V., 1999 – Endoskeleton, in Hamlett W. C. (ed.), Sharks, Skates, and Rays: The Biology of Elasmobranch Fishes. Baltimore: Johns Hopkins University Press, 69-92.
8. Cordova J. A. and Ebert D. A., 2021 – Apristurus manocheriani (Carcharhiniformes: Pentanchidae), a new species of catshark from the Southwest Indian Ocean, *Journal of the Ocean Science Foundation*, 38, 13-26
9. Devi N. T., Khumar F and Siddiqui M. S, 1991 – Observations on the morphometric characters of the catfish Rita rita (Ham.) of the river Yamuna, *Journal of Inland Fisheries Society of India*, 23, 52-58.
10. FAO, 1990 – FAO species identification sheets for fishery purposes, Field guide to the commercial marine resources of the Gulf of Guinea, 268.
11. Farrag M. M. S., Soliman T. B. H, Akel E. K. A., Elhaweet A. A. K. and Moustafa M. A., 2015 – Molecular phylogeny and biometrics of lessepsian puffer fish Lagocephalus sceleratus (Gmelin, 1789) from Mediterranean and Red Seas, Egypt, *Egyptian Journal of Aquatic Research*, 41, 323-335.
12. Grunow B., Reismann T. and Moritz T., 2022 – Pre-hatching ontogenetic changes of morphological characters of Small-Spotted Catshark (Scyliorhinus canicula), *Fishes*, 7, 3, 100.
13. Kern E. M. and Langerhans R. B., 2018 – Urbanization drives contemporary evolution in stream fish, *Global Change Biology*, 24, 8, 3791-3803.
14. Kohinoor A. H. M, Saha N. C., Akhteruzzaman M., Shah M. C. and Mahata S. C., 1995 – Morphometric characters and their relationship in red tilapia (mutant Oreochromis mossumbicus x Oreochromis niloticus), *Bangladesh Journal of Fish*, 15-18, 19-24.

15. Kousteni V., 2021 – Morphometric description and biological notes on the rare kitefin shark Dalatias licha (Chondrichthyes: Dalatidae) from the Hellenic waters, *Journal of Fish Biology*, 99, 1, 258-263.
16. Mahfuj M. S., Ahmed F. F., Hossain M. F., Islam S. I., Islam M. J., Alam M. A. and Nadia Z. M., 2022 – Stock structure analysis of the endangered Queen Loach, Botia dario (Hamilton 1822) from Five Rivers of Northern Bangladesh by using morphometrics: implications for conservation, *Fishes*, 7, 1, 41-50.
17. Mahfuj S., Islam S. I., Jinia S. S., Hossain M. F. and Atique U., 2023 – Stock identification of Congaturi halfbeak (Hyporhamphus limbatus): insight into conventional and truss-based morphometrics, *The Journal of Basic and Applied Zoology*, 84, 1, 10-19.
18. Mekkawy I. A. A. and Mohammed A. S., 2011 – Morphometrics and meristics of the three Epinepheline species*:* Cephalopholis argus (Bloch and Schneider, 1801), Cephalopholis miniata (Forskal, 1775) and Vardiola louti (Forskal, 1775) from the Red Sea, Egypt, *Journal of Biological Sciences*, 11, 1, 10-21.
19. Najmudeen T. M., Zacharia P. U., Seetha P. K., Sunil K. T. S., Radhakrishnan M., Akhildev S. and Sipson A., 2019 – Length-weight relationships of three species of pelagic sharks from southeastern Arabian Sea, *Regional Studies in Marine Science*, 29, 100647.
20. Narejo N. T., Jafri S. I. H and Shaikh S. A., 2000 – Studies on the age and growth of Palri, Gudusia chapra (Clupeidae: Teleostei) from the Keenjhar Lake (District Thatta) Sindhu, Pakistan, *Pakistan Journal of Zoology*, 32, 307-312.
21. Nayman, 1965 – Growth and ecology of fish population, *Journal of Animal Ecology*, 20, 201-219.
22. Notarbartolo di Sciara G., Adnet S., Bennett M., Broadhurst M. K., Fernando D., Jabado R. W. and Stevens G., 2020 – Taxonomic status, biological notes, and conservation of the longhorned pygmy devil ray Mobula eregoodoo (Cantor, 1849), *Aquatic Conservation*: *Marine and Freshwater Ecosystems*, 30, 1, 104-122.
23. Ozcan E. I. and Başusta N., 2018 – Preliminary study on age, growth and reproduction of Mustelus mustelus (Elasmobranchii: Carcharhiniformes: Triakidae) inhabiting the Gulf of Iskenderun, North-Eastern Mediterranean Sea, *Acta Ichthyologica et Piscatoria*, 48, 1, 27-36.
24. Pathak N. B., Parikh A. N. and Mankodi P. C., 2013 – Morphometric analysis of fish population from two different ponds of Vadodara city, Gujarat, India, *Journal of Animal Veterinary Fishery Science*, 1, 6, 6-9
25. Ramya V. L., Behera B. K., Das B. K., Krishna G., Pavankumar A. and Pathan M. K., 2021 – Stock structure analysis of the endemic fish, Barbodes carnaticus (Jerdon, 1849), for conservation in a biodiversity hotspot, *Environmental Science and Pollution Research*, 28, 55277-55289.
26. Rasheeq A. A., Rajesh M., Kumar T. A., Rajesh K. M., Kathirvelpandian A., Kumar S. and Singh P. K., 2023 – Stock structure analysis of the white-spotted spine foot fish (Siganus canaliculatus) along the Indian coast using Truss morphometry, *Regional Studies in Marine Science*, 65, 103072.
27. Reist J. D., 1985 – An empirical evaluation of several univariate methods that adjust for size variation in morphometric variation, *Canadian Journal of Zoology*, 63, 1429-1439.
28. Sampaio A. L. A., Pagotto J. P. A. and Goulart E., 2013 – Relationships between morphology, diet and spatial distribution: Testing the effects of intra and interspecific morphological variations on the patterns of resource use in two Neotropical cichlids, *Neotropical Ichthyology*, 11, 2, 351-360
29. Sidiq M., Ahmed I. and Bakhtiyar Y., 2021 – Length-weight relationship, morphometric characters, and meristic counts of the cold-water fish Crossocheilus diplochilus (Heckel) from Dal Lake, *Fisheries & Aquatic Life*, 29, 1, 29-34.

30. Pathak N. B., Parikh A. N. and Mankodi P. C., 2013 – Morphometric analysis of fish population from two different ponds of Vadodara city, Gujarat, India, *Journal of Animal Veterinary Fishery Science*, 1, 6, 6-9.
31. Ramya V. L., Behera B. K., Das B. K., Krishna G., Pavankumar A. and Pathan M. K., 2021 – Stock structure analysis of the endemic fish, Barbodes carnaticus (Jerdon, 1849), for conservation in a biodiversity hotspot, *Environmental Science and Pollution Research*, 28, 55277-55289.
32. Turan C., 1999 – A note on the examination of morphometric differentiation among fish populations: The Truss system, *Turkish Journal of Zoology*, 23, 259-263.